ISSN 1454-8518

ANNALS OF THE UNIVERSITY OF PETROŞANI

ELECTRICAL ENGINEERING

VOL. 20 (XLVII)

UNIVERSITAS PUBLISHING HOUSE
PETROŞANI - ROMANIA 2018

Annals of the University of Petrosani, Electrical Engineering, 20 (2018)

ISSN 1454-8518

Editorial office address: Ec. Radu Ioan, University of Petroşani, 20 University Street, 332006 Petroşani, Romania, Phone: (40) 254/54.29.94; 54.25.80; 54.25.81; 54.33.82; Fax: (40) 254/54.34.91; 54.62.38,

Contact person: **Susana ARAD**, e-mail: susanaarad@yahoo.com
This publication is spread in 28 countries.

CONTENTS

Annals of the University of Petrosani, Electrical Engineering, 20 (2018)

EVALUATION OF ENCAPSULATED EQUIPMENT

COSMIN COLDA[1], SORIN BURIAN[2], MARIUS DARIE[3], TIBERIU CSASZAR[4], DĂNUȚ GRECEA[5]

Abstract: This paper presents the explosion protection principles implemented for the type of protection encapsulation “m” which are based on the adoption of certain separations between the encapsulated circuits and the other circuits, by including them in a compound. The paper describes the test methodologies for explosion-proof electrical equipment with type of protection encapsulation “m”.

The use of electrical energy in potentially explosive atmospheres involves various particularities, fact for which there have been raised a lot of issues concerning the design, construction and exploitation of electrical equipment and installations intended to be used in these atmospheres.

Keywords: type of protection, encapsulation, electrical equipment, compound, type test

1. GENERAL CONDITIONS

In health and security domain, it is noted a rising trend of the security level in conformity with scientific knowledge state and with taking in consideration of the new risk factors due to economic development. It also follows the same trend the protection of low currents installations utilized in workplaces with risk of explosives atmospheres. Directive 2014/34/EU states that equipment and installations utilized in explosive atmospheres must have compatible specifications with the ones of explosive atmosphere there are about to work.

[1] *Ph. D.Eng., scientific researcher III, INDC-INSEMEX Petroşani*
[2] *Ph. D.Eng., scientific researcher I, INDC-INSEMEX Petroşani*
[3] *Ph. D.Eng., scientific researcher I, INDC-INSEMEX Petroşani*
[4] *Ph. D.Eng., scientific researcher I, INDC-INSEMEX Petroşani*
[5] *Ph. D.Eng., scientific researcher, INDC-INSEMEX Petroşani*

In order to evaluate the equipment for protection to explosion, encapsulation type, one has to follow an investigation process of the equipment in terms of its conformity with relevant standard requirements for protection to explosion. As to evaluate the electric equipment for protection to explosion, type encapsulation “m”, the current trend is to increase the evaluation share through applicable calculus on the equipment, using tables and diagrams presented in applicable standards SR EN 60079-0; SR EN 60079-18. This paper follows the study and assessment of the requirements concerning absorption test for electric equipment with type “m” protection.

2. CONSIDERATIONS ABOUT THE ENCAPSULATED EQUIPMENT TESTS

The conformity assessment of technical documentation for equipment used in potentially explosive atmospheres is made in accordance with Directive 94/9/EC, annex 3. The documentation submitted to the notified body must include the following:

•a general type-description;

•design and manufacturing drawings and layouts of components, subassemblies, circuits, etc.;

•descriptions and explanations necessary for the understanding of said drawings and layouts and the operation of the product;

•a list of the standards referred to in Article 5, applied in full or in part, and descriptions of the solutions adopted to meet the essential requirements of the Directive where the standards referred to in Article 5 have not been applied;

•results of design calculations made, examinations carried out, etc.;

•tests reports.

The notified body shall:

•examine the technical documentation, verify that the type has been manufactured in conformity with the technical documentation and identify the elements which have been designed in accordance with the relevant provisions of the standards referred to in Article 5, as well as the components which have been designed without applying the relevant provisions of those standards;

•perform or have performed the appropriate examinations and necessary tests to check whether the solutions adopted by the manufacturer meet the essential requirements of the Directive where the standards referred to in Article 5 have not been applied;

•perform or have performed the appropriate examinations and necessary tests to check whether these have actually been applied, where the manufacturer has chosen to apply the relevant standards;

•agree with the applicant the location where the examinations and necessary tests shall be carried out.

Equipment/installations of low currents are those equipment / electrical installation in which the electric components utilized for info transfer, for mini-macro movements also for the components whose nominal voltage doesn’t exceed 11 kV, are included in a compound.

A brief review on these protection type encapsulation installations following their objectives: equipment and installations in automation field, data communication, interlocks, controls; Monitoring and alarm equipment and installations for water leaks, explosive and toxic gases, respectively for fire; equipment and installations for access control, warning device for surveillance; equipment and installations for (video) intercom, telephony and sound; equipment and installations for data transmission and VDI; equipment and installations for data cable CATV and other circuit parts (Figure 1).

Fig. 1. Encapsulated equipment and electrical installations

The protection type in which the parts that can ignite an explosive atmosphere either by spark or by heating, are included in a compound, so that the given explosive atmosphere can't be lit in normal operating conditions is referred to as encapsulation "m".

The electric encapsulated "m" equipment can be with:

a) protection level "ma" (EPL "Ma, Ga, Da"),

b) protection level "mb" (EPL "Mb, Gb, Db") or

c) protection level "mc" (EPL "Gc, Dc").

The test sequence and number of samples are shown below:

2.1 Maximum temperature

A sample of "m" equipment shall be subjected to a type test to ensure that:

a) the temperature limits are not exceeded in normal operation;

b) for level of protection "ma" and "mb" the maximum surface temperature is not exceeded under fault conditions.

For "m" equipment without an external load, the test shall be carried out in accordance with the temperature measurements of IEC 60079-0 taking into account the supply conditions.

2.2 Thermal endurance test

2.2.1. Thermal endurance to heat

- for level of protection "ma" and "mb", the test shall be carried out in accordance with IEC 60079-0. The temperature to be used as the reference service temperature for the test shall be either:

a) the maximum surface temperature of the test sample under normal operation plus 20 K;

or

b) the maximum temperature at the component surface in the compound under normal operation;

- for level of protection "mc", the test shall be carried out in accordance with IEC 60079-0.

The temperature to be used as the reference service temperature for the test shall be the maximum surface temperature under normal operation.

2.2.2. Thermal endurance to cold

The test shall be carried out in accordance with IEC 60079-0.

After each test the sample shall be subjected to a visual inspection. No visible damage to the compound that could impair the type of protection shall be evident, for example cracks in the compound, exposure of encapsulated parts, failure of adhesion, inadmissible shrinkage, discoloration, swelling, decomposition or softening. A discoloration on the surface of the compound is permissible (for example oxidation in the case of epoxy resin).

2.3 Dielectric strength test

The test shall be carried out on the following arrangements of circuits as applicable:

a) between galvanically isolated circuits;

b) between each circuit and all earthed parts;

c) between each circuit and the surface of the compound or the non-metallic enclosure that, if necessary, can be clad with a conductive foil.

For arrangement a), the voltage U to be used shall be the sum of the rated voltages of the two circuits being tested and for arrangements b) and c), the voltage U to be used shall be the rated voltage of the circuit being tested.

For arrangement b), circuits that contain transient suppression components connected between the circuit and the earthed parts, a special test sample without these components shall be permitted for the type test.

Dielectric strength shall be verified by test:

- either as given in a relevant industrial standard for the individual items of electrical equipment or,
- at the test voltage according to 1) or 2) below, and increased steadily within a period of not less than 10 s until it reaches the prescribed value, and it shall then be maintained for at least 60 s without dielectric breakdown occurring.

The test voltage shall be increased steadily within a period of not less than 10 s until it reaches the prescribed value, and it shall then be maintained for at least 60 s.

2.4 Cable pull test

The test shall be carried out on one sample, previously unstressed and at 21 °C ± 2 °C.

A further test sample shall be subjected to the cable pull test after conditioning at the maximum temperature at the cable entry point. The tensile force (in Newton) applied shall either be 20 times the value in millimeters of the diameter of the cable or 5 times the mass (in kilograms) of the “m” equipment, whichever is the lower value. This value can be reduced to 25 % of the required value in the case of permanent installations. The minimum tensile force shall be 1 N and the minimum duration shall be 1 h. The force shall be applied in the least favorable direction.

After testing, the sample shall be subjected to a visual inspection. Visible displacement of the cable, which affects the type of protection, shall not be evident. No damage to the compound or cable that could impair the type of protection shall be evident, for example, cracks in the compound, exposure of the encapsulated components or failure of adhesion.

2.5 Pressure test for Group I and Group II electrical equipment

For level of protection “ma” with any individual free spaces between 1 cm^3 and 10 cm^3 and level of protection “mb” with any individual free spaces between 10 cm^3 and 100 cm^3, two test samples shall be prepared with a pressure connection. Where there is more than one free space of a size requiring testing, the pressure test shall be carried out simultaneously in all those free spaces. The pressure test shall be carried out on samples that have already been submitted to the thermal endurance tests. The test shall be carried out with a pressure as shown in Table 1 applied for at least 10 s.

Table 1. ***Test pressure***

Minimum ambient temperature °C	Test pressure kPa
≥ –20 [(a)]	1 000
≥ –30	1 370
≥ –40	1 450
≥ –50	1 530
≥ –60	1 620
[a)] This covers equipment designed for the standard ambient temperature range specified in IEC 60079-0.	

As an alternative for ‘mb’ equipment if the component with a free space up to 100 cm^3, prior to encapsulation, passes the Leakage test on sealed devices specified in IEC 60079-15 (without the conditioning, voltage, or dielectric withstand testing) it can be encapsulated without requiring the pressure test. After testing, the samples shall be visually inspected. No compound damage (such as cracks in the compound, exposure of the encapsulated components or failure of adhesion) that could impair the type of protection shall be evident. For constructions that are permitted to have no thickness of compound between a free space and a non-metallic enclosure wall, there shall also be no damage to the non-metallic enclosure wall(s).

2.6 Sealing test for built-in protective devices

The test is to be performed on five samples. With the test samples at an initial temperature of (25 ± 2) °C, they are suddenly immersed in water at a temperature of (50 ± 2) °C to a depth of not less than 25 mm for at least 1 min. The devices are considered to be satisfactory if no bubbles emerge from the samples during this test.

3. CONCLUSIONS

1) This paper presents the main tests for electrical apparatus with encapsulation protection type.
2) Analysis specific requirements of the standard SR EN 60079-18 on the evaluation equipment with type of protection encapsulation "m" highlighted compound role in the determination of applicable defects in the phase of explosion protection evaluation.
3) Presentation in the requirements of water absorption test for explosion-protected equipment through the types of protection encapsulation "m", being one of the basis tests for these.
4) The increased complexity of the circuits of the equipment involved in the production process using a compound and conceiving with regard to protection from explosion due to thermal effects to which they may be subjected to.
5) Standardized values imposed by the requirements of isolation distances resulting from the simplified assessment process are superior to those which can be implemented which often leads to rejection of rated equipment.
6) The aim is to study different types of compound to satisfy the mechanical and thermal resistance, to dissipate the thermal effects caused by overheating the electric and electronic components included in the compound without them affecting the electric equipment safety of use. This aspect is primarily important due to a high number of equipment which operates in explosive atmospheres hazardous areas where the temperature varies between - 30˚ C ÷ +50˚ C.

4. ACKNOWLEDGMENTS

This article uses the experimental results obtained within the project PN 18 17 02 01 of the „Nucleu” Program developed with the help of ANCSI.

REFERENCES

[1]. Burian S., Ionescu J., Darie M., Csaszar T., Andriş A., *Requirements for Installations in Areas with Explosive Atmosphere, Other than Mines, (in Romanian)*, INSEMEX – Petrosani Publishing House, Romania, (2007).

[2]. Colda C., Burian S., Darie M., Csaszar T., Grecea D., *Considerations about the encapsulated equipment tests*, 8th International Multidisciplinary Scientific Symposium SIMPRO 2018, 11-13 October 2018, Petroşani

[3]. Darie M., Burian S., Ionescu J., Csaszar T., Moldovan T., Colda C., Moldovan C., Andriş A., *Investigation of air humidity influence over the ignition sensitivity of gaseous explosive atmospheres from the underground of firedamp mines*. The Sixth Balkan Mining Congress Balkanmine 2015 Petrosani, Romania, (2015).

[4]. Directive 2014/34/EU of the European Parliament and of the Council of 26 February 2014 *on the harmonisation of the laws of the Member States relating to equipment and protective systems intended for use in potentially explosive atmospheres* (recastOn line at: http://ec.europa.eu/DocsRoom/documents/16402/attachments/1/translations/en/renditions/native), (2014).

[**5]. SR EN (IEC) 60079-18:2015**. *Explosive atmospheres. Equipment protection by encapsulation "m"*, (2015).

Annals of the University of Petrosani, Electrical Engineering, 20 (2018)

EVALUATION OF SIMPLE CIRCUITS WITH INTRINSIC SAFETY

DĂNUȚ GRECEA[1], SORIN BURIAN[2], MARIUS DARIE[3], TIBERIU CSASZAR[4], COSMIN COLDA[5], ADRIANA ANDRIŞ[6], GABRIELA PUPĂZAN[7], LUCIAN MOLDOVAN[8],

Abstract: In this paper are presented the analysis and characterization of linear sources from within intrinsic safety circuits and issues to be taken into account for the evaluation of these circuits.

For low current electrical equipment (interlocking, command, data communications, signalling) the assessment of explosion protection is often carried out by calculation using the technical data available in the specific standard related to protection to explosion requirements.

Currently, the method of calculation uses simplified but covering models. The major advantage of the outcome's certainty on the confirmation of the explosion protection is balanced by the increased rate of rejection. Complex equipment which cannot be assessed by calculation is tested in explosive atmospheres in compliance with the requirements set out in the relevant standard.

Keywords: explosive atmosphere, explosion protection; electrical equipment, type of protection, intrinsic safety.

[1] *Ph. D.Eng., scientific researcher, INDC-INSEMEX Petroşani*
[2] *Ph. D.Eng., scientific researcher I, INDC-INSEMEX Petroşani*
[3] *Ph. D.Eng., scientific researcher I, INDC-INSEMEX Petroşani*
[4] *Ph. D.Eng., scientific researcher I, INDC-INSEMEX Petroşani*
[5] *Ph. D.Eng., scientific researcher III, INDC-INSEMEX Petroşani*
[6] *Eng., scientific researcher , INDC-INSEMEX Petroşani*
[7] *Eng., scientific researcher, INDC-INSEMEX Petroşani*
[8] *Ph. D.Eng., scientific researcher I, INDC-INSEMEX Petroşani*

1. GENERAL CONDITIONS

In industrial installations in which are processed, used or stored flammable or combustible substances is likely to occur an explosive atmosphere, generating an explosion hazard. In this regard, in order to ensure explosion protection, the electrical equipment used in such installations must be correctly chosen to ensure the level of health and safety at the workplace and to prevent their being built into a source of ignition for explosive atmospheres, [1].

In this paper are presented the analysis and characterization of linear sources from within intrinsic safety circuits and issues to be taken into account for the evaluation of these circuits.

Explosion prevention and explosion protection are of major importance for occupational health and safety in order to minimize losses (both human and material). Explosive atmospheres are defined as a mixture with air, under atmospheric conditions, of flammable substances in the form of flammable gases, mist vapors or combustible dusts, in which, after ignition, combustion is spread throughout the unburned mixture, [7].

The mechanism of an explosion generated by a mixture of flammable gas, vapor or mist with air can be expressed by the well-known explosion triangle shown in Figure 1. Thus, the occurrence of an explosion is conditioned by the simultaneous presence of the following three factors:

1. fuel (flammable gases, vapours, dusts /powders, mists);

2.comburent (oxygen, oxidizing substances);

3. efficient ignition source for ensuring the activation of molecules in order to ignite and propagate the fast combustion reaction, [2].

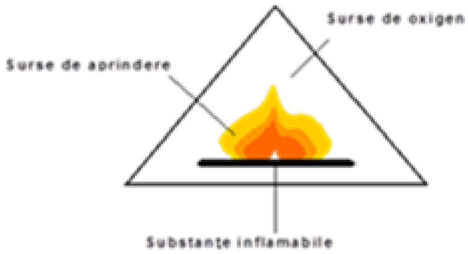

Fig. 1. The explosion triangle

Evaluation and testing of equipment which is part of an explosion protect system in purpose of certification, considers that the risk of explosion has to be minimized in order to ensure security of life and human health, as well as to prevent damage to property and, last but not least, the environment, [3].

All equipment included in a system under construction explosion-protected equipment used in spaces endangered by potentially explosive atmosphere shall meet the following requirements:

• be adequately protected from the explosion;

• to maintain the level of protection for the environmental conditions for which it was built;

• to be able to withstanding all requests (predictable) to which they are subjected during storage, transport, installation and operation of the system, [5].

Explosion protection for low current installations can be implemented using the intrinsic safety type of protection.

Intrinsic safety type of protection, based on the separation of the circuit is protected from other circuits and limiting the energy that is protected so that it cannot ignite the explosive atmosphere, [4].

The explosion protection evaluation for low current equipment involves a process of analyzing the equipment documentation with respect to compliance with the requirements of the relevant explosion protection standards.

The current trend in assessing explosion protection of low current electrical equipment protected by the type of explosion protection intrinsic safety is to increase the share of assessments by calculation applied to equipment using reference tables and charts presented in the relevant standard SR EN 60079- 0; SR EN 60079-11.

Intrinsic safety equipment and parts with intrinsic safety of the associated equipment are classified after recalled above standard as having levels of protection: ”ia”, ”ib” or ”ic”, [8].

2. EVALUATION CRITERIA FOR SIMPLE CIRCUITS WITH INTRINSIC SECURITY TYPE OF PROTECTION

Explosion protection implemented by intrinsic safety protection type is based on two main guidelines: limiting the transited and stored energy but also the adoption of separations between intrinsically safe circuits and other circuits.

To evaluate the active intrinsic safety circuits, it is necessary to know first the internal resistance and supply voltage.

For the simplest case, the source can be characterized by two electric constant values, either idle voltage U_0 and internal resistance R_i or the idle voltage U_0 and short-circuit current I_0 as shown in Figure 2.

When the circuit to be evaluated, in terms of capacity, is approximated as a simple circuit, for which there are experimentally curves determined in reference accredited laboratories and recognized at international level, the charts in carts A1 ÷ A6 can be used for evaluation.

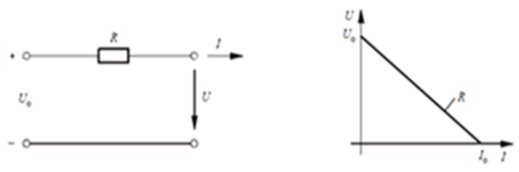

Fig. 2. Resistive circuit with linear characteristic

Specific values of these charts can be processed in tabular form. In both cases, however, the defective conditions and safety coefficients should be considered.

The information given by the following figures relate only to simple circuits and in some cases it can be difficult to apply the information to design practical circuits.

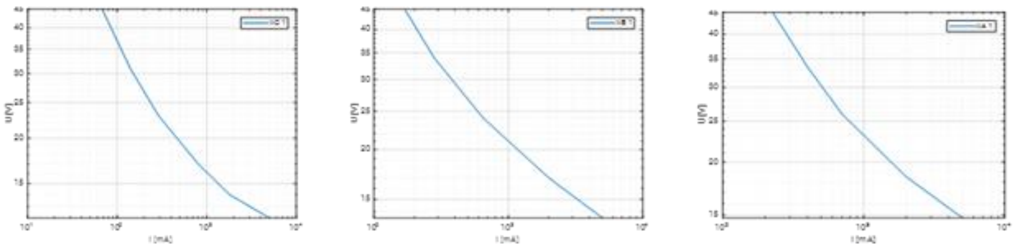

Fig. 3. Curves for evaluation of resistive circuits, group II, safety coefficient 1

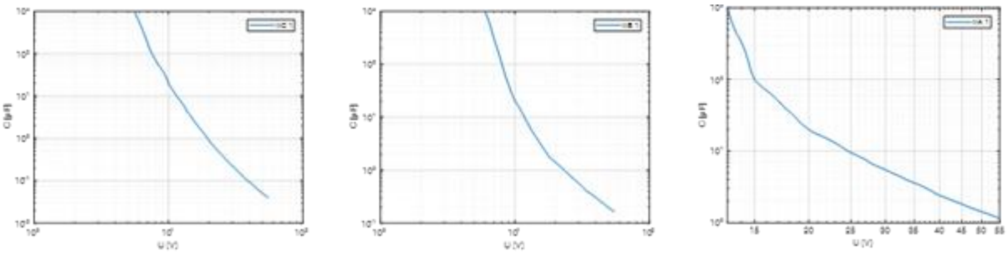

Fig. 4. Curves for evaluation of capacitive circuits, group II, safety coefficient 1

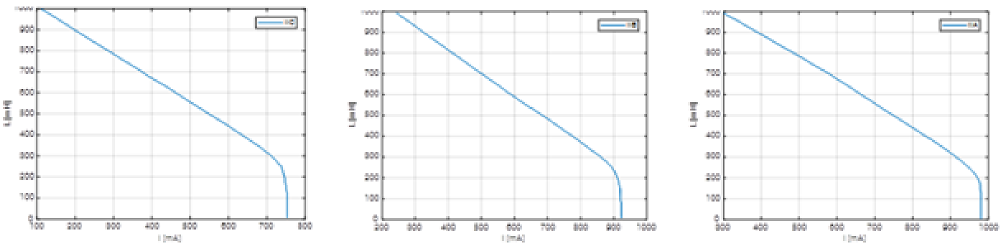

Fig. 5. Curves for evaluation of inductive circuits, group II

A circuit intended for use in potentially explosive environments, with the protection type intrinsic safety "i" must satisfy three basic criteria:

a) does not result in any electrical spark ignition owed when the circuit is rated or tried in accordance with the specified protection level and specified electrical equipment group. This requirement may be satisfied through evaluation, information, current and voltage information on circuit parameters such as inductance and capacity.

b) the temperature class of the equipment with the intrinsic safety is established so as to ensure that the ignition is not caused by hot surfaces. This requirement can be satisfied by estimating the maximum surface temperatures of the components, from the knowledge of their behavior and thermal maximum power to which they may be subjected in operation/fault conditions. The temperature classes of flammable substances (Table 1) are as follows:

Table 1. ***Temperature classes of flammable substances***

Temperature class	Auto-ignition temperature range (AIT) (°C)
T1	≥ 450
T2	$300 \leq$ AIT ≤ 450
T3	$200 \leq$ AIT ≤ 300
T4	$135 \leq$ AIT ≤ 200
T5	$100 \leq$ AIT ≤ 135
T6	$85 \leq$ AIT ≤ 100

c) the circuit should be separated by the other circuits. This can be satisfied by providing isolation distances on the surface and in air insulation distance, electro insulating material, compound or galvanic separation elements.

The following diagram is presented for the evaluation of a circuit intended for use in potentially explosive atmospheres having that type of protection intrinsic safety "i", Figure 6. The steps that you must follow are:

-faling the circuit in one of the levels of protection imposed: "ia", "ib" or "ic";

-identify the values for the U_m respective U_i;

- is determined by the coefficient shall be applied to the security parameters of the electrical circuit rated you as well as for evaluation of surface temperature;

-shall be determined points of application defects in circuit rated depending on the level of protection circuit is employed;

-calculate the maximum values for parameters U_i, I_i, respectively P_i, taking into account the tolerance values of components depends on the type of protection;

-compare the values obtained with the diagrams of acceptability standard.

Based on circuit analysis, a MATLAB computing application was developed to evaluate simple linear circuits using curves and reference tables. Specific values of these diagrams were processed and tabular form. In both cases, however, defective conditions and safety coefficients should be considered, [6].

In Figure 7 is represented the capture of the user interface. This interface allows you to choose the type of simple circuit, the coefficient of safety and gas subgroup required in the evaluation process, based on the charts values, in tabular form inserted and processed in MATLAB in the form of .mat file, graphically indicating validation or invalidation of the protection taking into account the input data (voltage U, resistance R, capacitance C, inductance L).

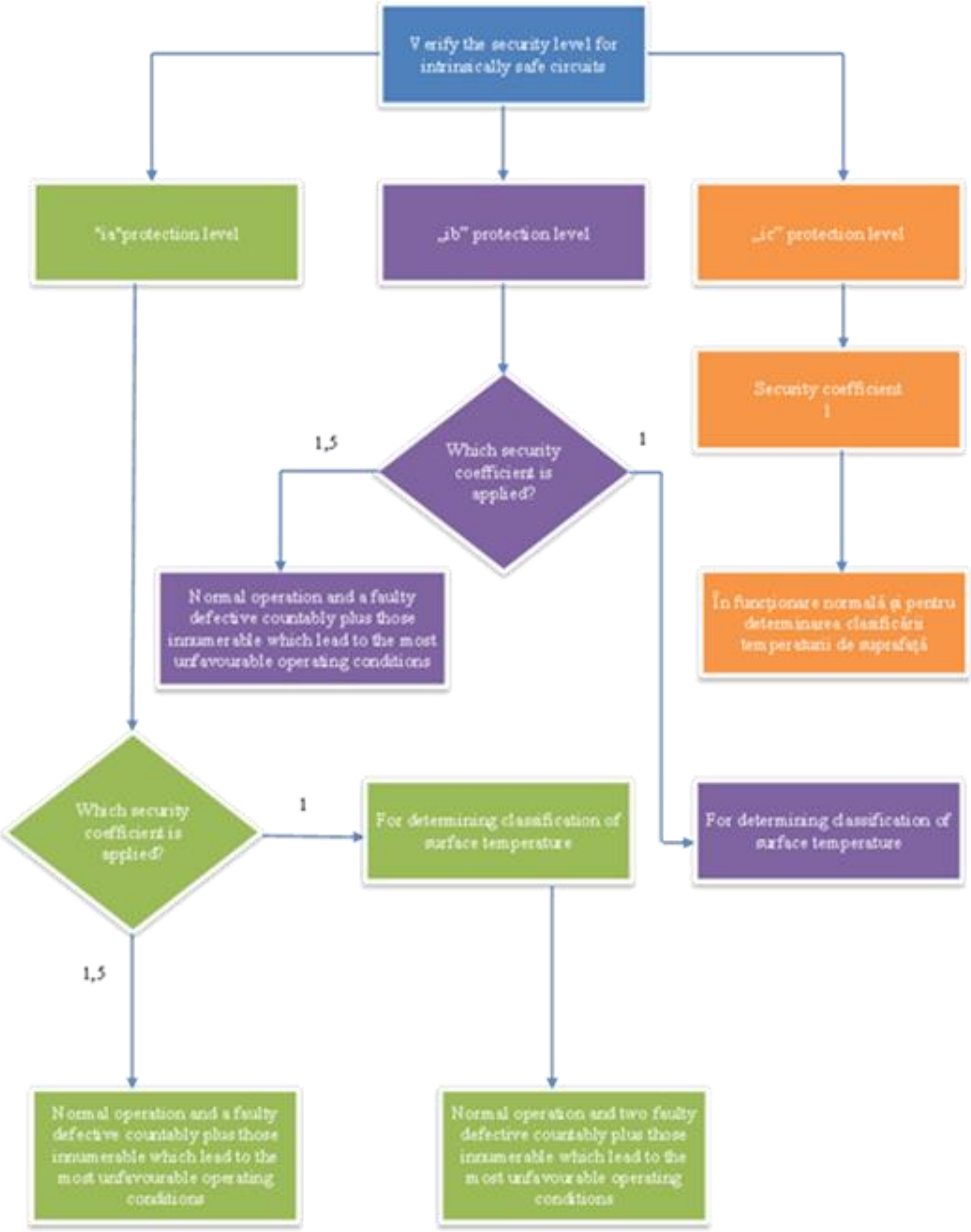

Fig. 6. Diagram of evaluation circuit with intrinsic safety "i"

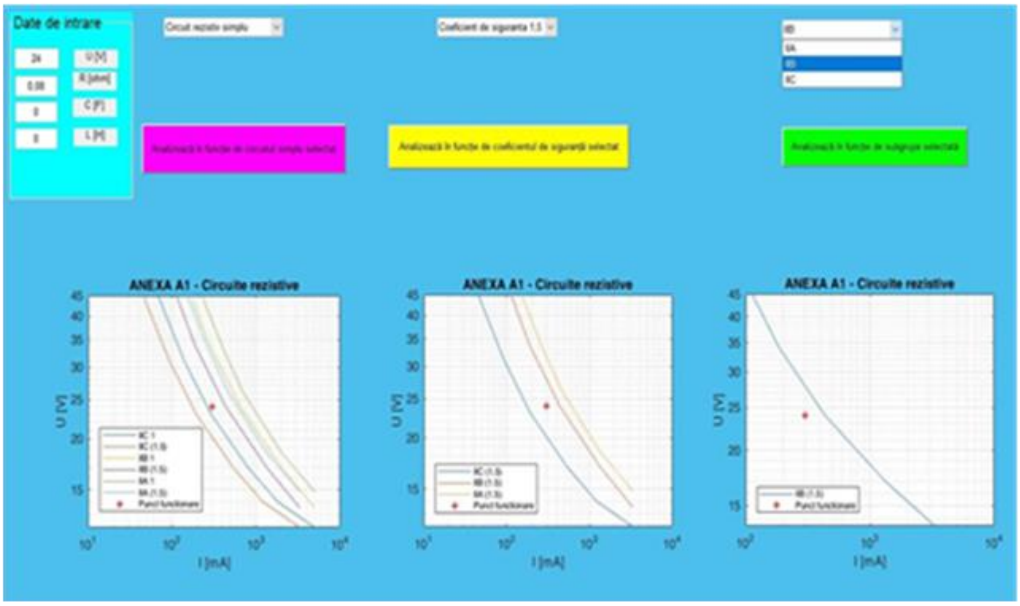

Fig. 7. The user interface of the application

3. CONCLUSIONS

1) This paper aims to increase the ability to evaluate intrinsically safe protection equipment by using the standardized means and the simulation based on the ignition diagrams within the equipment certification body to perform tests on low current equipment protected by the type of protection intrinsic safety intended for use in explosive atmospheres by implementing specific requirements

2) For simple circuits, especially those with a linear characteristic, it is possible to assess the non-ignition capability using the standardized means and the simulation based on the ignition diagrams.

3) The increased complexity for the circuits of the equipment involves in the evaluation process, the use of simplified models of circuits that are comprehensive in terms of explosion protection.

4) Joining the IECEx scheme for products certification has imposed the implementation of appropriate methods for assessing the low current circuits in testing laboratory infrastructure. This position involves maintaining a process of updating the procedures for conformity assessment and testing and suitability for carrying out the necessary tests required by the process.

5) Explosion prevention and explosion protection are of major importance for occupational health and safety in order to minimize losses (both human and material).

4. ACKNOWLEDGMENTS

This article uses the experimental results obtained within the project PN 18 17 02 01 of the „Nucleu" Program developed with the help of ANCSI.

REFERENCES

[1]. Burian S., Ionescu J., Darie M., Csaszar T., Andriş A., *Requirements for Installations in Areas with Explosive Atmosphere, Other than Mines, (in Romanian),* INSEMEX – Petrosani Publishing House, Romania, (2007).

[2]. Burian S., Ionescu J., Ghicioi E., Darie M., Moldovan L., Csaszar T.. *Influence of environmental conditions on test mixtures used for testing of equipment with type of protection intrinsic safety*, Proc. Science and technologies in geology, exploration and mining - SGEM 2014, Albena, Bulgaria, 16-22, June, 2014. 719-726, (2014)

[3]. Csaszar T., Pasculescu D., Darie M., Ionescu J., Burian S., *Method for assessing energy limited supply sources, designed for use in potentially explosive atmospheres*, Environmental Engineering and Management Journal, 11, 1281-1285, (2012).

[4]. Darie M., Ionescu J., Burian S., Csaszar T., Moldovan L, *Ignition probability assessment of low current circuits designed for use in explosive atmospheres*, Environmental Engineering and Management Journal, volume 11/2012, No.5, (2012).

[5]. EN Directive, ***Directive 2014/34/EU of the European Parliament and the Council*** *of 26 February 2014 on the harmonization of the laws of the Member States relating to equipment and protective systems intended for use in potentially explosive atmospheres,* Official Journal of the European Union, No L96/309, 29.03.2014, Brussels, (2014).

[6]. Grecea D., Burian S., Darie M., Csaszar T., Colda C., Andriş A., Pupăzan G., Moldovan L., *Issues concerning the requirements for the achievement of a spark test apparatus simulator for linear circuits,* 8th International Multidisciplinary Scientific Symposium SIMPRO 2018, 11-13 October 2018, Petroșani

[7]. Prodan M., Ghicioi E., Oancea D, *Correlation of explosion parameters and explosion-type events for preventing environmental pollution*, Environmental Engineering and Management Journal, 13, 1409-1414., (2014).

[8]. SR EN (IEC) 60079-11:2012. *Explosive atmospheres - Part 11: Equipment protection by intrinsic safety "i"*, ASRO, (2012). [7] R Core Team (2015). R: A language and environment for statistical computing. R Foundation for Statistical Computing, Vienna, Austria. URL http://www.R-project.org/.

REQUIREMENTS FOR TESTING AND VERIFICATION FOR BREATHING AND DRAINING DEVICES

MARCEL DANIEL RAD[1], SORIN BURIAN[2], MIHAI MAGYARI[3]
LUCIAN MOLDOVAN[4], DRAGOS FOTĂU[5], DIANA SĂLĂȘAN[6]

Abstract: The evaluation of explosion-proof electrical equipment for certification is particularly important given the risk of explosion and must be minimized. This in order to ensure the safety of life, health of workers, to prevent damage to goods and the environment when they meet the essential security requirements at European level.

Directive 2014/34 / EU states that equipment used in explosive atmospheres must be designed to operate without endangering the environment for which it is intended.

This paper proposes the study and evaluation of the requirements for the breathing and drainage devices. In order to verify explosion protection, the representative samples made available by explosion-protected equipment manufacturers are tested under the worst possible conditions that may occur in practice.

Keywords: Flameproof enclosure; explosion protection; breathing and draining devices; explosive atmosphere; permeable metallic materials.

1. INTRODUCTION

The paper deals with the study of the requirements for the testing of drainage and breathing devices used in electrical equipment with flameproof enclosures type of protection. Several studies have been conducted on the reliability of electrical equipment and installations.

[1] *Ph. D.Eng., scientific researcher, INDC-INSEMEX Petroşani*
[2] *Ph. D.Eng., scientific researcher I, INDC-INSEMEX Petroşani*
[3] *Ph. D.Eng., scientific researcher I, INDC-INSEMEX Petroşani*
[4] *Ph. D.Eng., scientific researcher I, INDC-INSEMEX Petroşani*
[5] *Ph. D.Eng., scientific researcher III, INDC-INSEMEX Petroşani*
[6] *Eng., scientific researcher , INDC-INSEMEX Petroşani*

Types of protection are all the specific measures applied to electrical equipment to avoid the ignition of an ambient explosive atmosphere.

According to Directive 1999/92/EC, users of technological installations in areas with explosive atmospheres have to follow successively three stages: preventing the formation of explosive atmospheres, avoiding the ignition of explosive atmospheres, limiting the harmful effects of an explosion to ensure the health and safety of workers [6].

2. REQUIREMENTS FOR DRAINAGE AND BREATHING DEVICES

2.1. General

Drainage and breathing devices are generally used for electric motors with a flameproof enclosure protection. For the design and construction of motors with a type of flameproof enclosure protection, it is necessary for the beneficiary to formulate precisely and in detail the requirements regarding the operation of the motors in accordance with the ATEX Directive [5].

Being designed to operate installations in explosive atmospheres (chemical industry, petroleum industry, mining industry, etc.), these engines are often built into the flameproof enclosure protection module, its outer part (case, shields, terminal box, clamping elements) having to withstand an internal explosion of an explosive mixture that penetrated the interior without suffering deformations and without transmitting the flame from the inside out to an explosive atmosphere surrounding the enclosure.

For this, it is necessary to have maximum admissible gaps at joints or other flamepaths, depending on explosion categories and subcategories [1]. The engines are distinguished by a robust mechanical construction, made in a wide range of constructive shapes normalized by the major manufacturers of electric machines. The external shape of the casing depends on the type of motor protection as well as on the cooling mode In the case of a closed machine equipped with an axial cooling system, the casing is constructed with ribs to increase the cooling surface. In the case of an internal cooling machine, the casing is smooth outside. [2]

Standard SR EN 60079-1 shows all types of possible joints encountered when making flameproof enclosures as well as joint parameter values. The standard also mentions the materials used for the enclosures.

3. BREATHING AND DRAINING DEVICES WHICH FORM PART OF A FLAMEPROOF ENCLOSURE

3.1. General

Breathing and draining devices shall incorporate permeable elements which can withstand the pressure created by an internal explosion in the enclosure to which they are fitted, and which shall prevent the transmission of the explosion to the explosive atmosphere surrounding the enclosure [3].

They shall also withstand the dynamic effects of explosions within the flameproof enclosure without permanent distortion or damage which would impair their flame-arresting properties. They are not intended to withstand continuous burning on their surfaces. [2]

These requirements apply equally to devices for the transmission of sound but do not cover devices for relief of pressure in the event of internal explosion, use with pressure lines containing gas which is capable of forming an explosive mixture with air and is at a pressure in excess of 1,1 times atmospheric pressure.[4]

3.2. Openings for breathing or draining

The openings for breathing or draining shall not be produced by deliberate enlargement of gaps of flanged joints [3].

The composition limits of the materials used in the device shall be specified either directly or by reference to an existing applicable specification.

The elements of breathing or draining devices for use in an explosive gas atmosphere containing acetylene shall comprise not more than 60 % of copper by mass to limit acetylide formation [3].

The dimensions of the breathing and draining devices and their component parts shall be specified.[4]

4. TYPE TESTS FOR BREATHING AND DRAINING DEVICES

4.1. General

Attachment of the sample device under test shall be made on the end of the test rig enclosure in the same manner as it would normally be mounted on a flameproof enclosure. The test shall be performed on the sample after the impact test. [3]

The impact test may be performed on the sample, separate from the test enclosure, when it is mounted on a plate that forms the end part of the test rig enclosure.

For devices with non-measurable paths, the maximum bubble test pore size of the sample shall be not less than 85 % of the specified maximum bubble test pore size. [3]

4.2. Bubble test

For bulloscopic verification of sintered materials, materials used for making drainage and breathing devices, is shown in Fig. 1.

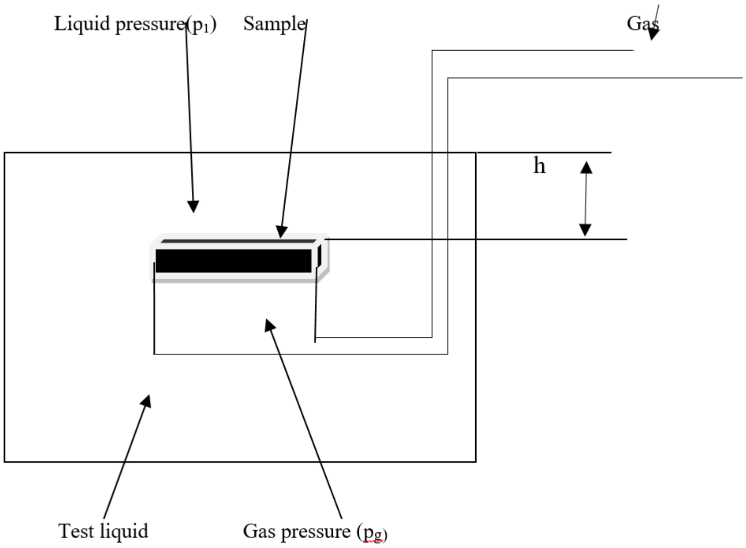

Fig. 1. Block diagram for buloscopic determination

The buloscopic hair size corresponds to the minimum differential pressure at which the first bubbles appear continuously. For this reason, this pressure is sometimes called the minimum bubble pressure or the first bubble. The appropriate capillary diameter is called maximum pore diameter or maximum pore size.

When the pressure exceeds the minimum burst pressure (the first bubble point), more bubbles appear on the sample. For a given aspect, the corresponding pressure can lead to the definition of a conventional pore size. [7]

4.3. Thermal tests

4.3.1. General

After the bubble test, breathing and draining devices as Ex components shall be subjected to the thermal tests based on the maximum intended flameproof enclosure volume, but no less than the volume of the test rig in Figure 2. [3]

Breathing and draining devices intended for multiple use in any single flameproof enclosure shall be tested additionally with the enclosure.

4.3.2. Test procedure

For enclosure volumes of less than or equal to 2,5 l, the test rig assembly with all four sections, as shown in Figure 2, shall be used, and the test procedure shall be carried out as follows [3]:

a) the position of the ignition source shall be at the enclosure inlet and 50 mm from the inside of the end-plate housing the device and the results observed;

b) the test mixtures shall;

c) the temperature of the external surface of the device shall be monitored during tests;

d) any device shall be operated as specified by the manufacturer's documentation. After each of five tests, the explosive mixture shall be maintained external to the device for a sufficient time to allow any continuous burning on the face of the device to become evident, for at least 10 min, so as to increase the temperature of the external surface of the device or to make temperature transfer to the outer face possible; and

e) the tests shall be carried out five times for each gas mixture for the gas groups in which the device is intended for use.

For enclosure volumes of greater than 2,5 l, a representative enclosure of the intended volume shall be used, and the test procedure shall be carried out as follows [3]:

- the test mixtures shall, as appropriate;
- the temperature of the external surface of the device shall be monitored during tests;
- any device shall be operated as specified by the manufacturer's documentation.

After each of five tests, the explosive mixture shall be maintained external to

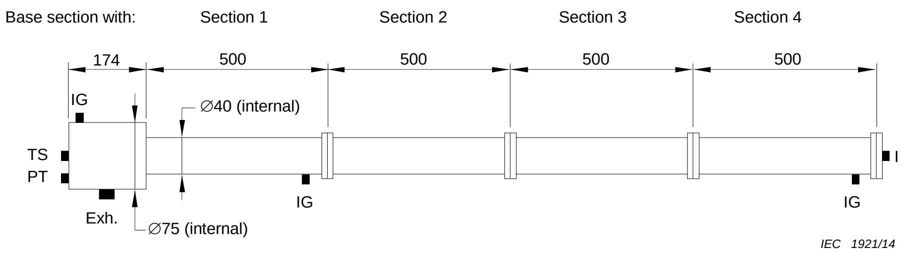

Fig 2. Component test rig for breathing and draining devices

the device for a sufficient time to allow any continuous burning on the face of the device to become evident, for at least 10 min, so as to increase the temperature of the external surface of the device or to make temperature transfer to the outer face possible; and the tests shall be carried out five times for each gas mixture for the gas groups in which the device is intended for use. [3]

4.3.3. Acceptance criteria

During the thermal tests, no flame transmission shall occur and no continuous burning shall be observed. The device shall show no evidence of thermal or mechanical damage or deformation which could affect its flame-arresting properties [3].

The measured external surface temperature rise of the device shall be multiplied by a safety factor of 1,2 and added to the maximum service temperature of the device for the determination of the temperature class of the electrical equipment.

4.4. Test for non-transmission of an internal ignition

4.4.1. General

After the bubble test, this test shall be carried out on a standard test rig, as illustrated in Figure 2, with the following additions and modifications [3].

4.4.2. Test procedure

The position of the ignition source shall be as shown in Figure 2:

a) at the inlet end; and
b) at 50 mm from the inside of the end-plate housing the device.

For the purposes of the test, the test rig shall be assembled for each gas group, in accordance with Figure 2, and have the following number of sections:

–Group I and Group IIA: one section of test rig assembly;
–Group IIB and Group IIC: four sections of test rig assembly.
–The gas mixture within the test rig enclosure shall be ignited and the tests shall be made five times at each ignition point.
–For breathing and draining devices of Groups I, IIA and IIB having either measurable paths or non-measurable paths.
–For breathing and draining devices of Group IIC with measurable paths,.

For breathing or draining devices of Group IIC with non-measurable paths.

4.4.3. Acceptance criteria

During the test, no ignition shall be transmitted to the surrounding test chamber [2].

4.5. Test of the ability of the breathing and draining device to withstand pressure

4.5.1. Test procedure

The reference test pressures in each gas group are:

Group I	1 200 kPa,
Group IIA	1 350 kPa,
Group IIB	2 500 kPa,
Group IIC	4 000 kPa.

For the purpose of the test, a thin flexible membrane is fitted over the inner surfaces of the breathing and draining devices. The reference pressure shall be one of the relevant pressures given above for the gas group for which the component is intended [2]. One of the following overpressure tests shall be applied:

- 1,5 times the reference pressure for a period of at least 10 s. Then each component shall be submitted to a routine test; or
- 4 times the reference pressure for a period of at least 10 s. If this test is successful, the manufacturer is not required to apply the routine test to all future components of the tested type.

4.5.2. Acceptance criteria

After the overpressure tests, the device shall show no permanent deformation or damage affecting the type of protection.

4.6. Ex component certificate [3]

The Ex component certificate shall include, in the schedule of limitations, the details necessary to properly select a breathing or draining device for attachment to a type tested flameproof enclosure. The schedule of limitations shall include, as a minimum, the following:

a) the maximum recorded surface temperature obtained during the type test corrected to 40 °C, or to the higher marked ambient;

b) service temperature range for non-metallic enclosures and non-metallic parts of enclosures;

c) the maximum permitted enclosure volume (based on the thermal test) if greater than 2,5 l;

d) a requirement that each Ex component or package of Ex components be accompanied by a copy of the certificate, together with the manufacturer’s declaration stating compliance with the certificate conditions, and confirmation of the material, maximum bubble test pore size and minimum density, where applicable; and special mounting instructions, if any.

5. CONCLUSIONS

As a result of the work titled: “Requirements for testing and verification for breathing and draining devices", the following conclusions were drawn:

- the requirements of standard SR EN 60079-0 for electrical equipment used in explosive environments have been analyzed;
- the requirements of standard SR EN 60079-1 for drainage and breathing devices have been analyzed;
- the requirements of standard SR EN 60079-1 have been analyzed regarding the necessary tests to be performed on drainage and breathing devices;

- the test requirements for the drainage and blowing devices in bulk, correlated with the other specific tests to which the equipment is to be subjected, have been presented in the paper, establishing the order of the tests in accordance with the specific standard;
- the components required to achieve the test bench for the pressure and non-explosion test for the drainage and blowing devices have been established;
- the required components for the test stand were prepared for the buloscopic test of drainage and breathing devices;
- the block diagram of stalls for pressure, explosion-proof and buloscopic test stands that meet the test requirements specified in the standard.

Acknowledgements

This work is part of the Core Program: "Researches for the development of evaluation capacity, testing of technical equipment for use in explosion risk areas and protective equipment" - PN 18 17 02 01.

REFERENCES

[1]. Rad M., *Increased reliability of electrical equipment used in explosive environments*, Doctoral Thesis, March, (2018).

[2]. Rad Marcel Daniel s.a. *Study and evaluation of requirements for breathing and draining devices*- SIMPRO 2018.

[3]. Romanian Standard, S**R EN 60079-1** *Explosive atmospheres - Part 1: Equipment protection by flameproof enclosures "d"*, Romanian Association for Standardization – ASRO, Bucharest, Romania, (2015).

[4]. Romanian Standard, SR EN 60079-0 *Explosive atmospheres - Part 0: Equipment – General requirements*, Romanian Association for Standardization – ASRO, Bucharest, Romania, (2013).

[5]. Directive 2014/34/EU *Of the European Parliament and of the Council of 26 February 2014 on the harmonization of the laws of the Member States relating to equipment and protective systems intended for use in potentially explosive atmospheres (recast)* Text with EEA relevance, (2014).

[6]. Directive 1999/92/EC *Of The European Parliament And Of The Council of 16 December 1999 on minimum requirements for improving the safety and health protection of workers potentially at risk from explosive atmospheres* (15th individual Directive within the meaning of Article 16(1) of Directive 89/391/EEC), (1999).

[7]. Standard SR EN 24003 -1996 - *Permeable sintered metallic materials*. Determination of pore size, (1996).

Annals of the University of Petrosani, Electrical Engineering, 20 (2018)

DETERMINATION OF THE INFLUENCE OF JAW MOVEMENT FREQUENCY OF JAW CRUSHER ON ENERGY CONSUMPTION

TEODORA HRISTOVA[1], ANGEL YANEV[2], NIKOLAY SAVOV[3]

Abstract: In the paper, in accordance to the theory, it is shown that the relative energy consumption of a jaw crusher depends on the average diameter of the material entering the crusher and the width of the discharge port. An experimental study has shown that the energy consumption depends also on the frequency of the jaw swing. In the study a jaw crusher with a complex swing of a moving jaw is used and it is driven by an asynchronous motor with a squirrel-cage rotor. The rotational speed of the asynchronous motor is controlled by an inverter, and this frequency determines the swing frequency of the jaw. A statistical model developed in the middle of the STATGRAPHICS program demonstrates the influence of the rotation speed of the engine driving the crusher.

Keywords: jaw crusher, asynchronous engine, energy consumption, particle size distribution, discharge port, jaw movement frequency.

1. INTRODUCTION

The new standard EN 50160 replaces the previous one from 1980 - BDS 10 694-80, which introduces stricter criteria for energy quality indicators. The aim is to reduce electricity consumption and to increase its quality compared to the previous one, which is active in Bulgaria. Also, in accordance to the 1972 Rome Club Agreement, it is necessary to abide by the criteria for sustainable development in all sectors. In the mining industry, one of the most energy intensive objects is the crusher. For the implementation of the legal norms it is necessary to determine the factors that affect energy consumption. To determine the factors affecting the energy consumption of the crusher, it is necessary

[1] *PhD., Associate Professor, Eng., University of Mining and Geology "St. Ivan Rilski" -Sofia,* teodora@mgu.bg
[2] *Assistant Professor, Eng., University of Mining and Geology "St. Ivan Rilski"-Sofia,* angel.yanev@mgu.bg
[3] *Assistant Professor, Eng., University of Mining and Geology "St. Ivan Rilski"-Sofia,* nsawow@abv.bg

first to clarify the mechanism of crushing the ore and the method of determining the productivity.

2. THEORETICAL DETERMINATION OF THE OPTIMAL ANGULAR VELOCITY OF THE ECCENTRIC SHAFT OF JAW CRUSHERS

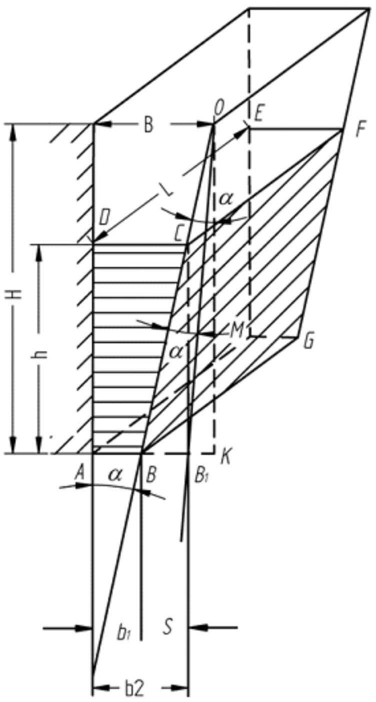

Fig. 1. Unloading the produced stuff from a jaw crusher at an optimum eccentric shaft rotation speed

Fig. 1 shows a drawing of a jaw crusher with an eccentric shaft. When the moving jaw is removed from the static [4], the crushed product is freely discharged through the disharge port of the crusher under its own weight. With each move of the jaw, only ore pieces located below the level of the CD surface can fall. At this level, the width of the crushing chamber at the time of completion of the working stroke is equal to the width of the crushing disharge port of the crusher at maximum movement of the swinging jaw. The disharged material is located in the ABCDEFGM prism volume. The size of the ore fragments present in the volume of this prism may be larger or smaller than the minimum width of the discharge port. If the size of ore fragments is larger, it can be assumed that this is as a result of the limited time of unloading the crushed material constituting half a turn of the eccentric shaft.

The time for one move of the jaw must be sufficient to pass the crushed ore fragments under their own weight to the horizontal level *CDEF* located at a height *h*. The time for one swing of the jaw is equal to the half stroke of the eccentric shaft. It is given by the mathematical equation:

$$\boldsymbol{t = \frac{1}{2}\frac{60}{n} = \frac{30}{n}, s} \qquad (1)$$

where *n* is the eccentric shaft rotation speed, $\boldsymbol{min^{-1}}$. In accordance to the law of the free fall of bodies, the path *h* is determined by the dependency: $\boldsymbol{h = \frac{1}{2}gt^2}$ from which it follows that

$$\boldsymbol{t = \sqrt{\frac{2h}{g}}}, \qquad (2)$$

where *g* is the acceleration of the earth, *m/s*^{2}.

Equalizing the equal parts of (1) and (2) for *n* the result is:

$$\boldsymbol{n = 30\sqrt{\frac{g}{2h}}\,min^{-1}} \tag{3}$$

The height *h* is calculated from the rectangular triangle BB_1C.

$$\boldsymbol{h = \frac{s}{tg\alpha} = \frac{b_2 - b_1}{tg\alpha}, m.} \tag{4}$$

By replacing the right part of (4) in (3) the result for *n* is:

$$\boldsymbol{n = 30\sqrt{\frac{g.tg\alpha}{2(b_2 - b_1)}} = 30\sqrt{\frac{g.tg\alpha}{2s}}, min^{-1}} \tag{5}$$

where: $\boldsymbol{\alpha}$ - is the angle of gripping; $\boldsymbol{b_1}$- the minimum width of the discharging port, *m*; $\boldsymbol{b_2}$- the maximum width of the discharging port, *m*; *s*- swing of the moving jaw, m.

The resulting revolutions are called theoretical. The actual revolutions will be obtained by entering a correction coefficient:

$$\boldsymbol{n_{Д} = k_1 n, min^{-1}} \tag{6}$$

where: $\mathbf{n, min^{-1}}$ is the theoretical rotation speed of the eccentric shaft; $\mathbf{k_1 = 0,75 \div 0,9}$ - a friction coefficient between the crushed product and the crushing plates.

3. DETERMINING THE PRODUCTIVITY OF THE JAW CRUSHER

The bulk of the crushed product that is unloaded for one turn of the eccentric shaft at optimum rotational speed is equal to the prism volume *ABCDEFGM* (fig.1). Taking into account this volume, the material with reduce size of the crusher is calculated:

$$\boldsymbol{Q_v = 60k_1k_pnV = 60k_1k_pn \frac{(b_2+b_1)(b_2-b_1)}{2tg\alpha} L, m^3/h} \tag{7}$$

where: *L*,*m* is the length of the crusher receiving port; $\boldsymbol{k_1}$ is a coefficient for the crusher type. For crushers with simple swing of the jaw $\boldsymbol{k_1 = 1}$, and for crushers with complex swing $\boldsymbol{k_1 = 1,2}$; $\boldsymbol{k_p}$ - a coefficient of bulk density of the ore. The mass productivity is calculated by considering the density of the ore:

$$\boldsymbol{Q = \rho . Q_v, t/h} \tag{8}$$

where $\boldsymbol{\rho, t/m^3}$ is the density of the crushed product.

4. DETERMINING THE ENGINE POWER OF THE JAW CRUSHER

The load of the engine when operating a jaw crusher depends on many factors, some of which cannot be identified. This explains why no precise theoretical formula has been created until now, that will make be possible to determine the driving power of the crushers. The required power of the Alice-Chalmer crushers, for example, is determined in accordance to the Bond hypothesis using the Bond index [4]. It represents the relative energy absorption of ores and is determined on the basis of experimental results. In accordance to the theory of Bond, the energy consumed for crushing a ton of ore will be:

$$\boldsymbol{W} = \boldsymbol{k}_{\text{СТ}}\left(\frac{\mathbf{10}\boldsymbol{w_i}}{\sqrt{\boldsymbol{b}}} - \frac{\mathbf{10}\boldsymbol{w_i}}{\sqrt{\boldsymbol{D}}}\right), \boldsymbol{kWh/t} \tag{9}$$

where: $\boldsymbol{w_i}$ is the Bond index, $\boldsymbol{kWh/t}$; *b* - the dimensions of the square holes of the sieve through which 80% of the finished product passes or the width of the discharge port of the crusher, *m*; *D*- the dimensions of the square holes of the sieve through which 80% of the product entering the crusher or the average diameter of the class fraction entering the crusher port, *m*; $\boldsymbol{k}_{\text{СТ}}$ - the crushing stage coefficient. For crushing the big class fractions $\boldsymbol{k}_{\text{СТ}} = \mathbf{0,75}$.

Then the equation for crushing power is:

$$\boldsymbol{N}_{\text{ДВ}} = \frac{\boldsymbol{W}.\boldsymbol{Q}}{\mathbf{1000}\boldsymbol{\eta}_{\text{М}}}, \text{kW} \tag{10}$$

where $\boldsymbol{\eta}_{\text{М}} = \mathbf{0,85} \div \mathbf{0,88}$ is the mechanical efficiency of the asynchronous motor of the crusher.

5. DETERMINING THE RELATIVE ENERGY CONSUMPTION OF THE JAW CRUSHER

In accordance to the reviewed theory, the relative energy consumption can be determined by the formula:

$$\boldsymbol{E} = \frac{\boldsymbol{N}_{\text{ДВ}}}{\boldsymbol{Q}} = \frac{\boldsymbol{W}}{\mathbf{1000}\boldsymbol{\eta}_{\text{М}}} = \frac{\boldsymbol{k_{CT}}}{\mathbf{1000}\boldsymbol{\eta}_{\text{М}}}\left(\frac{\mathbf{10}\boldsymbol{w_i}}{\sqrt{\boldsymbol{b}}} - \frac{\mathbf{10}\boldsymbol{w_i}}{\sqrt{\boldsymbol{D}}}\right), \boldsymbol{kWh/t} \tag{11}$$

The conclusion from the above discussed theory is that the energy consumption depends only on the parameters: *D*, *b* and the type of crushed product but does not depend on the eccentric shaft revolution.

6. EXPERIMENT

6.1. Experiment Planning

The purpose of the experiment is to determine the effect of the speed of the engine on energy consumption. The following input parameters are defined and they will change:

1. The average diameter of the class fraction entering the crusher - $\boldsymbol{D}, \boldsymbol{mm}$. Prior to the experiment, some material with the following 50, 40 and 30 mm class fraction was selected and pre-sieved. They are compliant with the width of the feed port of the crusher [3].
2. The width of the discharge port of the crusher - $\boldsymbol{b}, \boldsymbol{mm}$. The width of the discharge port has the following values: 8 ,12,16 and 19mm. The parameter has also been selected in accordance to the dimensions and capabilities of the laboratory machine.
3. The frequency of rotation of the asynchronous motor f, Hz. The following frequencies were selected: standard - 50 Hz, reduced 40 Hz and 30 Hz. At lower frequencies of 25 Hz it was found out that the feed port of the crusher has been obstructed.

The relative power consumption as a target function is obtained through the ratio of the average crusher engine power measured by the measuring and recording device per unit time - $\boldsymbol{E}, \boldsymbol{Ws/g}$.

Homogeneous material is delivered continuously during the measurement [1]. During the experiment, the values *D, mm*, - *b, mm* and *f, Hz* were changed. The following parameters are measured in the experiment:

- $\boldsymbol{M_{CYM}}, \boldsymbol{g}$ - the weight of the crushed material;
- $\boldsymbol{P_1}, \boldsymbol{W}$ – the average power of one phase of the engine;
-$\boldsymbol{t}, \boldsymbol{s}$- time to crush the sample.

6.2. Description of the experimental pattern

The experiment was made with a laboratory jaw crusher with complex swing of a moving jaw driven by an asynchronous motor with a squirrel-cage rotor with the power of 2.2kW. The frequency of the stator voltage is regulated by the Electroinvent ELDI / B -2.2k / 380V frequency PWM inverter. The three-phase digital multi-function, AC powermeter of SATEC PM130EH is used as a measuring instrument.

6.3. Results

It is necessary to create a mathematical model for determining the function of the energy consumption, which depends on the values of the measured parameters: the inverter frequency, the average diameter of the class fraction entering the crusher and the width of the discharge port of the crusher. This model will take into account the real statistical properties of the dependencies in the object. In this case, it is appropriate to make a non-deterministic, rather than a statistical model [2], because we consider the change in a number of factors such as the engine power and the engine speed, the engine load. The calculation of the data from the experiment was done by statistical analysis [2, 5] through the STATGRAPHICS program. This is a program that finds out the proper target function for minimum energy consumption according to the frequency inverter settings. The program has synthesized energy consumption patterns, and the adequacy of the model is proved by the following criteria: Student's t-criterion, the P -criterion, the

F-criterion, the multiple correlation criterion, the corrected multi-correlation coefficient and the mean absolute error. The actual value of the evaluated parameter is in the so-called trusted interval. The importance of the individual criteria is as follows:

- The P-criterion determines the trusted probability and its value should be less than 0.05;

- Student's t-criterion determines the significance of the coefficients for certain degrees of freedom, which in this case should be more than 8;

- the F-criterion shows the influence of the controllable factors on the output parameter and the aim is that its value be high, i.e. the energy consumption is manageable.

-the $\boldsymbol{R^2}$ и $\boldsymbol{R^2_{(adj)}}$ are the criteria for the multiple correlation and the multiple correlation coefficient. They provide information for the extent of the relationship between the output parameter and the functions included in the model, as well as the adequacy of the resulting model.

Table1. ***Values of model parameters***

model	$\mathbf{R^2}$, %	$\mathbf{R^2_{(adj)}}$, %	P-ratio- b	P-ratio -	P-ratio	F-ratio
M 1	94,743	94,042	b -0,491	D - 0,743	f- 0,001	90,12
M 2	95,583	95,245	D*b–0,1.10^{-3}	Constant - 0	f- 0,025	139,7
M 3	30,872	21,655	D/b - 0,024	Constant-0,015	f- 0,921	3,35
M 4	86,509	85,666	D/b - 0,358	Constant - 0	f -0,1.10^{-3}	51,3
M 5	94,569	94,229	b - 0,1.10^{-3}	Constant - 0	f -0,277	139,31
M 6	89,552	88,899	D/b - 0,067	Constant - 0	sqrt(f) - 0	68,57
M 7	89,307	88,639	D -0,084	Constant - 0	sqrt(f)-0,502	66,82
M 8	94,498	94,154	b – 0, 3.10^{-3}	Constant - 0	sqrt(f)-0,322	137,42
M 9	46,131	42,764	f/b – 0,001	Constant - 0	---	13,70
M 10	61,256	61,256	f/D - 0,1.10^{-3}	Constant - 0	--------	26,88
M11	87,021	87,021	b/f- 0	Constant - 0	--------	113,99
M12	91,233	90,685	b/f - 0,06	Constant - 0	D - 0,0136	83,25
M13	89,494	88,837	D -0,029	Constant - 0	f -0,395	68,15
M14	81,826	81,826	D/f	Constant - 0	--------	76,54

Different models were obtained after examining the dependencies determined by the STATGRAPHICS program. The basic values of the parameters of all models are given in Table 1. Various models have been obtained from the statistical surveys, most of them having good correlation values - $\mathbf{R^2}$ (e.g., 94.743% for M1, or 94.57% for model M5), and the corrected multiple correlation coefficient $\boldsymbol{R^2_{(adj)}}$ (e.g., 94.0425% for M1 or 94.2298% for M5). These coefficients are at the border value of the recommended 95%. The drawback of the models is that the trust P-criterion has high values (P-criterion = 0.77437 for the D parameter in model M1 or P criterion for the f parameter -0.277). These values for the cited models are above the critical one, i.e. it can be assumed that these models are inadequate.

Based on the model data in the table, it can be determined that M2 has the best parameters.

Table 2. ***M2 model parameters***

Parameter	**Estimate**	**Standard Error**	**T statistic of Student**		**P-Value**
constant					
D*b	2,21432E-05	4,33642E-06	5,10633		0,0001
f	0,000152824	6,18155E-05	2,47226		0,025
	Sum of Squares	*Df*	*Mean Square*	*F-Ratio*	P-Value
Model	0,00676644	3	0,00338322	139,7	0
Residual	0,000387475	27	2,42172E-05		
Total	0,0071539	30			
R-squared				95,5837%	
R-squared (adjusted for d.f.)				95,2452%	
Standard Error of Est				0,0049211	
Mean absolute error				0,00396103	
Durbin-Watson statistic				2,33315	

The $\boldsymbol{R^2}$ correlation coefficient of M2 is 95.5837% and the corrected multiple correlation coefficient $\boldsymbol{R^2_{(adj)}}$) is 95.2452% (Table 2). The recommended multiple correlation coefficient is 95% and can therefore be accepted as a proper. The value of the trust probability indicator (P-criterion = 0.0001 and 0.025) for the model is below the critical one and the model can be assumed to be adequate. The model with natural variables to be:

$$\mathbf{E} = \mathbf{0,0000221432 * D * b + 0,000152824 * f} \quad \mathbf{, KWh/t} \tag{12}$$

This is the model for which the frequency inverter should be set at certain parameters of the class fraction of input ore and the width of the discharge port. For the same study, more accurate models with a higher correlation coefficient can be obtained with more experiments (more than 30). In a previous study [3] it has been found out that the function of the energy consumption depending on the size of the input pieces and the width of the discharge port is:

$$\mathbf{E = 2,8310^{-3}\frac{D}{b}, KWh/t} \tag{13}$$

In the present study, this dependence was not confirmed - M3, M4 and M6. The reason is that in this case there is a complex interaction of three factors. Thus, when adjusting the frequency of the engine speed, the result will be changes of the time for crushing the material and hence its load. Therefore, in the statistical surveys, a connection was sought for between the individual parameters. From the results, it can be concluded that the width of the crusher discharge port is directly proportional to the energy consumption (M8, M9 and M11). Also, the diameter of the pieces entering the crusher - M7, M10, M13 and M14 is also directly proportional to the energy consumption.

7. CONCLUSIONS

The results obtained from the measurements and the statistical analysis for the relative energy consumption of the crusher show the following:

- the relative power consumption is influenced largely by the three parameters, namely the diameter of the input pieces, the width of the discharge port of the crusher and the rotation speed of the engine;
- the relative energy consumption of the asynchronous motor increases as the diameter of the input pieces increases. The reason is most likely that larger pieces of material increase the degree of crushing, which increases the power needed to crush the material;
- when reducing the width of the discharge port of the crusher, the relative energy consumption due to the increase in the crushing rate is also increased.
- when reducing the swing frequency of the jaw, the crusher decreases the relative energy consumption due to the increase in the crush chamber discharge time and reduces the engine load.

For future research, the team aims at measuring and detecting the presence of harmonics in regulating the engine speed through a frequency inverter. The presence of harmonics leads to a distortion of the sine wave of the supply current. Thus, through control of the energy consumption by means of the frequency swing of the jaw, it is possible to generate harmonic constituents above the allowed ones in the standard. The experiment data will be useful in finding an appropriate target function for the control of the frequency inverter.

Acknowledgements This research was supported by the Ministry of Education and Science through the Project" Energy Quality Test for Asynchronous Motor Operation, Driving Crusher", contract 155/2018).

REFERENCES

[1]. Ackerman Yu, G. Bukats, V. Olevskyi et al., *Reference Book on Processing Rough, Moscow*, Nedra, 1982.

[2]. Bojanov E. S., Ivan N. Vuchkov, *Statistical Decisions in Production and Research*, Sofia, Technika, 1979.

[3]. Hristova T., Minin I., D. Mitev, *Determination of relative energy consumption of a jaw crusher in depending on the width of the discharge port and the particle size distribution of the crushing product*, Journal of Mining and Geological science, 61s, part Mechanization, Electrification and Automation in Mines, 2018, p.13-17, ISSN 2535-1192.

[4]. Minin I.S., *Technique and Technologies for Processing of Minerals - I part*, Avangard Prima, Sofia, 2012.

[5]. Nalimov, V.V., I.A. Tchernova, *Statistical Methods Planning*, Exploratory, Moscow, Science, 1965.

Annals of the University of Petrosani, Electrical Engineering, 20 (2018)

THE USE OF LIDAR TECHNOLOGY IN THE MANAGEMENT OF CAR TRAFFIC IN URBAN AREAS

NICOLAE PĂTRĂȘCOIU[1], COSMIN RUS[2], CECILIA ROȘULESCU[3], GABRIEL ILCEA[4], NICOLETA NEGRU[5]

Abstract: In this paper we propose a solution to realize a mobile system for traffic management by counting the vehicles on a road with one or two lanes. The traffic intensity is measured using the transducers based on lidar principle. The acquired data are local stored into a local data logger and simultaneous are transmitted via radio communication to a dedicated server. The novelty of this system is represented by the communication facility provided by the new LoRa technology. System performance is evaluated by field tests and simulations. Based on the analyzes and evaluations, some solutions for monitoring and controlling processes are proposed using this communications infrastructure. Also, it is highlights that this system is mobile and it is not invasive on the road structure.

Keywords: LoRa, data acquisition, non-invasive technology, urban traffic management, LabView.

1. INTRODUCTION

In recent decades there has been a steady increase in the number of private cars in traffic, while public transport is steadily declining. The current road infrastructure no longer meets the demands. Accidents and congestion caused by traffic have an important impact on life, reduce productivity and reduce energy. Traffic congestion, which causes environmental problems and accidents, is becoming increasingly acute. The benefits of transport are diminished by the increasing number of negative impacts (air pollution and accidents, increased stress on road users), resulting in a vicious circle in urban transport. The spectacular increase in road traffic can't be met in the short term by a corresponding increase in road space. For this reason, in all developed economic environments, two-directional solutions were dealt with: improving the design of road space to increase utilization and improving the parameters of the traffic through control and monitoring.

[1] *Ph.D., Associate Prof. Eng., University of Petroşani, nicolaepatrascoiu@upet.ro*
[2] *Ph.D. student., Eng., University of Petroşani, cosminrus@upet*
[3] *Professor, Grigore Geamănu School*
[4] *Ph.D., Eng., Energy Complex Hunedoara*
[5] *Ph.D. student, University of Petroșani*

Developing an intelligent transport system requires the collection of high-quality and real-time information about the traffic flow. Increasing pressure to improve the traffic management, the collection of traffic data methods has evolved considerably, and the access to real-time traffic information becomes usual. [11],[5]

For planning the road development or the management of traffic it is very important to collect the traffic data and use them in anticipation of traffic volume. The traffic flow can be considered as a function having a random distribution because it differs from many parameters including the time of day for measurement, season, geographical position, environmental conditions. It follows that the data collected is a methodological statistic and, despite such complexities, it follows some well-defined models that can be classified and analyzed. Thus, the collection of traffic data can be done in different ways and plays an important role in the evaluation and management of road networks.[7] Generally, the traffic flow consists of vehicle count on the road and the technologies used for this can be split into two categories: the intrusive and non-intrusive.

The intrusive methods consist of transducers which are placing on or in the road and a data recorder. The most usual transducer used in intrusive methods are: pneumatic road tubes, piezoelectric and almost inductive loops. For all of them, it is necessary to bury in the construction layers of the road, becoming fixed or permanent installation.

The non-intrusive techniques are based on the remote data recording. Eliminating the manual counting that is often used, new technologies use transducers based on passive and active infrared, microwave radar, ultrasonic and passive acoustic, or video image detection.

2. LIDAR SENSORS

To achieve the system, Lidar sensors have been selected due to their features, such as influence reduced of the dust or ambient light, the operation is not influenced by the color or optical transparency of the reflective surface.

Small dimensions and low power consumption make this sensor ideal for projects where energy sources are batteries and energy consumption should be as low as possible. The sensor can be used for drones, robotics, 3D image scanning, collision avoidance, fluid / solid level measurement, medical imaging and more. This device measures the distance by calculating the delay between transmitting an infrared laser signal and receiving it after reflecting at a target meeting. This delay translates away using the known lightning speed. The sensor transmits through the laser beam a coded signature and searches for that signature in the reflection of the signal, allowing for an extremely efficient detection. Signal processing techniques are used to achieve high sensitivity, speed and accuracy using a low power source and a low-cost system. [8]

To perform a measurement, this sensor first performs a receiver polarity correction, correcting the change of ambient light level and allowing maximum sensitivity. Then the device sends a reference signal directly from the transmitter to the receiver. Store the transmission signature, set the delay for the "zero" distance and recalculate this delay periodically after several measurements.

Then the device initiates a measurement by making a series of data acquisitions. Each acquisition is a transmission of the main laser signal while recording the return signal to the receiver. If there is a signal match, the result is stored in memory as a correlation record. The next purchase is summed up with the previous result. When an object at a certain distance reflects the laser signal back to the device, these repeated acquisitions cause a peak of signal coming out of the "noise" area at the corresponding location of the distance from the correlation record.

The device integrates purchases until the peak of the correlation record signal reaches a maximum value. If the returned signal is not strong enough for this to occur, the device stops from making purchases.

The signal strength is calculated from the magnitude of the signal recording peak and from a valid signal, the reference threshold is calculated from the noise level. If the tip is above this threshold, the measurement is considered valid and the device will calculate the distance, otherwise it will report 1 cm. From the next measurement, the sequence is resumed.

At startup or reset, the device performs a self-test sequence and initializes all registers with the default values. Approximately 22 ms the distance can be taken with the I2C interface.

This device has a serial interface compatible with I2C. It can be connected to an I2C bus as a slave device under the control of an I2C master. The I2C circuit works internally at 3.3 V. An internal level switch allows the device to run at a maximum of 5 V. The 3k ohm pull-up internal resistances provide this functionality and allow easy use and easy connection to the I2C host. The device has a 7-bit slave address with a default value of 0x62. After initializing the system, the most significant bit of the I2C address byte is set to automatically increment the register address with successive reads or writes in a transfer data block. This is commonly used to read the two bytes of a 16-bit value in a single transfer and is used in the following example.

The hardware structure of the mobile system is represented in Fig. 1 and consists of the following:

- Arduino Uno/Nano development board;
- Lidar Lite v3 sensor connected to Arduino digital inputs;
- ESP32 a low-power system on a chip (SoC) with Wi-Fi and dual mode Bluetooth capabilities, that is connected to the Arduino between a serial communication bus;
- A simple local LCD display also connected to the Arduino between a serial communication bus;

The LiDAR sensor will be connected according to the technical specifications to the Arduino module either using an I2C connection or using a PWM connection. [6] The ESP32 will connect to Arduino using a serial connection and will allow the retrieved information to another module or to a LoRa gateway. The LCD display allows you to display information on the number of vehicles on a traffic arc, thus testing the entire system to the specified parameters. The entire system will be powered either from the power grid where it is possible or from an external battery in case of necessity. In the future, it is also desirable to create a power system using other types of renewable energy. ESP32 module allows communication using wireless communication protocol LoRa and so these modules can be integrated simply in any equipment regardless of its physical size tends to be minimized and a more reliable all components.

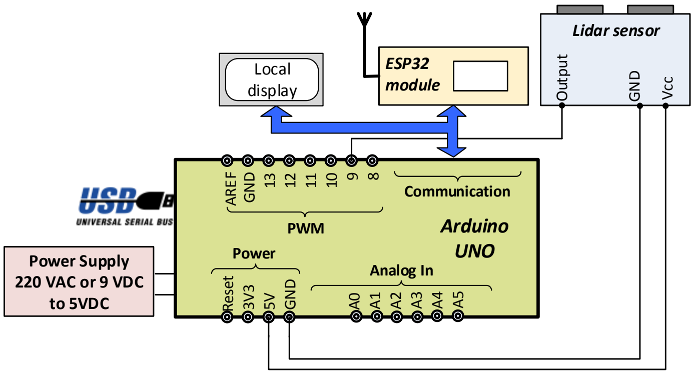

Fig. 1. Hardware structure diagram

For this system the supply voltage is provided from an alternative voltage source or from a battery through the 5 VDC controller on the Arduino board. In this way, the autonomy of the system can be assured. The monitoring system using a Lidar sensor, in addition to allowing for special portability, also ensures a fast and secure acquisition of data in traffic management (the number of machines crossing an intersection, their speed, and distance measurements). Laser scanning of the Lidar type has other applications in many areas of activity. LiDAR laser scanning provides an interactive topographic map with a height accuracy of up to 20 cm. Current data has an accuracy of up to 1.5 m. As a complement to topographic measurements, technology can be used to build roads, other construction sites, etc. It can also be used to evaluate different alternatives in the field of construction, education and research, engineering.

Since LiDAR is based on air scanning, the system is able to scan large areas of land in a relatively short time. An aircraft / helicopter mounted LiDAR system can scan a 300 km² area with a precision of 0.15 m over a 4-hour flight. Unlike photogrammetry involving manual, time-consuming work, LiDAR processing is largely automatic, with the possibility of obtaining the land model within weeks and not months after obtaining the data.

LiDAR is an automated system and does not involve a prior objective visit. Topographic maps can be obtained even in less accessible areas with reduced visibility and complexity at ground level.

Fast and automatic data collection for LiDAR allows designers to consider a multitude of options and alternatives in the design that will be performed. It also allows them to study alternative routes to suggest to the beneficiary. Normally, only 3-4 flights will be required to get a precise representation of the land and buildings, respectively alternate routes in an area with increased complexity. The optimal option will then be selected to meet the expectations of the beneficiary.

LiDAR is able to penetrate dense vegetation, which means that the team of designers can get information from hard-to-reach areas much faster and more accurately.

The experimental model setup is shown in Fig.2.

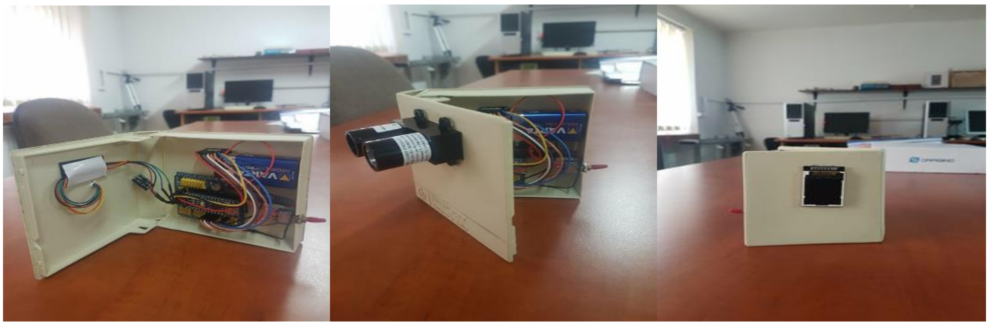

Fig. 2. Experimental model setup

The sensor is used to count vehicles on a lane at a time. Calculate the distance from the sensor to a particular reference point between it and the sidewalk, or consider the maximum distance that can be measured with this type of sensor when another value is found count a vehicle. The resulting number of counting vehicles on lane is locally displayed through a local LCD display and also are sent to the ESP32 radio module. Through this module, the information can be sent by radio transmission in 2.4 GHz band to long distance till a LoRa (Long Range Wireless Network) gateway connected to a network server from where it can be taken through internet network.

3. LoRa

The term LoRa (or LoRa technology) refers to a category of high-power low power long range radio communications. Unlike conventional digital radio transmission technologies, LoRa technologies have the capability of communicating data over tens of kilometers, with extraordinary applicability in wireless sensor networks, the Internet of Things (IoT), and networking of smart devices. [9] Behind the term LoRa is actually a multitude of proprietary or open technologies, similar to functionality but totally incompatible as implementation - the field of long distance radio communications is currently in a pioneering phase in which standardization stability and technological interconnection methods are a far-reaching goal. Other terms used to refer to high-bandwidth digital radio networks are LoRaWAN (Low Range Power Network), LPWAN (Low Power Wide Area Network), Low Power Network (LPN). Some of these terms are registered as brands belonging to certain companies or consortia being used to identify a particular LoRa technology (even the term LoRa is a registered trademark of Semtech). LoRaWAN is a radio transmission protocol capable of forms a smart grid. [1] The setup network uses a star-of-stars topology, with gateways serving as transparent bridges that transmit information between sensors and the central server. Gateways connect to the network through traditional IP connections, and sensor devices use single-pass wireless communications for one or more gateways. [3]

The structure of LoRa network is similar to one cellular network, but instead of having a single interconnected network, LoRa allows the deployment of more independent networks over the same infrastructure. [2]

LoRa can covers 15-20 kilometers. The compromise for such a distance is a reduced power and a lower bit rate, about 0.3 to 50 kbps.

The elements components of the system structure in "end-to-end" way of LoRaWAN are shown in Fig.3 and these are:

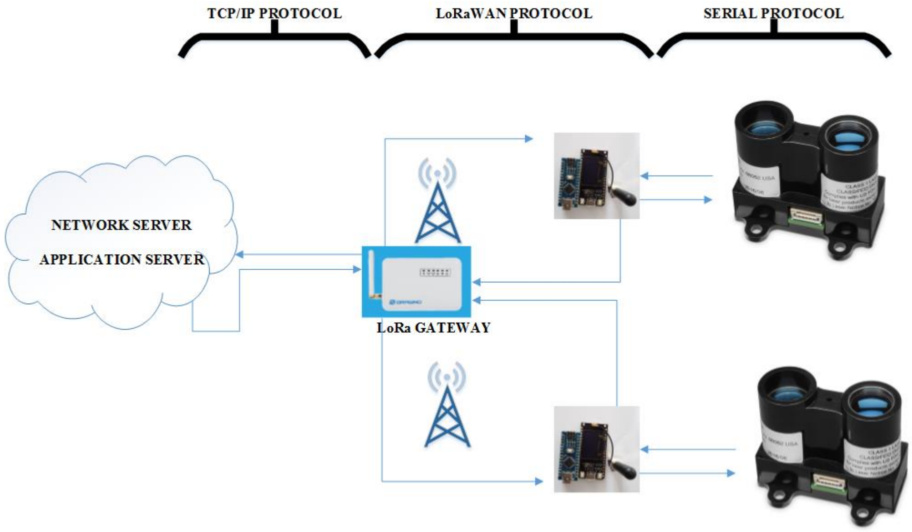

Fig. 3. The architecture of LoRa system

Nodes

Represents the elements of the LoRa network that monitors and controls the infrastructure devices which are usually located at distance, the ESP32 - LoRa – OLED which transmit the data taken from the LiDAR sensors via an Arduino Nano development board in this case. The ESP32 - LoRa - OLED has a 0.96 inch blue OLED display for displaying local information and a Lora transceiver, the SX1276 transceiver for the 868 MHz band. It has a high sensitivity over -148dBm, + 20dBm output power, high reliability and long transmission distance. The onboard Wi-Fi antenna, lithium battery charging circuit, CP2102 interface and USB serial chip, make it the perfect support for Arduino development environment. [4]

Operating voltage is from 3.3V to 7V. It have support for Sniffer software protocol analysis, Station, SoftAP, and Wi-Fi Direct modes. Data rates are comprised between: 11 Mbps and 150 Mbps and the transmit power is between 15.5 dBm and 19.5 dBm. This development board has a receiver sensitivity up to -98 dBm.

LoRa Gateway

This is the device that receives data from network nodes (ESP32) through the LoRaWAN protocol and then is transferred over the Internet to the main application server. The connection to the application server may be Ethernet, GSM data, or any other cable or wireless telecommunications connection that provides an Internet connection. In fact this base stations (LoRa Gateway) are connected to the network server using standard IP connections. In this way, the data uses a standard protocol that can be connected to any public or private telecommunications network. Given the resemblance of a LoRa network with a mobile network, the LoRa base stations can often be integrated into a cellular base station. In this way, the unused capacity of the cellular station can be used to transmit the data to the network server.[10]

Fig. 4. Dragino LoRa gateway used for system

Network server

The network server manages entire LoRa network. The network server acts to remove duplicate packets, recognition programs, and control the data transmission speed. Given the way it can be deployed and connected, the complexity of implementing a LoRa network is very low.

Application server

From the application server that is installed on the network server, we can access applications that retrieve data from network nodes through the gateway and display them to provide the most relevant information for the client. In addition, LoRa allows bidirectional communication between nodes and the network server, remote commands can be sent to the nodes, these commands can be related to node management (remote software update) and control of elements in a system (change of green time of traffic lights).

4. CONCLUSION

The realization of this mobile system of counting the vehicles crossing a road artery from an urban center is the first step in the direction of developing a traffic management system. The most important feature of this system is that it does not use invasive techniques on vehicle runways and can easily be moved from one location to another location. Through the LoRa network, real-time data can be obtained on the car traffic characteristics of the monitoring points, thus obtaining sufficient data to formulate new directions for the development of the automotive infrastructure plans. LoRa is a long-range telecommunication and low-power telecommunication system for the "Internet of Things". The physical layer of the entire system uses the LoRa module, a proprietary technology with a MAC protocol. LoRaWAN is an open standard with the specifications available for free. This paper provides an analysis of the bidirectional operation of the LoRa protocol on an experimental platform specifically designed to study the performance of the network, documented in this paper. The results obtained during the preparation of this paper show that LoRa modulation, due to modulation of spectrum dispersion and high sensitivity of the receiver, offers good interference resistance. Field trials demonstrate that LoRa can provide satisfactory network coverage of up to 3 km on a network in a suburban area with not very dense residential dwellings. LoRa is therefore suitable for low power, low speed and long range. The experimental results also show that the protocol is reliable and very simple to implement.

REFERENCES

[1]. Adelantado F., Vilajosana X., Tuset-Peiro P., Martinez B., Melià-Seguí J. and Watteyne T., *Understanding the Limits of LoRaWAN*, IEEE Communications Magazine, 2017.

[2]. Bankov D., Khorov E., Lyakhov A., *On the Limits of LoRaWAN Channel Access*, International Conference on Engineering and Telecommunication (EnT): 10–14. doi:10.1109/ent.2016.011, 2016.

[3]. Dongare A., Hesling C., Bhatia K., Balanuta A., Pereira R. L., Iannucci B., Rowe A., *OpenChirp: A Low-Power Wide-Area Networking architecture*, 2017 IEEE International Conference on Pervasive Computing and Communications Workshops (PerCom Workshops), pg. 569–574, 2017.

[4]. Espressif Systems, *ESP32 Series Datasheet*, 2015.

[5]. Leduc G., *Road Traffic Data: Collection Methods and Applications*, European Commission-Institute for Prospective Technological Studies, JRC, 2008.

[6]. Marcu M. Niculescu T. Popescu F. Slusariuc R., *Incremental conductance algorithm used in a programmable microcontroller as maximum power point traker*, 17th International multidisciplinary Scientific Geoconference SGEM 2017 Conference Proceedings, Vol. 17-Energy and Clean Technology, ISBN 978-619-7408-07-2 / ISSN 1314-2704, Albena, Bulgaria, pag. 369-376, 2017.

[7]. Massa P.D., *Chosing an Ultrasonic Sensor for Proximity or Distance Measurement*, Sensor Magazine, 2008.

[8]. Niculescu T., Marcu M., Popescu F., Slusariuc R., *MATLAB applications in the study of connection schemes of inductive circuits to alternative power source*, 17th International multidisciplinary Scientific Geoconference SGEM 2017 Conference Proceedings, Vol. 17-Informatics, Geoinformatics and Remonte Sensing, ISBN 978-619-7408-01-0 / ISSN 1314-2704, Albena, Bulgaria, pag. 407-412, 2017.

[9]. Sanchez-Iborra R., Cano M.D., *State of the Art in LP-WAN Solutions for Industrial IoT Services*, http://www.mdpi.com/1424-8220/16/5/708, 2016.

[10]. Sornin N. et al., *LoRaWAN Specification*, https://www.lora-alliance.org/, 2017.

[11]. Steinset B.K., *Traffic Data Collection and Analysis, Ministry of Works and Transport*, ISBN 99912-0-417-2, 2004.

Annals of the University of Petrosani, Electrical Engineering, 20 (2018)

BRIEF ANALYSIS OF THE BITCOIN PHENOMENON BY PRIVATE USER

COSMIN RUS[1], ILEANA – SORINA RAKOȘ [2], NICOLETA NEGRU [3]

Abstract: This paper highlights aspects of the Bitcoin digital paradigm that use decentralized technology for secure payments and the storage of money that does not require banks or names of people. The main objective of the paper is to understand the bitcoin phenomenon both in terms of economic implications and in terms of the technical notions of the entire process of producing the virtual coins. Also, there are some clear remarks about the need to try to reduce the electricity consumption used in the virtual coin mining process or the more frequent use of renewable energy resources.

Keywords: bitcoin, mining, ledger, renewable energy resources, blockchain, technology

1. INTRODUCTION

In 2009, due to the increasing popularity of electronic payment systems, a person or a group of unknown people, under the pseudonym Satoshi Nakamoto, created Bitcoin. It can be defined as a decentralized electronic payment system, but also a digital coin. The purpose of this coin is to ensure security and transaction anonymity, free business finance, and investment protection without resorting to public or private financial institutions, thus excluding dependence on a certain financial structure. As we know, the world currencies have a special issuer: The dollar is issued by the US Federal Reserve System, the Euro is issued by the Central Bank of Europe, etc. Unlike these coins, Bitcoin does not use a central issuer, being totally decentralized. Economically speaking, Bitcoin has no value, and is used as a measure of the value of traded items, basically fulfilling the original money function. Bitcoin's value is based on the confidence of all participants in this coin's trading network.[1],[5]

Next we will address the technical aspect of this coin, because without it, we can not understand its principle of operation. It's a bit heavy, but we'll try to make it as suggestive as possible. Due to its construction, the Bitcoin can be anonymously transmitted, and saved on the user's computer as a portfile. In order to make a transaction,

[1] Ph.D. student, Eng., University of Petroşani, cosminrus@upet
[2] Ph.D, Associate Prof.,University of Petroşani, nihilsinedeo_68@yahoo.com
[3] Ph.D. student, University of Petroşani, negru.ioananicoleta@yahoo.ro

users need two "keys", a public one, which is used to encrypt the transaction code and BitTorrent, and a private one, with which the code is decoded, and finalizing the transaction, offering anonymity and security.[2],[3],[7]

In our opinion, the concept of crypto-labeled is perspective, but Bitcoin does not have a high practical capacity, because of how paradoxically it would be, its main plus: decentralization. Because of this facility, this currency can not be controlled by the state, it does not depend on any bank, it can not suffer inflation (the number of bitches being controlled), what is the problem then? The problem is the financial value of a Bitcoin coin. The course of this cryptocurrency is very unstable, sensitive to crises in economic life and investor actions.[7]

2. BITCOIN MINING

Bitcoin is a digital currency (also called cryptocurrency) that is not backed by any country's central bank or government. Bitcoins can be traded for goods or services with vendors who accept Bitcoins as payment. Mining is the process of adding transaction records to Bitcoin's public ledger of past transactions (and a "mining rig" is a colloquial metaphor for a single computer system that performs the necessary computations for "mining"). This ledger of past transactions is called the block chain as it is a chain of blocks. The blockchain serves to confirm transactions to the rest of the network as having taken place. Bitcoin nodes use the blockchain to distinguish legitimate Bitcoin transactions from attempts to re-spend coins that have already been spent elsewhere.[5]

Mining is intentionally designed to be resource-intensive and difficult so that the number of blocks found each day by miners remains steady. Individual blocks must contain a proof of work to be considered valid. This proof of work is verified by other Bitcoin nodes each time they receive a block. Bitcoin uses the hashcash proof-of-work function. The primary purpose of mining is to set the history of transactions in a way that is computationally impractical to modify by any one entity. By downloading and verifying the blockchain, bitcoin nodes are able to reach consensus about the ordering of events in bitcoin.

Mining is also the mechanism used to introduce Bitcoins into the system: Miners are paid any transaction fees as well as a "subsidy" of newly created coins. This both serves the purpose of disseminating new coins in a decentralized manner as well as motivating people to provide security for the system. Bitcoin mining is so called because it resembles the mining of other commodities: it requires exertion and it slowly makes new units available to anybody who wishes to take part. An important difference is that the supply does not depend on the amount of mining. In general changing total miner hashpower does not change how many bitcoins are created over the long term.

Mining a block is difficult because the SHA-256 hash of a block's header must be lower than or equal to the target in order for the block to be accepted by the network. This problem can be simplified for explanation purposes: The hash of a block must start with a certain number of zeros. The probability of calculating a hash that starts with many zeros is very low, therefore many attempts must be made. In order to generate a new hash each round, a nonce is incremented.

The difficulty is the measure of how difficult it is to find a new block compared to the easiest it can ever be. The rate is recalculated every 2,016 blocks to a value such that the previous 2,016 blocks would have been generated in exactly one fortnight (two weeks) had everyone been mining at this difficulty.

This is expected yield, on average, one block every ten minutes. As more miners join, the rate of block creation increases. As the rate of block generation increases, the difficulty rises to compensate, which has a balancing of effect due to reducing the rate of block-creation. Any blocks released by malicious miners that do not meet the required difficulty target will simply be rejected by the other participants in the network.When a block is discovered, the discoverer may award themselves a certain number of bitcoins, which is agreed-upon by everyone in the network.

Currently this bounty is 12.5 bitcoins; this value will halve every 210,000 blocks. Additionally, the miner is awarded the fees paid by users sending transactions. The fee is an incentive for the miner to include the transaction in their block. In the future, as the number of new bitcoins miners are allowed to create in each block dwindles, the fees will make up a much more important percentage of mining income.[10]

3. BLOCKCHAIN AND CRYPTOCURRENCY

We have to understand that creating cryptocurrency is not the only single use of Blockchain. In 2015, the Ethereum network was launched that generated far more modern technologies than Blockchain and other concepts such as smart-contracts. Ethereum was a Blockchain, but more technically advanced not only to perform currency transactions but also to initiate and process smart-contracts, create its own Token devices (identifies you as a user and authorizes your transactions) for use in any other (third) projects.[4]

Smart-Contracts is a new direction, which became known with the development of the Blockchain. Imagine a smart electronic contract that records all business conditions and cannot be changed by anyone. This technology will generate the complete disappearance of scams and lies, both from simple people and from the state. For example, you have created a smart contract for the sale of a good (your own house), you have scheduled the necessary conditions after which the smart-contract will create the necessary events (in our case the sale of the house (sale of the private-real estate)). Therefore, the buyer transfers the necessary amount of money to the smart-contract to the corresponding smart-contract, after which the smart-contract verifies daily the update in the State Property Register. As soon as the property registration letter is displayed after the new owner, the smart-contract will transfer to your account the amount equal to the price. If within one month this inscript will not be displayed, the smart-contract will return the buyer's crypt.

This is one of the simplest examples that make it clear that in front of Blockchain technology there is a big future. Blockchain and cryptocurrency are now like the Internet in 1993, everything that's more interesting is going to happen. And it is very important that we all understand this new direction, and if we have the opportunity, let us even take part in it.

4. THE HAZARDS ASSOCIATED WITH BITCOIN

As we know, the creator of Bitcoin is a person, or a group of people, known under the pseudonym Satoshi Nakomoto, who first launched the Bitcoin network. For testing and verification, around 7% of all Bitcoin coins were extracted, and today, in a few years, those 7% represent colossal amounts, approximately $ 20 billion, and after forecasts only 7% will almost equal $ 200 billion, and by 2050, these percentages will turn to $ 5-10 trillion. And it is very possible that at that moment to be the opposite of the present, ie the value of the dollar to be calculated in bitcoins, even if that sounds funny, this is likely to happen. So funny sounded for that boy who bought a 10,000 Bitcoin pizza in 2010, hearing that in 2018 the equivalent of that price would be $ 150 million. Ask a financial analyst or economist who you know about the danger of this phenomenon.

What will happen if 7% of all Bitcoins are extracted in a single day at cryptocurrency exchanges? We will see how soon Bitcoin, but also the other cryptocurrency, will be destroyed. Their value will decrease hundreds of times, creating such a catastrophe in the world that most financial organizations, traders and others will have to stop trading and sales. In fact, the entire world economy will stop in just two or three days. Stores, pharmacies, no trader will be able to accept payments, because everyone, a day ago, bought goods at a price hundreds of times higher.

Everyone will wait for clarifications, which they will not receive. Imagine that in your house there is a room that is full up to the bridge with $ 100 banknotes, so if you want to open the door, you will be covered with waves of money. And you have been living in that 9-year-old house, and in all these 9 years you've passed that room without taking even $ 1.[7]

Mining is a very wasteful electricity process, for the location of large mining devices, very cheap electricity access is needed, as is a favorable climate area. Mining equipment produces a large amount of heat that needs to be absorbed. After these clues, in your opinion, in which country are the capabilities and basic tools that Bitcoin is shuffling for? This is China. In the percentage ratio, it looks like this: China 81%; Japonia5%; Czech Republic 2%; Georgia1% etc. If most of Bitcoin's power is in a single country, it allows for a simpler connection between mining equipment owners, which causes danger. It is enough that these owners, uniting themselves, form 51% of the administrative equipment to make changes to the Bitcoin network. Mining pools already have their own brands and names, they have long known each other, and possibly keep in touch with each other.[10]

Today's modern cryptocurrency are no longer in need of mining. More secure and cheaper Blockchain projects have been designed and are already in place, where the role of mining is diminished, not much electricity is needed (Bitcoin currently consumes energy as a city with a population of 1 million people). Here too we can add accelerated demodulation of mining equipment, it will be an endless race. The equipment purchased yesterday, tomorrow, may be old and out of date with the release of new ones.[7][8]

I reviewed and analyzed the most important hazards that Bitcoin might pose. But what to do to avoid all this? Everything is simple and complicated at the same time. Cryptocurrency's company must not change Bitcoin's price higher than it has at present.

Most believe that $ 50-60 thousand is a reasonable limit for the Bitcoin value and safe for the cryptocurrency market, because if someone tries to destroy Bitcoin, the rest of the cryptocurrency will fall. We need to assess the situation correctly and not lift the Bitcoin up to those heights that may prove dangerous. We, society, can create a more positive future in this respect, which we will continue to talk about.[9]

5. CONCLUSIONS

We have approached Bitcoin from the multitude of cryptocurrency on the market because of its popularity, being the most used electronic money. From the ideas outlined above we can deduce that Bitcoin has no practical value, but it is not. Even if bitcoin use is somewhat more difficult because of its volatile course, the popularization of this coin has led to the development of cryptocurrency itself, which is economically important.

More stable and more practical cryptoscopes appear: Etherium, Litecoin, Yota, which, over time, may replace the concept of paper money, and move to electronic money.

Technologies are growing at an accelerated rate, and financial security is getting bigger every day, so implementation of cryptobodies might be an action that would provide economic prosperity in the future, yet they eventually meet the concept of money base: measuring the value of a product, and facilitating the exchange, that is money is a tool with which the exchange becomes effective.

Money presents our economic capacity, and cryptocurrency is a concept that attempts to implement this money feature in reality. As mentioned earlier, once and spices were considered "gold", which means that the nature of money is flexible, and what seems impossible now can be widely used in the future. Currently 12 TWh/year and rising will be consumed through Bitcoin Mining, and another 6 TWh/year by Ethereum Mining, this is the equivalent of 8 million average German households therefore in the context of smart city and sustainable development it is vital to step up efforts to increasingly use renewable energy sources in production of cryptocurrency (mining).

REFERENCES

[1]. Davis J., *The Crypto-Currency: Bitcoin and its mysterious inventor,* The New Yorker, pg. 93-96, 2011.

[2]. Detrixhe J., *The secret to crypto investing is there is no secret*, (https://qz.com/1321633/), 2018.

[3]. Jason M., *Cracking the Bitcoin: Digging Into a $131M USD Virtual Currency*, Daily Tech, 12 June 2011.

[4]. Timothy B., *An Illustrated History Of Bitcoin Crashe*, Forbes, 07 August 2011.

[5]. Antonopoulos M., *Mastering Bitcoin: Unlocking Digital Crypto-Currencies. O'Reilly Media*, 2014.

[6]. Merkle R.C., *Protocols for public key cryptosystems*, In Proc. 1980 Symposium on Security and Privacy, IEEE Computer Society, pg. 122-133, April 1980.

[7]. Nakamoto S., *Bitcoin: A Peer-to-Peer Electronic Cash System*, www.bitcoin.org, 2008.

[8]. Nakamoto S. et al., *Bitcoin source code - amount constraints*, GitHub, 2016.

[9]. Wilson T., *Twitter and LinkedIn ban cryptocurrency adverts – leaving regulators behind*, Independent, 28 March 2018.

[10]. *** http://bitcoindaily.org/bitcoin-guides/what-is-bitcoin-mining/

Annals of the University of Petrosani, Electrical Engineering, 20 (2018)

ACTIVE POWER FILTERS IN ORDER TO LIMIT THE HARMONIC DISTURBANCE FROM ELECTRICAL NETWORKS

ILIE UȚU[1], MARIA DANIELA STOCHIȚOIU[2], LILIANA SAMOILĂ[3], ALINA DANIELA HANDRA[4]

Abstract: This paper addresses a high-current field of research, under the conditions of proliferation of nonlinear loads - generally static converters with power semiconductors - generating current harmonics. A series of simulations of the voltage and current harmonics compensation system are made and control and adjustment methods are proposed. A nonlinear consumer simulation model was created with the Matlab-Simulink software package. The simulation results are analyzed to determine the compensation issues that the active filter will have to solve.

Key words*:* Nonlinear loads, harmonics, power converters, active filters, parallel filters, series filters.

1. INTRODUCTION

Active filters are static power converters that can perform various functions. Current filter schemes allow the synthesis of any current form with relatively high harmonic components [1].

The consumer may choose one of the following solutions:

- waives the equipment that absorb the current distorted and invests in new equipment,
- maintain the equipment and invest in tools for limiting issuance in the form of disruptive harmonics: passive or active filters.

[1] *Associate Professor Eng., Ph.D. at the University of Petrosani,ilieutu@upet.ro*
[2] *Associate Professor Eng., Ph.D. at the University of Petrosani, daniela_orban@yahoo.com*
[3] *Associate Professor Eng., Ph.D. at the University of Petrosani, branaliliana@gmail.com*
[4] *PhD., Trainer, Eng., Soft Skills Training SRL*

2. CONNECTION MODE AND TOPOLOGY OF ACTIVE FILTERS

Harmonic filters are available to the user or to the electricity supplier. Filters from energy suppliers are of great powers and in most cases it is passive filters. Users can place filters:

- common connection points (CCP), which takes a global information;
- at the point of connection of a consumer important, current harmonics generator.

Power circuit can be connected in two ways: in parallel or in series. Parallel structure (fig. 1.a) is the most widespread. Active filter compensates current harmonics content, which would have been injected into the supply network in the absence of such compensation [2], [5]. Such filters are implemented with voltage inverters in the current.

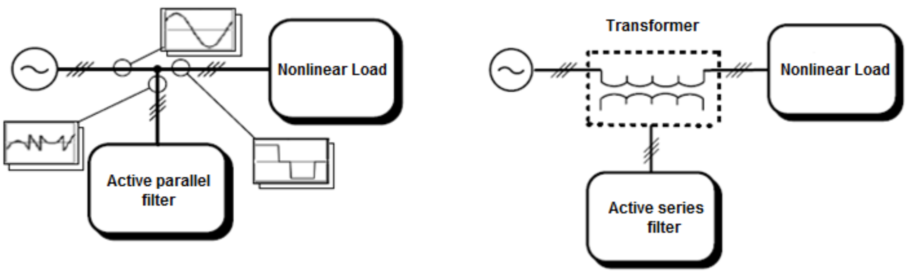

a) b)

Fig.1 Active filter connected in parallel (a) and in series (b)

Active filter fig.1.b is connected in series with the load through a nonlinear transform. The strategy of the command filter series aims to produce such a voltage transformer, the mayor who ensures a pure sine wave voltage at the terminals. Such filters are implemented with voltage inverters without current loop [3], [8]. The main disadvantage is that the series of filters should drive the entire current task.

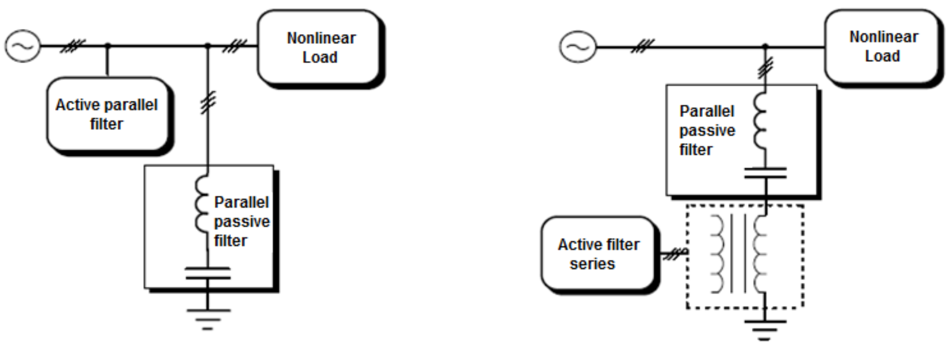

a) b)

Fig.2. Combinations of filters a) Active parallel filter – parallel passive filter;
b) Active filter series – parallel passive filter

Special interest presents the combination of parallel active filter and passive filter. From passive filter fig. 2.a shall be designed so as to largely eliminate low harmonics - e.g. 5, 7, 11, 13 - who is important, and the active filter is sized for a lower rated current.

Active filter fig. 2.b shall be installed in series with the battery of capacitors to compensate reactive power or with a passive filter. Active filter topology is voltage inverter with the command in the current directory[4],[7].

3. SIMULATION OF ACTIVE POWER FILTERS

3.1. Nonlinear Simulink model of the consumer

To study the harmonic content of the nonlinear consumer to be compensated, a model of the thyristor rectifier was developed using the Matlab-Simulink software package and modules from the PowerSys auxiliary tool kit [6]. The rectifier (Fig. 3.) consists of a three-phase tri-phase bridge, a pulse generator and a current regulator. On each thyristor two pulses are applied at 60 degrees.

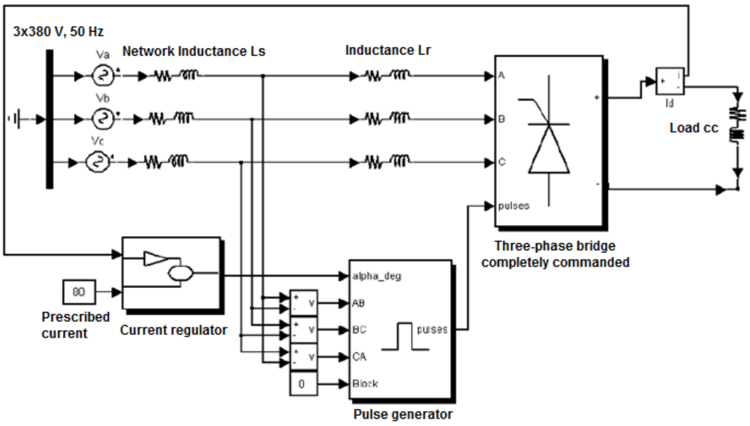

Fig. 3. Simulink model of three-phase rectifier with thyristors

In Fig. 4 the simulation results and the waveforms obtained for the nonlinear consumer are presented. The evolution over time and spectrum of current recovered by the rectifier at different current values were compared. It has been found that the current distortion factor decreases as the current increases.

3.2. Simulink model of the active filter

With the Matlab-Simulink software package, a simulation model was developed (fig. 5.). The model's structure contains the network and rectifier (nonlinear consumer) models and the active filter model.

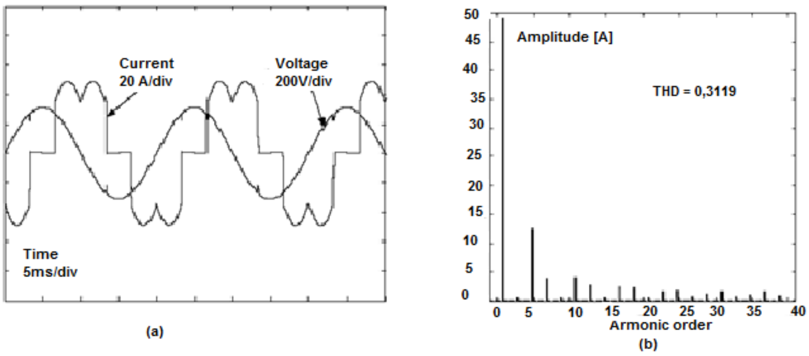

Fig. 4. The current absorbed from the mains voltage and phase (a) and the spectrum of current drawn from the mains (b)

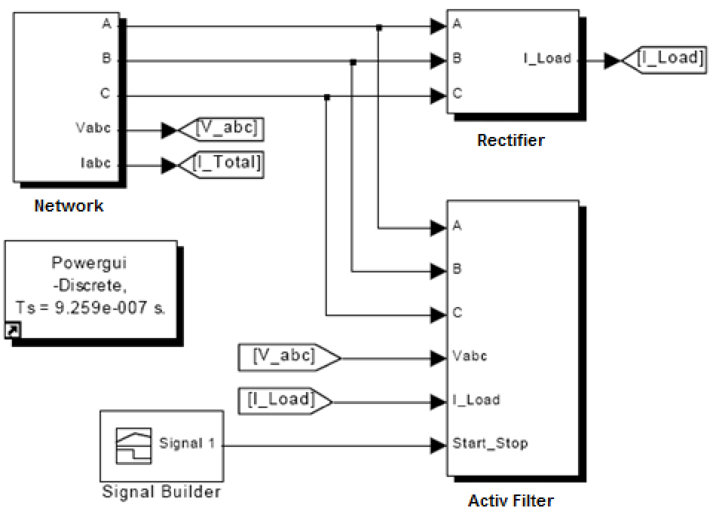

Fig. 5. Simulink model of nonlinear consumer assembly; active filter

3.3. Active filter simulation results

The effect of the passive filter for the wavelength waves and its multiples is emphasized by comparing the absorbed current in the presence of the filter (Fig. 7) and the current absorbed in the absence of the filter (Fig. 6).

It is observed the effect of the circuit given on the switching frequency, which removes the harmonics of current with this frequency and the effect of the reactive power compensation.

Mains voltage in the CCP has a high content of harmonics in the absence of passive filter, which can have a negative influence on other consumers. In Fig. 8 shows the simulation results for the reference signal and the measured value of the filter current for a phase in coordinates (a, b, c).

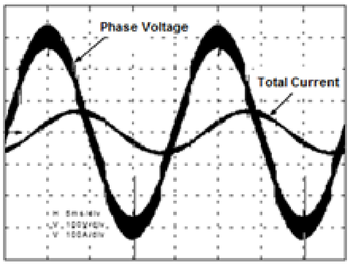

Fig. 6. Phase voltage and total current without passive filter

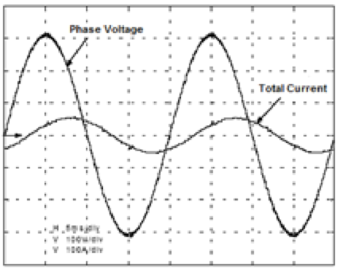

Fig. 7. Phase voltage and total current with passive filter

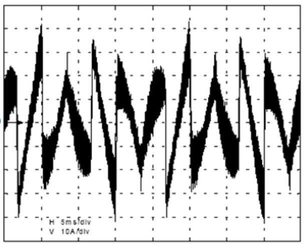

Fig. 8. Reference signal and measured value of filter current in coordinates (a, b, c)

As the consumer's current is slow, it is possible to calculate the current reference based on the preceding period but with one or more switching steps to compensate for the delay introduced by the current regulators and the execution element.

In Fig. 9 shows the reference signal and the measured value of the filter current on the q axis.

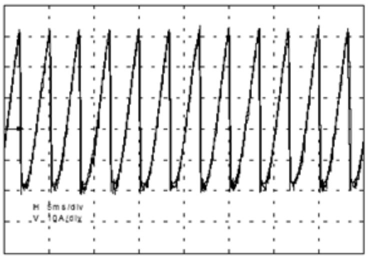

Fig. 9. The reference signal and the measured value of the filter current on the q axis.

4. CONCLUSIONS

We developed a method of compensation of the harmonic current absorbed by the adjustable drives with DC or AC motors, which that are most prevalent industrial consumers. We achieved two active filter structures in parallel topology, with a voltage inverter, at two different power levels and two harmonic generator test benches, on which the experimental method of compensation was implemented and tested.

The paper presents the elements of the active filter. It makes a classification of active filters depending on power and response speed. Then the different ways of locating the active filters, the main topologies, and the way in which the active filters can be connected to the network and the nonlinear consumer are treated.

To mitigate the impact of an active filter's price, there are additional features that the filter could offer besides compensating the harmonics: reactive power compensation, resonance damping, protection against temporary voltage drops.

With the Matlab-Simulink software package a simulation model of the nonlinear consumer and the power supply network was created. The simulation results are analyzed to determine the compensation issues that the active filter will have to solve and at a future stage to be validated by comparing with the experimental results.

Based on mathematical models, simulation schemes were developed as follows:

- Simulation scheme of a disturbed source with fully rectifier structure and thyristor supply network at the test bench connection point;
- Parallel active filter simulation scheme with voltage inverter structure with Matlab, Simulink and PowerSys modules.

The experimental results are similar to those obtained by simulation. This concordance allows us to conclude that the computational assumptions and mathematical models underlying this work are correct.

REFERENCES

[1]. Marcu, M., Popescu, F.G., Samoila, B. L., *Modeling and simuling power active filter using method of generalized reactive power theory*, IEEE International Conference on Computer Science and Automation Engineering, Shanghai, China, 10-12 June 2011.

[2]. Marcu M.D., Popescu F.G., Niculescu T., Pana L., Handra A.D., *Simulation of power active filter using instantaneous reactive power theory*, Harmonics and Quality of Power (ICHQP), IEEE 16th International Conference, Page(s):581 – 585, Bucharest, 2014.

[3]. Niculescu T., Marcu M., Popescu F., Slusariuc R., *MATLAB applications in the study of connection schemes of inductive circuits to alternative power source*, 17th International multidisciplinary Scientific Geoconference, Vol. 17-Informatics, Geoinformatics and Remonte Sensing, pp. 407- 412, Albena, Bulgaria, 2017.

[4]. Popescu F.G., Arad S., Marcu M.D., Pana L., *Reducing energy consumption by modernizing drives of high capacity equipment used to extract lignite*, Papers SGEM2013/Conference Proceedings, Vol. Energy and clean technologies, pp. 183 - 190, Albena., Bulgaria, 2013.

[5]. Popescu F.G., Marcu M.D., *Metode moderne de analiză şi reducere a armonicilor de curent şi tensiune*, Editura Universitas, Petroşani, pag. 265, 2016.

[6]. Shklyarskiy Y. E., Skamyin A. N., *Compensation of the reactive power in the presence of higher voltage harmonics at coke plants*, Coke Chem., vol. 59, no. 4, pp. 163–168, Apr. 2016.

[7]. Solovev S. V., Kryltcov S. B., Voytyuk I. N., *Static load characteristics consideration for determination of transmission line power capacity*, in Proceedings of the 2018 IEEE Conference of Russian Young Researchers in Electrical and Electronic Engineering, ElConRus 2018, 2018, vol. 2018–Janua.

[8]. E. O. Zamyanit, Y. E. Shklyarskiy, *Concept for electric power quality indicators evaluation and monitoring stationary intellectual system development*, Int. J. Appl. Eng. Res., vol. 11, no. 6, pp. 4270–4274, 2016.

Annals of the University of Petrosani, Electrical Engineering, 20 (2018)

OVERVIEW OF CONTROL METHODS FOR INDUCTION MOTOR DRIVES

MARIUS MARCU[1], FLORIN GABRIEL POPESCU[2], RĂZVAN SLUSARIUC[3], SUSANA ARAD[4], ALINA DANIELA HANDRA[5]

Abstract: The paper presents an analysis of the operation of asynchronous motor drive systems. The control method used is the vectorial one, being presented indirect and direct vector control, stator flux oriented direct vector control, and direct torque and flux control methods. The analysis of the operation of the electric drive systems is done by simulation with the help of the program package MATLAB-Simulink.

Keywords: vector control, direct torque, flux control, simulation, stator flux oriented control.

1. INTRODUCTION

The development of vector or field-oriented control, and the demonstration that ac motor can be controlled like a separately excited dc motor, brought renaissance in the high performance control of induction motor drives [1]. The advent of microprocessors made the vector control increasingly acceptable from the 1980's. In fact, with vector control, induction motor drive outperforms the dc drive because of higher transient current capability, increased speed range and lower rotor inertia. High performance adaptive and optimal control techniques can be easily applied on vector-controlled drives because of simple dc machine-like transient model [3], [8].

The advent of modern digital signal processors, powerful personal computers, user-friendly simulation and CAD tools, artificial intelligence (AI) techniques, and advancement of control and estimation theories are continuously extending the frontier of high performance AC drives, [9] [10].

[1] *Ph.D., Associate Prof. Eng., University of Petroşani, mariusmarcu@upet.ro*
[2] *Ph.D., Lecturer Eng.,University of Petroşani, floringabriel@yahoo.com*
[3] *Ph.D., Lecturer Eng., University of Petroşani, razvansir@yahoo.com*
[4] *Ph.D., Prof. Eng., University of Petroşani, susanaarad@yahoo.com*
[5] *PhD., Trainer, Eng., Soft Skills Training SRL*

2. VECTOR OR FIELD-ORIENTED CONTROL

Vector control is the foundation of modern high performance drives. It is also known as decoupling, orthogonal, or transvector control [4].

Vector control techniques can be classified as indirect method, and direct method depending on the method of unit vector generation for vector transformation. There is also classification of control based on orientation with rotor flux (Ψr) or stator flux (Ψs) [2].

Fig. 1 shows the indirect vector control block diagram with rotor flux orientation. The synchronously rotating vector components of stator current iqs and ids are controlled independently to control the torque and rotor flux, respectively.

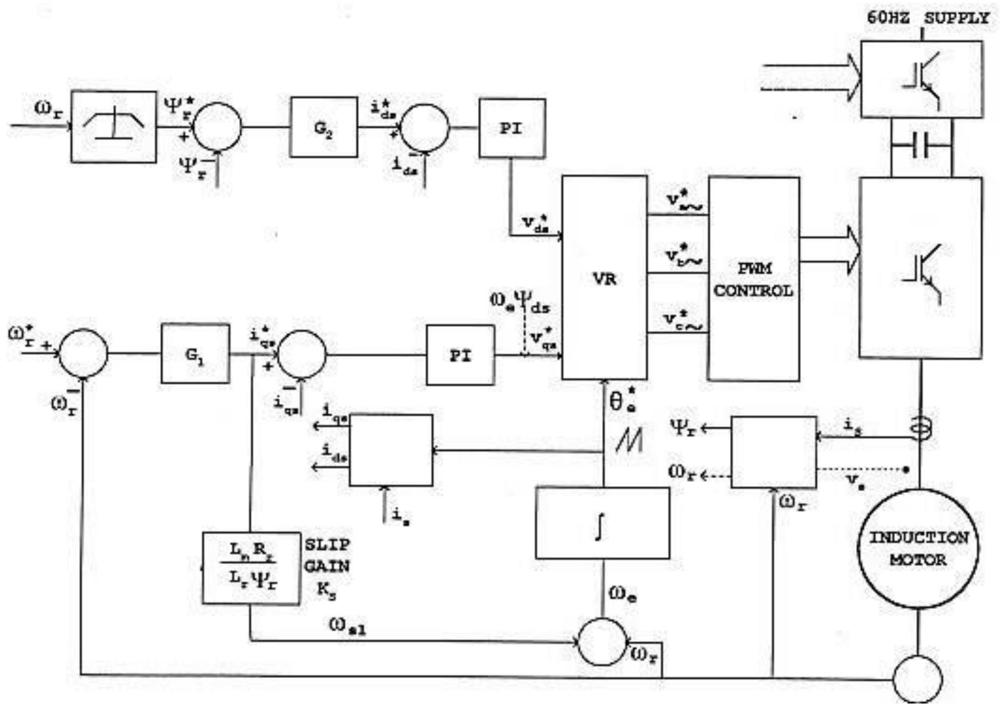

Fig. 1. Indirect vector control

It can be shown that rotor flux orientation (in contrast to stator flux orientation) tends to give true decoupling control. Within the synchronous current control loops, as shown, the respective counter emf (electromotive force) signals can be added (or subtracted) to enhance the current loop response [6], [11]. The unit vector signal θe that transforms the synchronously rotating stator voltages into stationary frame signals has been generated from the speed signal and slip signal which is a function of iqs*, as shown. The slip gain Ks is a function of machine parameters, which should track with the actual machine parameters to get true decoupling. The feedback flux can be estimated from machine terminal voltages and currents (voltage model), or from currents and speed (current model) [7]. The voltage model works well typically above 2% of base speed but the current model works from zero speed. Of course, the current model is more sensitive to machine parameter variation. The flux can also be simply controlled by open loop as a function of ids*. The drive can easily be operated from zero speed to constant power field-weakening region. It is the most popular vector control method in industry. However, the machine parameter variation affects the slip gain and correspondingly, both static and dynamic performances of the drive are affected [5]. The initial tuning of Ks can be done by automated parameter measurement with inverter-injected signals. The on-line tuning for parameter variation is more difficult.

Fig.2 shows the simulation waveforms for this method. The simulation was made by MATLAB-Simulink packages [12], [13].

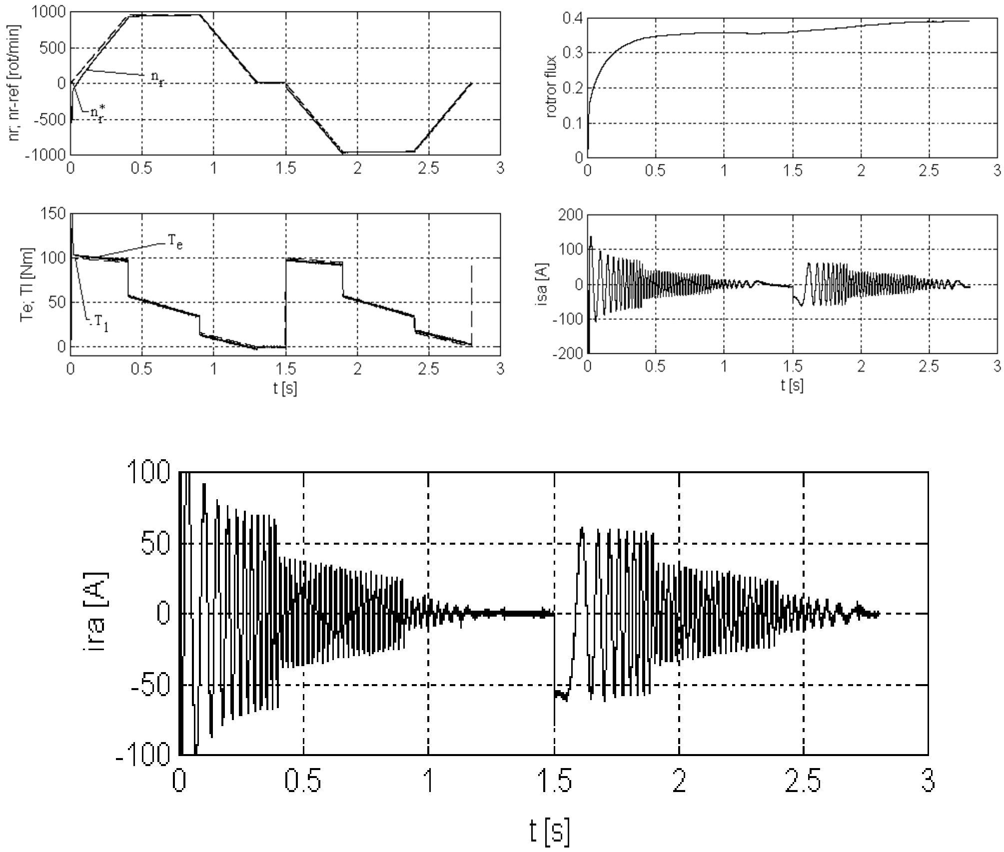

Fig.2. Simulation results for indirect vector control with rotor flux orientation

Fig. 3 shows the direct vector control based on rotor flux orientation.

All the basic elements of the control are essentially the same as indirect vector control except the unit vector signal θe which is derived from the flux vector that can be estimated either by voltage model, current model, or by close loop observer. It is also possible to estimate the speed signal from the voltage and current signals. The flux vector estimation with voltage model does not work near zero speed, but with current model it can be easily extended to zero, as indicated before [2].

Fig. 4 shows the stator flux oriented direct vector control method. It can be shown by analysis that stator flux oriented vector control introduces coupling effect that slows down the transient response, and therefore, decoupling compensation (idq) is required in the flux control loop. In spite of this drawback, the control has the advantage that the flux vector signal derived by integration of the voltage behind the stator resistance is sensitive to stator resistance only, and can be compensated somewhat easily. In fig.5 the authors present the simulation results for stator flux oriented vector control.

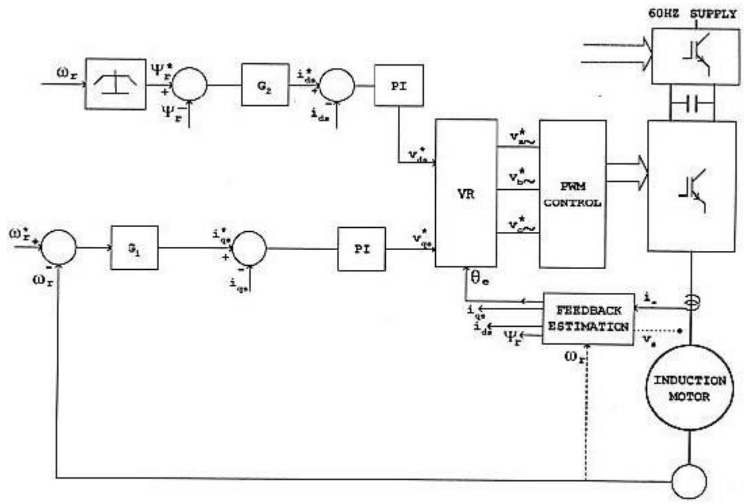

Fig. 3. Direct vector control

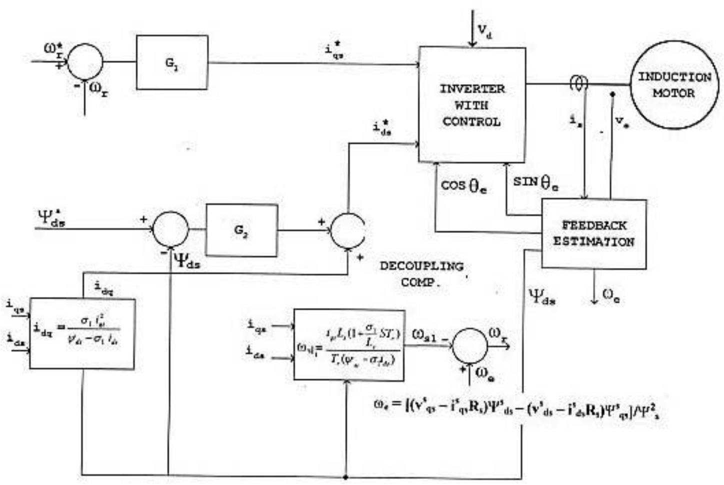

Fig. 4. Stator flux oriented direct vector control

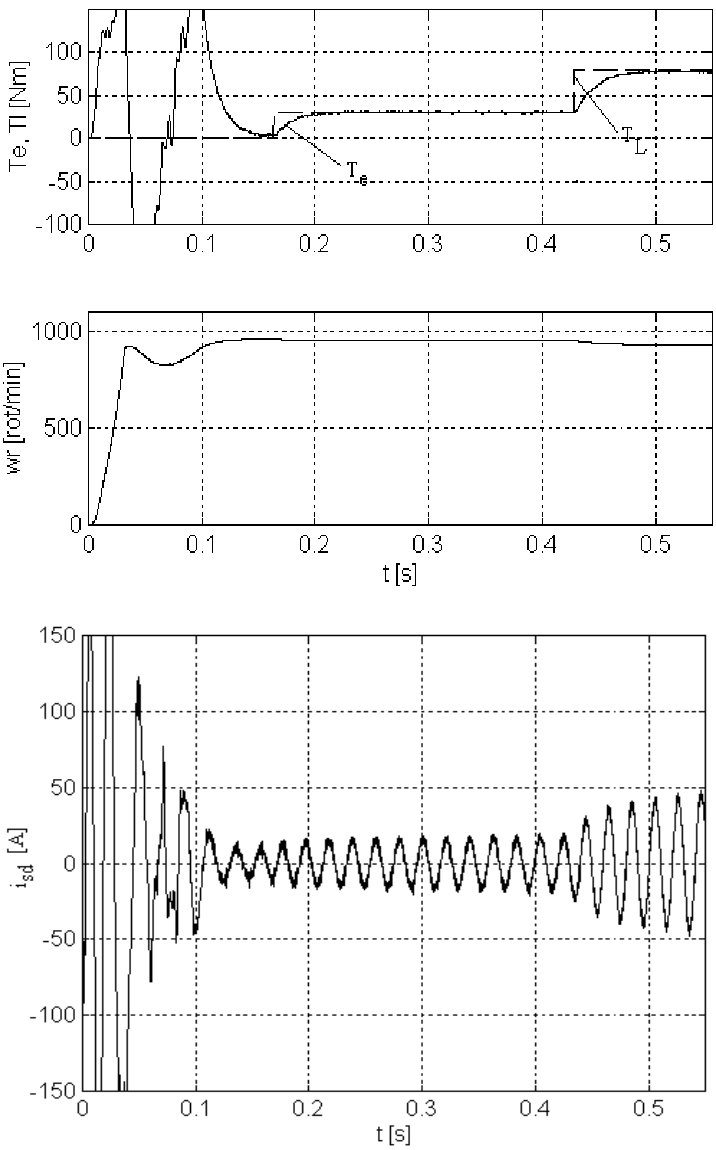

Fig.5. Simulation results for stator flux oriented vector control

3. DIRECT TORQUE AND FLUX CONTROL (DTFC)

The DTFC method, shown in Fig. 6, is basically a performance-enhanced scalar control method and is popularly known as direct torque control (DTC). It can be shown that the developed torque of a machine is proportional to the product of synchronously rotating stator flux (Ψs), rotor flux (Ψr) and the angle (δ) between them. In a PWM inverter-fed machine, Ψr vector is more filtered than Ψs, and therefore, Ψr vector rotates more smoothly. The motion of Ψs, dictated by the impressed voltage vector, is discontinuous, but its average velocity is same with Ψr in steady state. The Ψs magnitude is easily controlled within a hysteresis-band by limit cycle control [1].

Basically, DTC has torque and stator flux control in the outer loops, as indicated. The speed loop can be added on the torque loop with the speed encoder or estimated speed. The machine voltages and currents are sensed to estimate the torque and flux vector that gives information about Ψs location in one of the 60-degree sectors.

The control loop errors Es and ET generate the digital signals Ds and DT through the respective hysteresis-band comparators. A three-dimensional look-up table then selects the most appropriate voltage vector to satisfy the flux and torque demands. Since the feedback signals are being estimated from the machine terminal, the low-speed limitation and parameter variation problem are similar to Ψs-oriented direct vector control.

The drive has fast transient response, and has the simplicity of implementation due to absence of close loop current control, traditional PWM algorithm and vector transformation. However, the inherent limitations of limit cycle control, such as pulsating torque, pulsating flux and additional harmonic loss exist. Recently, a large number of papers are appearing in literature to improve the DTC control.

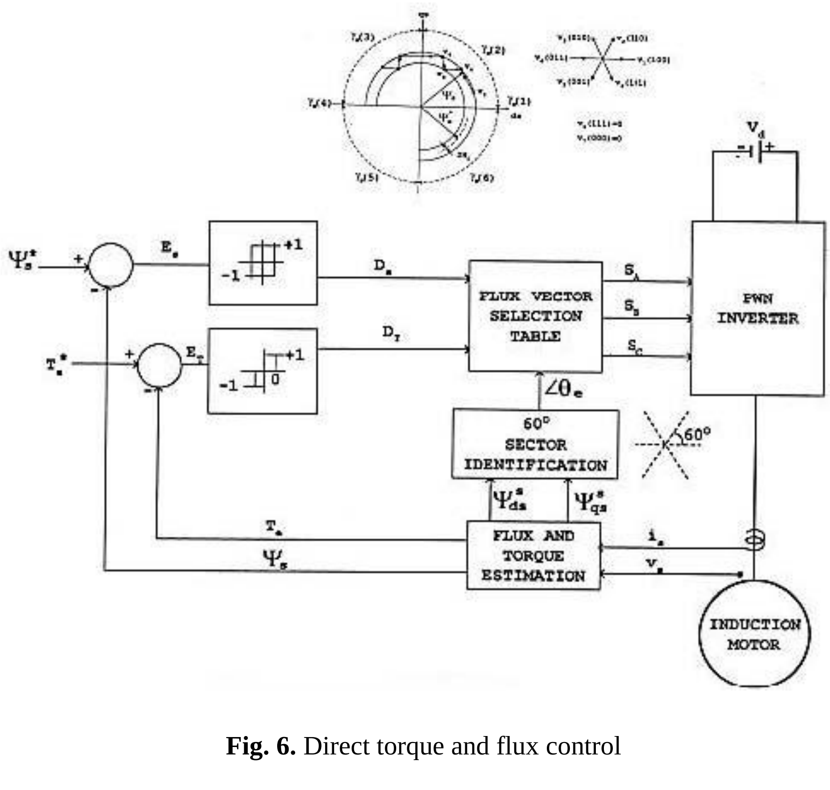

Fig. 6. Direct torque and flux control

Fig.7 shows the simulation waveforms for this method control of induction motor drive.

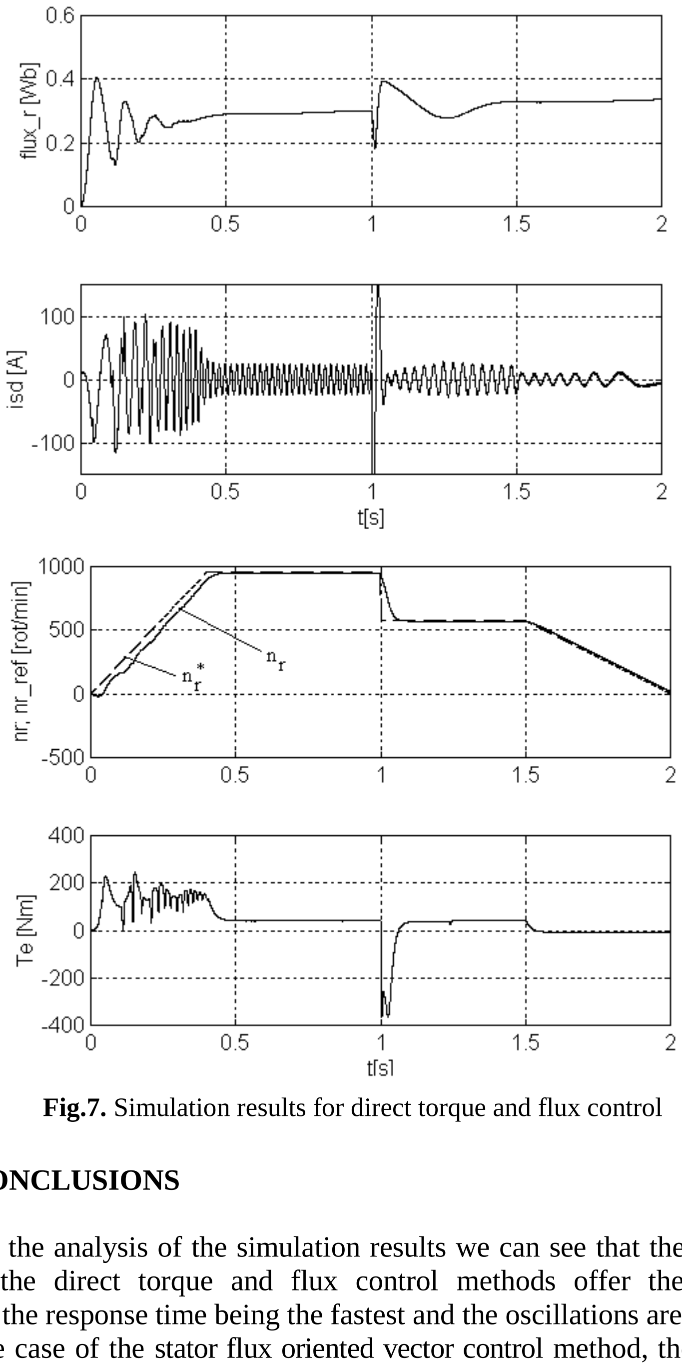

Fig.7. Simulation results for direct torque and flux control

4. CONCLUSIONS

From the analysis of the simulation results we can see that the indirect vector control and the direct torque and flux control methods offer the best transient performance, the response time being the fastest and the oscillations are minimal.

In the case of the stator flux oriented vector control method, the response time increases and the oscillations are more pronounced.

REFERENCES

[1]. Bose B. K., *Power Electronics and Variable Frequency Drives*, IEEE Press, 1997.

[2]. Marcu M., Utu I., *Sisteme de reglare vectoriala ale masinilor asincrone*, Ed. Universitas, Petrosani, 2000.

[3]. Pop E., Pătrăşcoiu N., *Practically algorithm, modelling and simulation of Luenberger observer*, Proceedings of the 12th International Conference on Applied Computer and Applied Computational Science (ACACOS'13), Kuala Lumpur, 2013.

[4]. Pop E., Pătrăşcoiu N., *Simulation and design algorithm for identifiers. Applications*, Proceedings of the 12th International Conference on Applied Computer and Applied Computational Science (ACACOS'13), pp. 53-58, Kuala Lumpur 2013.

[5]. Popescu F.G., Arad S., Marcu M.D., Pana L., *Reducing energy consumption by modernizing drives of high capacity equipment used to extract lignite*, Papers SGEM2013/Conference Proceedings, Vol. Energy and clean technologies, pp. 183 - 190, Albena., Bulgaria, 2013.

[6]. Popescu F.G., Slusariuc R., Uţu I., *Maşini şi acţionări electrice -lucrări de laborator*, Editura Universitas, Petroșani, 2017.

[7]. Samoila, L., Arad, S., Petre, M., *Application for simulating the short-circuit current and the transient recovery voltage*, IEEE 16th International Conference on Environment and Electrical Engineering (EEEIC), pp. 2159-2163, Florence, Italy, 2016.

[8]. Skamyin A. N., Shklyarskiy Y. E., *High harmonic minimization in electric circuits of industrial enterprises,* World Appl. Sci. J., vol. 30, no. 12, pp. 1767–1771, 2014.

[9]. Solovev S. V., Bardanov A. I., *Efficiency estimation method of three-wired AC to DC line transfer,* in Journal of Physics: Conference Series, 2018, vol. 1015, no. 3.

[10]. Stochițoiu, M.D., Uțu, I., - *Some aspects about using the modern high efficiency motors for driving the conveyor belts in lignite open pits*. Proceedings of the 7th International Symposium Occupational Health and Safety, SESAM, Poiana Brasov, Octombrie, 2015.

[11]. Uțu, I., Stochiţoiu M. D., *Voltage and current harmonics simulation*. Annals of University of Petroșani, 2015, pp. 53 - 60.

[12]. * * * *Drives simulation library. User's manual.*

[13]. * * * *Simulink. User's manual.*

Annals of the University of Petrosani, Electrical Engineering, 20 (2018)

ROMANIA'S ELECTRICITY MIX - ONE OF THE MOST BALANCED IN THE EUROPEAN UNION

MARIA DANIELA STOCHIȚOIU[1], ILIE UȚU[2]

Abstract: In nowadays the Romanian production structure keeps all kinds of energy production to coal, nuclear, hydro, and thermal from renewable. The objectives of the energy sector in Romania in accordance with the sustainable development are: providing the security of electricity and power supply for all consumers to an appropriate quality level, through diversification of generation sources, increasing the economic competitiveness and reduction of environmental impact.

Keywords: sustainable development, primary energy security of supply.

1. INTRODUCTION

For develop a sustainable economic growth, the main measurements that can be taken are in the National Energy System that can support the increasing security in energy supply through reducing the import dependence of energy. Energy and natural resources are the keys for launching the economy. Romanian energy evolution is in dependence with economy development but it is influenced by the evolution of energy and European Union economy [2].

The Romanian and European Union energy and geopolitical realities require the development of a new strategy till 2035 for enabling the provision for energy supplies needed a more efficient and secure operation of the National Power System, a more efficient electricity market in regional and European market and decreasing the dependence of imports [4].

2. ENERGY OBJECTIVES – FACTORS FOR SUSTAINING ECONOMY

Safe operation of power system is a priority even in the functioning of the electricity market, whether national, regional or European. An important problem of the European Union is the development of the single market for electricity and gas.

---

[1] *PhD., Associate Professor, Eng., University of Petrosani*
[2] *PhD., Associate Professor, Eng., University of Petrosani*

The objectives of the energy sector in Romania in accordance with the sustainable development are: providing the security of electricity and power supply for all consumers to an appropriate quality level, through diversification of generation sources, increasing the economic competitiveness and reduction of environmental impact. [3] More important is the sustainable development in assuring the energy needs nowadays on long term at the lowest price, suitable for a decent life and a modern economy taking into account the quality and safety supply. The sustainable development is based on:

- efficient using of primary energy sources;
- decreasing the negative impact of the energy on the environment through reducing of greenhouse gas;
- increasing the energy efficiency;
- promotion of electricity and heat in high efficiency cogeneration plants.[9]

The energetically intensity shows the energy PIB in relationship with national economy. The primary energy intensity is an indicator which characterizes economical efficiency of using the energy to a national level and is in dependence with the national economy results. That indicator has to turn to account with care when the energetically efficiency of technical problems are debated. The energetically intensity value is fundamental dependence by the calculation mode of PIB in Romania, typical for emerging economies. For developed countries the differences are insignificant. One of the main objectives for Romania is to rich an appropriate value of energetically intensity of developed countries, unconcerned of chosen measurement unit. This desideratum it is possible in condition as the Romanian economical results are almost like in developed countries.[4]

2.1. Forecast for the future

Romania's electricity mix is one of the most balanced in the European Union, with coal, hydropower, natural gas, nuclear energy and wind power having comparable shares of capacity and power generation (tab.1). With the exception of wind and solar, almost all units are fairly old. As of 2018, units over 50 MW have an average age of 39 years: 40 years for coal, 47 years for gas (some previously ran on coal), 31 years for hydropower and 18.5 years for nuclear. Although, the average capacity used to deliver to the system is around 7 GW, [1], [5].

Romania's energy sector has gone through several inflexion points in the past 20 years, marked by a wave of privatizations and attempts by the state to start new investment projects that have yet to materialize. In the gas sector, the eyes of investors are fixed on the Black Sea, where discovered deposits could help the country maintain its energy sufficiency for decades to come. Meanwhile, the sector requires an estimated EUR 10 billion in fresh investments on the long term to replace aging infrastructure. In the past decade, the country has fully liberalized the prices on the electricity market and on the gas market for consumers [6]. Through to 2021, gas prices for households should also be fully liberalized, according to the latest government targets.

In the electricity production sector, in close to two decades Romania has seen the gradual transition of the economy to cleaner production capacities. In 2004, coal had a share of 40 percent in Romania's electricity output, followed by hydrocarbons with 25,8% and hydro power with 24% . Nuclear energy had a share of 9% in the production mix, according to energy regulator ANRE. Overall electricity production has touched 56.91 TWh [7].

Table 1. ***Power generating capacity***

Net generating capacity GW		2018	2019	2020
Fossil Fuels				
	Lignite	2676	2626	3217
	Hard coal	0,428	0,428	0,428
	Gas	1831	1955	1845
	Mix fuels	1625	1625	1583
Total		**6559**	**6634**	**7072**
Renewable Energy Sources				
	Wind Power	3000	3150	3200
	Solar Power	1350	1420	1480
	Biomass Power	0,150	0,160	0,180
	Hydro	6436	6490	6505
Total		**10936**	**11220**	**11365**
	Nuclear Power	**1300**	**1300**	**1300**
TOTAL		**18795**	**19154**	**19737**

Fast forward to 2017 and close to 35% of Romania's electricity production came from renewable sources, mainly hydro power and wind capacities with shares of 23.42% and 11.64%, respectively (fig.1). The share of coal in the production mix has felt to 26.56%, while nuclear and natural gas capacities generated 18.11% and 15.22% of Romania's electricity respectively [8]. The country's electricity output has richened 61.3 TWh. Starting from 2011 the country has started to involve a massive influx of investments in the renewable sector. More than seven billion of euro went into green power production facilities. Capacities in the wind sector increased in six years from 826 MW to 3.1 GW at the end of 2017.[7]

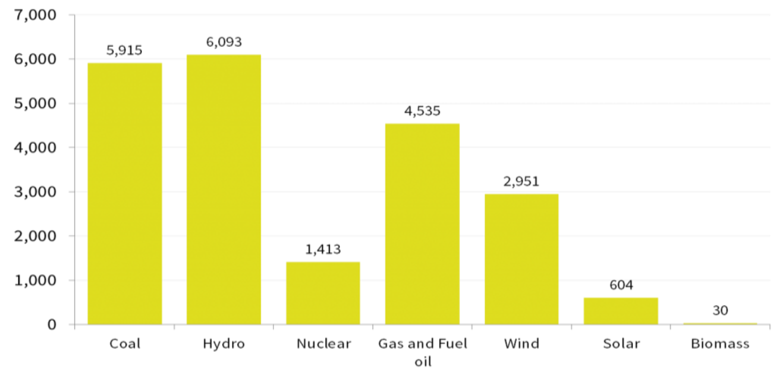

Fig.1 Installed capacity in MW

3. EXHAUSTIBLE COAL ENERGY RESOURCES

According to the expert, Romania could wean off coal dependency by relying increasingly on a mix of gas and nuclear to ensure the base load supply. Over the last two decades, coal mines have been shutting down in Romania every couple of years, as coal ran out or was becoming too expensive to dig out. None of the coal power plants are fully compliant with the Industrial Emissions Directive (two power plants benefited from derogation for NO_x emissions under the Accession Treaty, which expired on January 1st 2018), some are operating without an environmental (IPPC) permit and some of the hard coal units have emissions 10-15 times more than the allowed threshold for SO_x. There are also plans for a new 600 MW unit at Rovinari, being pursued more actively by Chinese government officials than by the Romanian authorities. There are two main coal companies, managing both power plants and mines: Oltenia Energy Complex manages 4 plants and 10 mines, all lignite-based, and it normally delivers 80% of the country's coal-based electricity. The main hard coal processing company, located in the neighboring county, is Hunedoara Energy Complex. Both companies are over-staffed, involved in corruption cases, and their finances depend on the success of other companies. 2017 was a bad year for hydropower and wind energy, therefore Oltenia Energy Complex made a hefty profit, while Hunedoara Energy Complex decreased its losses.[6]

4. CONCLUSIONS

Improvement of energy efficiency has an important role in achievement of security of supply; to sustainability and competitiveness and decreases the greenhouse gas emissions. Taking in consideration the effects of the commitments made for 2020 stage, Romania cannot afford to support a mandatory national target for energy efficiency and renewable sources for 2030 stage. Romania respects the EU objective of reducing greenhouse gas emissions.

REFERENCES

[1]. Belsky A. A., Skamyin A. N., Yakovleva E. V., *Configuration of a standalone hybrid wind-diesel photoelectric unit for guaranteed power supply for mineral resource industry facilities*, Int. J. Appl. Eng. Rese arch, vol. 1, no. 11, pp. 233–238, 2016.

[2]. Marcu M.D., Niculescu T., Slusariuc R.I., Popescu F.G., *Modeling and simulation of temperature effect in polycrystalline silicon PV cells*, International Conference on Innovative Research 2016 - ICIR Euroinvent 2016, Iasi 2016.

[3]. Marcu M., Niculescu T., Popescu F., Slusariuc R., *Incremental conductance algorithm used in a programmable microcontroller as maximum power point traker*, SGEM 2017 Conference Proceedings, Vol. 17, Albena, Bulgaria, pp. 369-376, 29 June-5 July 2017.

[4]. Stochitoiu M.D., *About the power generating plants demands as energy management feature*, Annals of electrical engineering, University of Petrosani, 2016.

[5]. www.energypost.eu

[6]. www..business-review.eu

[7]. www.jurnaldeafaceri.ro

[8]. www.ziarulfinanciar.ro

[9]. ****Univers ingineresc*, nr.19, 2018.

Annals of the University of Petrosani, Electrical Engineering, 20 (2018)

STUDY ABOUT THE CATHODIC PROTECTION AND DIAGNOSIS OF A BURIED GAS PIPELINE IN HUNEDOARA COUNTY

SUSANA ARAD[1], LILIANA SAMOILĂ[2], ILIE UȚU[3], FLORIN GABRIEL POPESCU[4], DUMITRU SFARLOAGA[5]

Abstract: The paper deals with an important issue concerning the corrosion of gas underground metallic pipelines. Some general consideration about the corrosion phenomenon are made and the main methods of anti-corrosive galvanic protection are presented. A cathodic protection station is presented and details about its use in monitoring the pipelines network are given. A specific pipeline in Hunedoara County is diagnosed.

Key words: corrosion, cathodic protection, diagnosis, pipeline.

1. INTRODUCTION

Machinery and metal constructions are exploited in the conditions of contact with different chemical-active environments: wet atmosphere, water, solutions of chemicals, industrial gases, etc.

Corrosion is the process of degradation and destruction in time of metals under the action of chemical, electrochemical or biochemical agents in the technological environment or the environment in which they are located. The degradation process begins at the surface of the metal and propagates into the mass of the material, which can lead to complete destruction of parts or subassemblies over time [3], [4].

Excepting the so-called noble metals, all other metals are unstable in contact with atmospheric air. The way this instability manifests, as well as the extent to which it occurs, depends on the nature of the metal and the aggressiveness of the environment. The damage caused to the world economy by corrosion reaches huge proportions, as an important amount of metal production is out of use due to corrosion. Damage due to corrosion is often related not only to direct metal losses but mostly to indirect losses through plant stagnation and repair or replacement of affected parts.

[1] *PhD, Professor, Eng., University of Petrosani, susanaarad@yahoo.com*
[2] *PhD, Associate Professor, Eng., University of Petrosani, branaliliana@gmail.com*
[3] *PhD, Associate Professor, Eng., University of Petrosani, ilieutu@ yahoo.com*
[4] *PhD, Lecturer, Eng., University of Petrosani, floringabriel82@yahoo.com*
[5] *PhD, Student, University of Petrosani*

The anti-corrosive galvanic protection methods are intended to protect against electrochemical corrosion of metal installations and structures, metal tanks, buried metal pipes, metal pillars, etc. Anticorrosive galvanic protection is achieved by cathodic polarization (the potential shift to negative values in the immunity area) called cathodic protection or anodic polarization (the shift of potential to passive values) called anodic protection [3].

These methods are [1], [2], [6]:

• cathodic protection with sacrificial anodes;
• cathodic protection with external power supply;
• anodic protection with external power supply;
• anode protection with protection cathode.

Cathodic (active) protection is one of the major means of reducing corrosion speed, especially in the case of large metal structures in contact with natural environments.

2. METHODS OF ANTI-CORROSIVE PROTECTION OF UNDERGROUND METALLIC PIPELINES

The degradation of the underground metallic networks (gas, oil, water, electric cables, etc.) produced by electrochemical underground corrosion leads to significant economic damage as well as to the risk of explosions and fires, with special social, economic and ecological implications. Corrosion protection measures are imperative for the reliability and long-term exploitation of underground networks [1]. These fall into two groups:

• passive protection, i.e. anticorrosive insulation with special materials;
• cathodic protection.

The classical protection system against corrosion of underground pipelines consists in covering them with insulating materials and applying cathodic protection. Only insulation coating is not sufficient to prolong the life of the pipeline. Cathodic protection is the one that applies to all insulated pipes.

Cathodic protection is one of the most cost-effective anticorrosive protection of large, costly installations and constructions with long service life. This method can be used to protect any kind of metallic structures such as underground metallic pipes, drilling platforms, ships, storage tanks and other equipment and is effective for combating both general and localized corrosion [2].

The cathodic protection of a metallic structure in contact with an electrolyte consists in shifting its electrical potential to a value more negative than the natural metal-soil potential (its equilibrium potential or base potential) after a sufficiently long contact with soil or water so that corrosion becomes thermodynamically impossible.

The choice of a cathodic protection system is made by the following criteria:

• electrical resistance of the soil;
• the state of the pipe insulation;
• cost of protection.

3. MONITORING THE WORKING CONDITIONS OF THE PIPELINES CATHODIC PROTECTION SYSTEMS

The monitoring of the operating conditions of the cathodic protection systems (Fig. 1) of the natural gas transport pipelines consists in the follow up, the surveillance and the systematic gathering of information on the state of the protection against corrosion.

The monitoring of cathodic protection status is an integral part of the Pipeline Network Security Management System [5] and has the main objectives:

• Preventing and avoiding damage to the components of the pipelines Cathodic Protection System (CPS) that would affect the safe operation of the pipeline;

• promptly detecting the damages in order to make decisions for their operative solving.

• pipeline-soil potential on the pipeline which is protected by an injection station or galvanic anode;

• the technical state of the outer insulation on the pipe line by performing intensive potential measurements using one or more specific methods, as well as by direct measurements (thickness, adhesion, specific strength, continuity);

• the technical condition of the outer insulation in the area of the air crossings and valves, traps, the underground separators along the pipeline;

• the technical state of the electrical separations to the aerial crossing support elements, obstacles under passages provided with protective tubes, insulating joints;

• resistivity of the soil along the pipeline.

Monitoring includes activities that capture signals from the cathodic protection system related to functional parameters. These signals are not only those indicated by the equipment mounted on the cathodic protection stations, but also those resulting from the planned measurements taken along the pipeline.

It is necessary to monitor the parameters and conditions that may lead to the materialization of time-dependent hazards (corrosion processes, damage to the electrical and electronic components of the CPS, etc.), but also the parameters and conditions that can create time-independent hazards (unauthorized third-party interventions, landslides, floods, earthquakes) that cause CPS components to fail or rapid and significant damage to their normal and safe operation [6].

Verification of the technical state of the CPS and the assessment of its integrity must be carried out periodically throughout its lifetime [7].

Defects detected on CPS components are subject to evaluations using appropriate methods and equipment. Based on these evaluations it is determined whether defects do not intolerably affect the functionality of the component and therefore do not require the follow up and / or subsequent application of corrective maintenance. If the defects have significant negative influences on the functional capacity of the components, appropriate surveillance and corrective maintenance measures be taken.

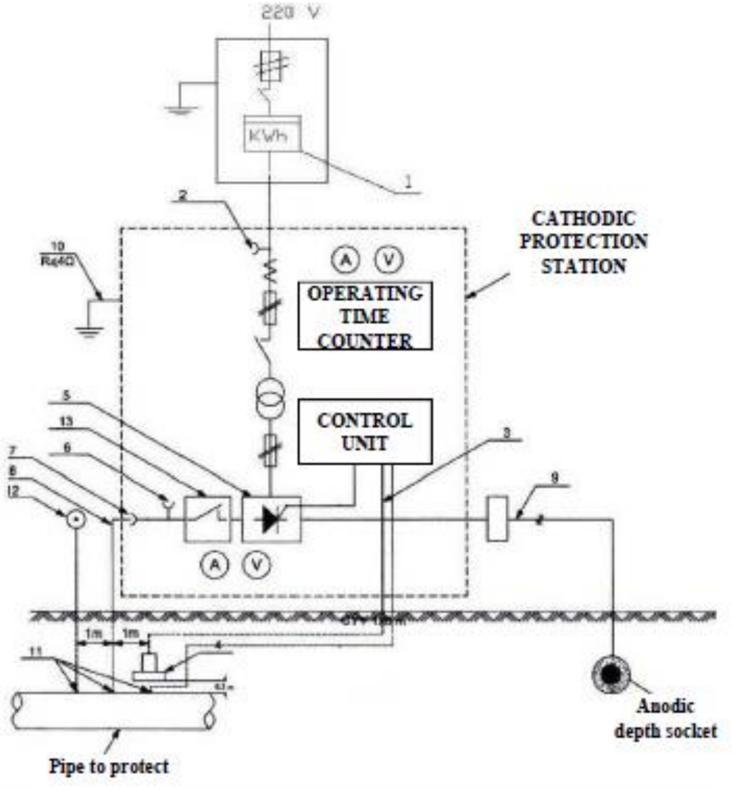

Fig. 1 Schematic of a cathodic protection station
1 - Single-phase electric counter. 2 - Socket for measuring the supply voltage. 3 - Copper conductor, 4 - Cu / CuSO4 permanent reference electrode. 5 - Transformer-rectifier set. 6 - Socket for measuring the rectified voltage. 7 - Socket for measuring the protection current intensity. 8 - Grounding conductor. 9 - Cyclic circuit breaker. 10 - Electrical cable for connection to the buried metal pipe, 11 - Anodic connection cable, 12 - Potential outlet

4. DIAGNOSIS OF THE PIPELINE SECTION BETWEEN ORASTIE AND BACIA

The general pipework data are:
- Diameter: Ø 20"
- Year of commissioning: 1962
- Operating pressure: 40 bar
- Length: 19.5 km

The general working data of the cathodic protection stations in the inspected area during the measurements are presented in Table 1.

Table 1 ***General data for the operation of the cathodic protection stations***

CPS Name	Injection voltage [V]	Injection current [A]	Potential ON [mV]	Potential OFF [mV]
CPS Orăştie	46	4	1100	900
CPS Spini 2	11,2	17,4	2250	1200

Intensive potentiometric measurements were performed using the Quantum CIPS instrument and CPS temporarily installed in the measuring area on the Vest 2 pipeline, on the synchronization sequence 4 sec ON / 1 sec OFF under temperature conditions of 30-35 °C, dry soil and grown vegetation.

Intensive potential measurements were made on the above-mentioned section on a length of 19,500 m, according to the data provided by the Quantum GPS equipment.

Following the intensive field measurements, it resulted the potential diagram ON / OFF (fig. 2).

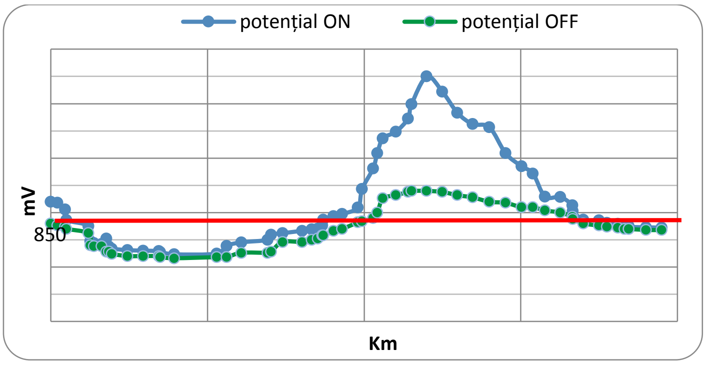

Fig. 2 Potential diagram along the main pipeline

Throughout the pipeline, soil resistivity measurements were made, whose results are presented in fig. 3.

To measure the soil resistivity, a Megger Det 5/4 R appliance was used, with the measuring range of 0.02 - 20 kΩ (measurement uncertainty 0.3 Ω) [8]. The next formula was used to determine the soil resistivity:

$\rho = 2\, \pi\, a\, r\, k$ [Ωm];

where: a - distance between the electrodes; r - the indication of the appliance; k - coefficient which varies with the degree of freezing of the soil (k = 0.9 for thawed soil and k = 0.65 for frozen soil).

For the interpretation of soil aggressiveness following soil resistivity measurements we used Table 2.

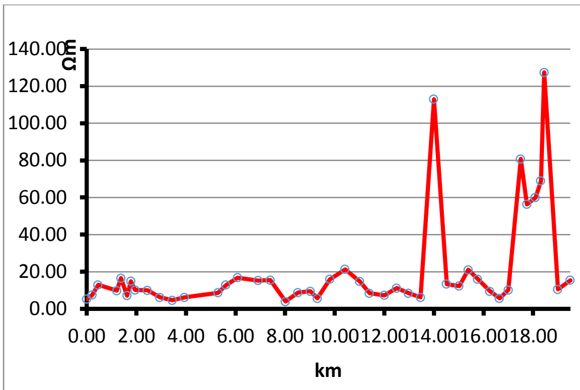

Fig. 3 Soil resistivity diagram

Table 2 ***Soil aggressiveness interpretation***

Indication	**Soil aggressiveness**
0 – 5	Very high aggressiveness
5 – 20	High aggressiveness
20 – 100	Medium aggressiveness
> 100	Low aggressiveness

5. CONCLUSIONS

The measurements along the pipeline gave that it mostly passes through a soil with high aggressiveness, according to the norm in force.

Interpreting the potential measurements, one can see some insulation defects, which are located in an area where the soil has high and very high aggression. Pipeline potential along the insulation faults has values below the corrosion protection limit (-850mV).

REFERENCES

[1]. Ionescu C., Matei A., Moldovan C., *Electrochimie si coroziune,* Universitas Publishing House, Petroşani, 2009.

[2]. Koptev V. Y., Kopteva A. V., *Structure of energy consumption and improving open-pit dump truck efficiency*, IOP Conf. Ser. Earth Environ. Sci., vol. 87, p. 022010, Oct. 2017.

[3]. Kopteva A. V, Voytyuk I. N., *The algorithm of measuring parameters of separate oil streams components*, IOP Conf. Ser. Mater. Sci. Eng., vol. 177, p. 012006, Feb. 2017.

[4]. Samoila L., Arad S., *Materiale electrotehnice. Caracteristici şi utilizări.* Universitas Publishing House, Petroşani, 2001.

[5]. Stochitoiu M.D., *About the power generating plants demands as energy management feature,* Annals of electrical engineering, University of Petrosani, 2016.

[6]. Technical rules for the maintenance of pipelines.

[7].http://new.transgaz.ro/ro/clienti/sistemul-de-transport/norme-tehnice-de-mentenanta

[8]. http://www.biddlemegger.com/biddle-ug/

Annals of the University of Petrosani, Electrical Engineering, 20 (2018)

ELECTRO-DYNAMIC FORCES IN SHORT CIRCUIT REGIME USING MATLAB - SIMULINK SOFTWARE

TITU NICULESCU[1]

Abstract: Nowadays, computer simulation is more and more used in engineering applications. Powerful IT software helps researchers from all engineering branches to gain fast and accurate results. One of these tools is represented by the MATLAB software package which is a powerful tool used worldwide in electrical engineering. The key features of MATLAB are matrix-oriented programming, excellent plotting capability and the included graphical environment – Simulink – which highly simplifies the control scheme design. This paper focuses on the MATLAB-Simulink software application for studying electro-dynamic forces. The single-phase short circuit and the three-phase short circuit are presented and for these situations the graphical correlation between these forces and time are presented for transitory phenomena. Simulation models and theoretical basement are presented also.

Keywords: electro-dynamic force, model, simulation, single-phase short circuit, three-phase short-circuit.

1. SINGLE-PHASE SHORT CIRCUITS

The electro-dynamic forces result in the distribution and transport of electric energy with two conductors and with three conductors when the short circuit occurs between three conductors [3], [11]. The mathematical expression of electro-dynamic forces for the transitory regime is:

$$F = CI^2(e^{-\lambda t} - \cos\omega t)^2 \tag{1}$$

Where λ is the equivalent time constant, and:

$$C = \frac{\mu_0}{2\pi} \cdot \frac{l}{a} \cdot \varphi_{CD} \cdot \varphi\left(\frac{a}{l}\right) \tag{2}$$

[1] *Ph.D., Associate Prof. Eng., University of Petroşani*

In equation (2) φ_{CD} is a function which depends on Dwight's diagrams, and:

$$\varphi\left(\frac{a}{l}\right) = \sqrt{1 + \frac{a^2}{l^2}} - \frac{a}{l} \tag{3}$$

where "l" is the length of the conductors and "a" is the distance between them.

Circuit Simulation Model: The explicit function (1) leads to the simulation model from (Fig.1), which generated the explicit diagram for dependence between electro-dynamic force and time (Fig.2) [8], [10]. The explicit diagrams have been obtained for specific values of the circuit parameter as follows:

$R = 100\Omega$; $L = 2H$; $l = 100m$; $a = 0.5m$; $\varphi_{CD} = 0.8$; $I = 100A$.

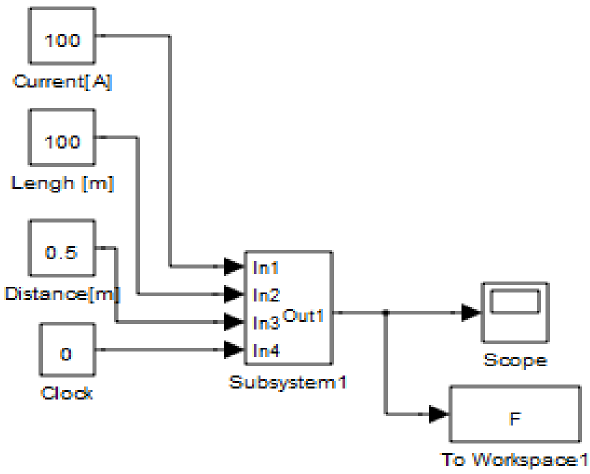

Fig.1. Simulink model for single-phase short circuit

The subsystem 1 is shown in Figure 8.

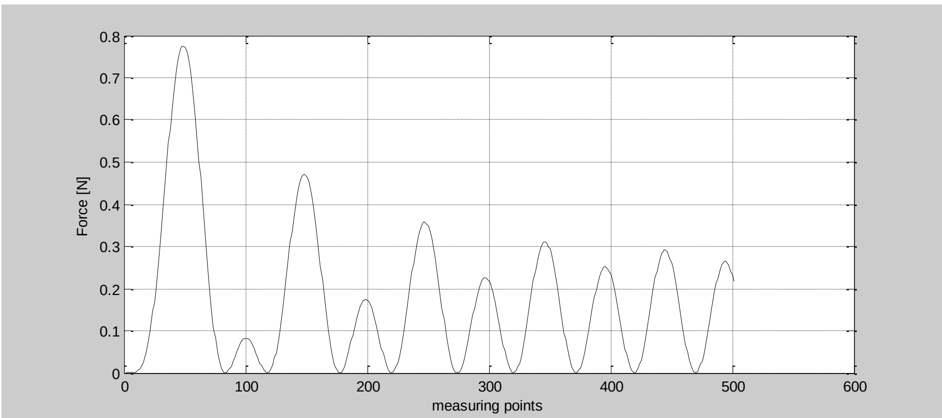

Fig.2. Force diagram for single-phase short circuit

2. THREE-PHASE SHORT CIRCUITS

The electro-dynamic forces occur in the transport and distribution of energy in three-phase systems. Short circuit is performed between the three active conductors of the system [2]. In Fig. 3 we have the case of three parallel conductors, the location and sign convention for the forces exerted on the median conductor, respectively on a side conductor [9].

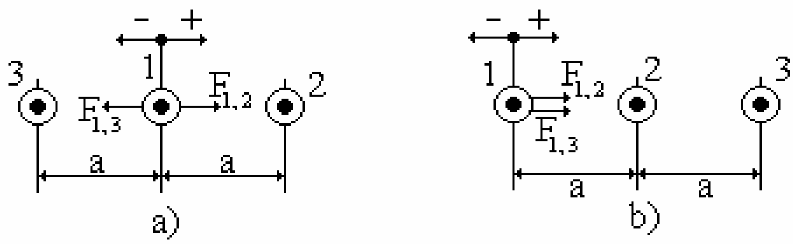

Fig.3. Disposition of conductors in the same plane: a) Forces exerted on the median conductors b) Forces exerted on the side conductor

Force Exerted on the Median Conductor: If a short circuit between conductors is performed in three phase system, the electro-dynamic force acting on the median conductor is [5]:

$$F_m = C \cdot i_1 \cdot (i_2 - i_3) \tag{4}$$

with the expressions of currents in the three conductors:

$$\begin{cases} i_1 = \hat{I} \cdot \left[e^{-\lambda t} \cdot sin\,\alpha + sin(\omega t - \alpha)\right] \\ i_2 = \hat{I} \cdot \left[e^{-\lambda t} \cdot sin\left(\alpha + \frac{2\pi}{3}\right) + sin\left(\omega t - \alpha - \frac{2\pi}{3}\right)\right] \\ i_3 = \hat{I} \cdot \left[e^{-\lambda t} \cdot sin\left(\alpha - \frac{2\pi}{3}\right) + sin\left(\omega t - \alpha + \frac{2\pi}{3}\right)\right] \end{cases} \tag{5}$$

The force exerted on the median conductor is obtained by inserting the expressions of currents presented in equation (5) into equation (4):

$$F_m = C \cdot \hat{I}^2 \cdot \left[e^{-\lambda t} \cdot sin\,\alpha + sin(\omega t - \alpha)\right] \cdot \left[e^{-\lambda t} \cdot sin\left(\alpha + \frac{2\pi}{3}\right) + \right.$$

$$\left. sin\left(\omega t - \alpha - \frac{2\pi}{3}\right) - e^{-\lambda t} \cdot sin\left(\alpha - \frac{2\pi}{3}\right) - sin\left(\omega t - \alpha + \frac{2\pi}{3}\right)\right] =$$

$$= C\cdot \hat{I}^2\cdot\left[e^{-\lambda t}\cdot sin\alpha + sin(\omega t-\alpha)\right]\cdot\left\{e^{-\lambda t}\cdot\left[sin\left(\alpha+\frac{2\pi}{3}\right)-\right.\right.$$

$$\left.\left.-sin\left(\alpha-\frac{2\pi}{3}\right)\right]+sin\left(\omega t-\alpha-\frac{2\pi}{3}\right)-sin\left(\omega t-\alpha+\frac{2\pi}{3}\right)\right\}=$$

$$= C\cdot \hat{I}^2\cdot\left[e^{-\lambda t}\cdot sin\,\alpha + sin(\omega t-\alpha)\right]\cdot\left[e^{-\lambda t}\cdot\left(-\frac{1}{2}\cdot sin\,\alpha+\right.\right.$$

$$\left.\frac{\sqrt{3}}{2}\cdot cos\,\alpha+\frac{1}{2}\cdot sin\,\alpha+\frac{\sqrt{3}}{2}\cdot cos\,\alpha\right)-\frac{1}{2}\cdot sin(\omega t-\alpha)-$$

$$\left.\frac{\sqrt{3}}{2}\cdot cos(\omega t-\alpha)+\frac{1}{2}\cdot sin(\omega t-\alpha)-\frac{\sqrt{3}}{2}\cdot cos(\omega t-\alpha)\right]$$

and finally, the relation becomes:

$$F_m=\sqrt{3}\cdot C\cdot \hat{I}^2\cdot\left[e^{-\lambda t}\cdot sin\,\alpha+sin(\omega t-\alpha)\right]\cdot\left[e^{-\lambda t}\cdot cos\alpha-cos(\omega t-\alpha)\right]$$

The maximum force occurs for the angle $=\frac{\pi}{4}$. The final force expression is:

$$F_m=\frac{\sqrt{3}}{2}\cdot C\cdot \hat{I}^2\cdot\left[e^{-\lambda t}+sin\,\omega t-cos\,\omega t\right]\cdot\left[e^{-\lambda t}-sin\,\omega t-cos\,\omega t\right] \qquad (6)$$

The simulation model of the force is presented in Fig. 4 and the generated diagram in Fig.5.

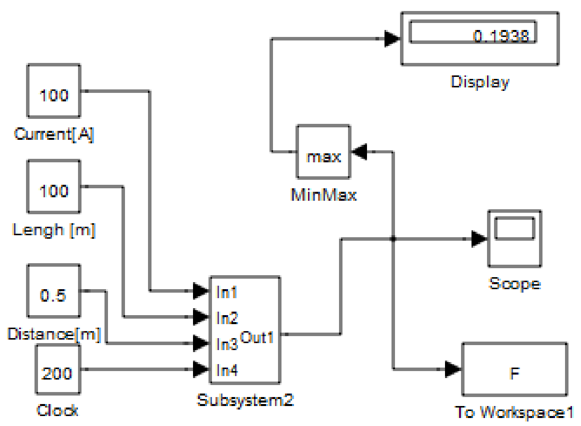

Fig.4. Simulink model for three-phase short circuit, median conductor

Subsystem 2 is shown in Fig. 9.

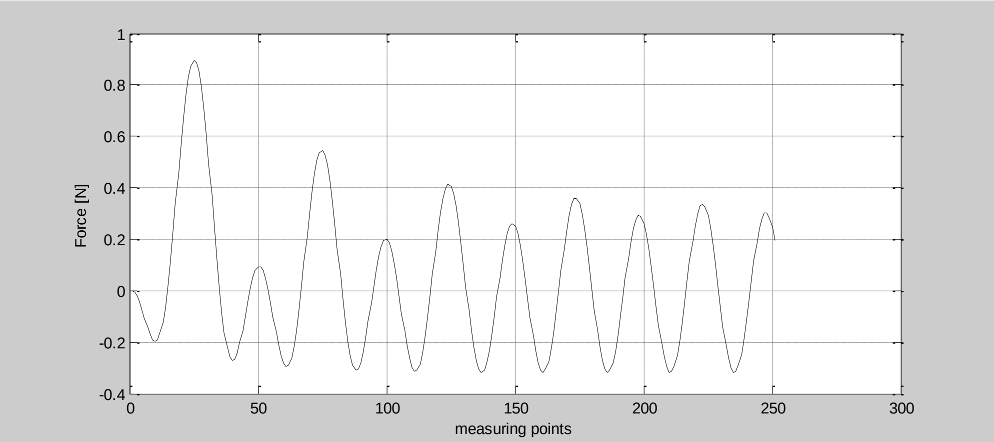

Fig.5. Force diagram for three-phase short circuit, median conductor

Force Exerted on the Side Conductor: If a short circuit between occurs between the conductors of a three phase system, the electro-dynamic force acting on the side conductor is [6]:

$$F_l = C \cdot i_1 \cdot \left(i_2 + \frac{i_3}{2} \right) \tag{7}$$

If the previous calculation method is applied, this force becomes:

$$F_l = -\frac{\sqrt{3}}{4} \cdot C \cdot \hat{I}^2 \cdot \left[e^{-\lambda t} \cdot sin\,\alpha + sin(\omega t - \alpha) \right] \cdot$$
$$\cdot \left[e^{-\lambda t} \cdot \left(\sqrt{3} \cdot sin\,\alpha - cos\,\alpha \right) + \sqrt{3} \cdot sin(\omega t - \alpha) + cos(\omega t - \alpha) \right] \tag{8}$$

The simulation model of the force is presented in Fig. 6 and the generated diagram is presented in Fig.7 [7].

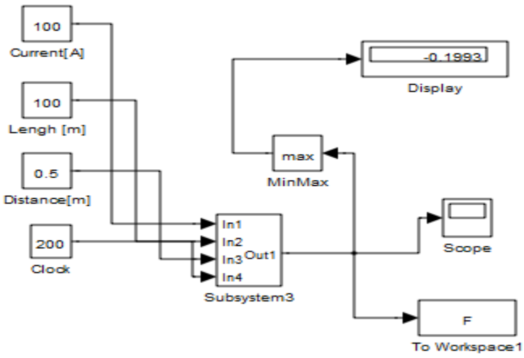

Fig.6. Simulink model for three-phase short circuit, side conductor

Subsystem 3 is shown in Figure 10.

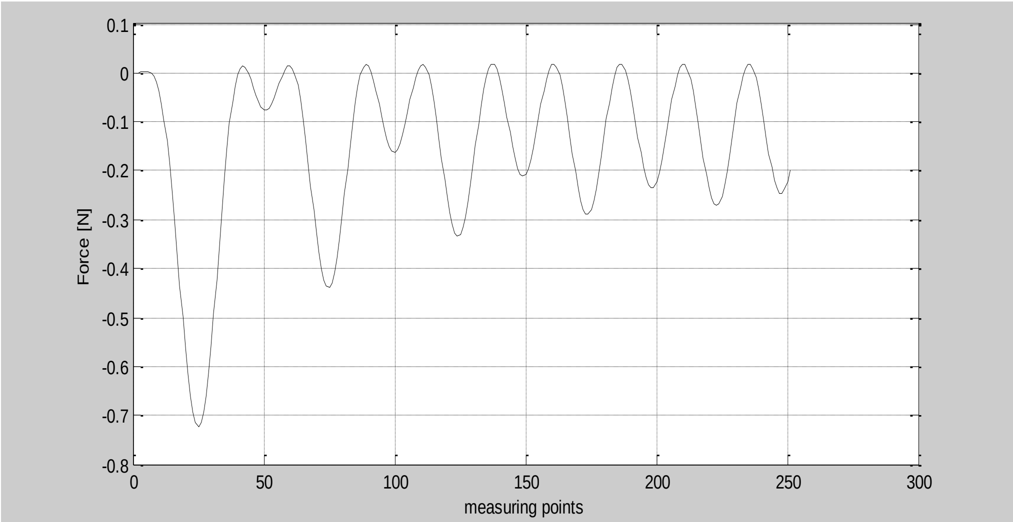

Fig.7. Force diagram for three-phase short circuit, side conductor

Simulation models have been designed so that input quantities are grouped separately to be modified and thus allow study of the influence of each input parameter on electro-dynamic forces for each situation [1], [4]. Each simulation model includes one subsystem. The three subsystems are presented below:

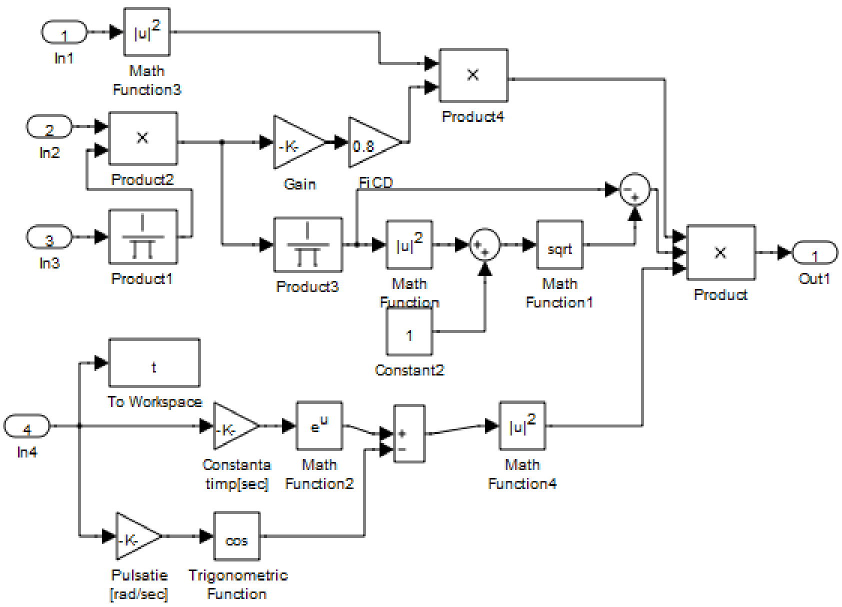

Fig.8. Subsystem 1

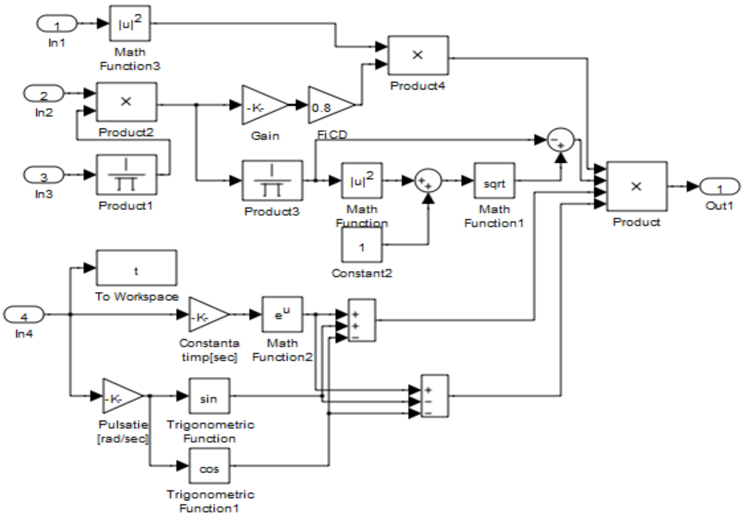

Fig.9. Subsystem 2

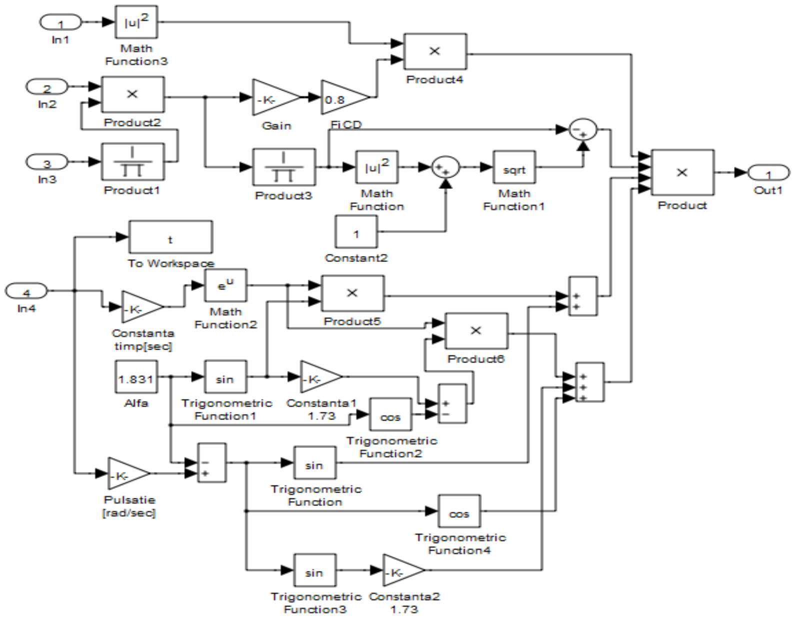

Fig.10. Subsystem 3

3. CONCLUSIONS

In single-phase short circuits, the highest mechanical strain for devices occurs at the beginning of the transient regime, when the shock occurs (highest a-periodic component) after which the current gradually decreases. From the simulations there may be observed that pulsations of force are uneven during the transient short-circuit and become equal after a sufficiently long period of time.

In case of three-phase short circuits, the forces on the median conductor are pulsed, in both directions. It is noticed that unlike the case of single-phase short circuit, for this one, the senses of force don't remain the same, but change over time. The amplitude of the force reaches the highest value at the beginning of the transient regime, after which it stabilizes until it reaches the steady state value.

For three-phase short circuits, the amplitude of the force in this system is much higher than the steady state value, but the dominant action is the same: pushing outward the lateral conductors system.

REFERENCES

[1]. Halunga-Fratu S., Fratu O., Simulating analogic and digital transmission systems using MATLAB/Simulink, (in Romanian), Matrixrom Publishing House, Bucharest, Romania, 2005.

[2]. Saracin C.G., *Electrical Installations*, (in Romanian), Matrixrom Publishing House, Bucharest, Romania, 2008.

[3]. Golovanov N. et al., *Electricity consumers. Materials, Measurements, Devices, Installations*, (in Romanian), AGIR Publishing House, Bucharest, Romania, 2009.

[4]. Niculescu T., *Analysis of electrical circuits through MATLAB simulation*, (in Romanian), Focus Publishing House, Petrosani, Romania, 2006.

[5]. Tudorache T., *Calculation environments for electrical engineering*, (in Romanian), Matrixrom Publishing House, Bucharest, Romania, 2006.

[6]. Surianu F.D., *Industrial electrical networks*, (in Romanian), Orizonturi Universitare Publishing House, Timisoara, Romania, 1999.

[7]. Niculescu T., Niculescu M., *The study of fundamental electrical circuits transitory phenomena using MATLAB software*, International Multidisciplinary Symposium Universitaria SIMPRO 2010, Electrical Engineering and Energetics System Control, Applied Informatics and Computer Engineering, Petrosani, Romania, 2010.

[8]. Pasculescu V.M., Radu S.M., Pasculescu D., Niculescu T., *Dimensioning the intrinsic safety barriers of electrical equipment intended to be used in potentially explosive atmospheres using the SimPowerSystems software package*, 13th International Multidisciplinary Scientific Geoconferences SGEM, Albena, Bulgaria, 2013.

[9]. Samoila, L., Arad, S., Petre, M., *Application for simulating the short-circuit current and the transient recovery voltage*, IEEE 16th International Conference on Environment and Electrical Engineering (EEEIC), pp. 2159-2163, Florence, Italy, 2016.

[10]. Uţu, I., Samoilă L., *Măsurarea mărimilor electrice*, Editura Universitas, Petroşani, 2010.

[11]. Uţu, I., Păsculescu, D., *Power Quality Study in Order to Comply with European Norms*. Publicat in Revista Calitatea, Supplement of "Quality - Access to Success" Journal, Vol.18, S1, January 2017, ISSN 1582-2559, pag. 366-371.

Annals of the University of Petrosani, Electrical Engineering, 20 (2018)

DESIGN AND IMPLEMENTATION OF A 360° IMAGING SYSTEM AND ANDROID APPLICATION FOR REMOTE CONTROL

LORAND BOGDANFFY[1], GABRIEL ILCEA[2]

Abstract: The panoramic photograph has been used for some time, even before the digital era, the classic method being the merging of several photos to obtain a very wide field of view. With the advent of digital cameras, smartphones, much has been done to create photos with a wide field of view, even 360° panoramas, but sometimes, especially with phone cameras, quality is below acceptable.

This paper focuses on making a remote controlled rotating support system for a large DSLR camera in order to take high quality, very high resolution 360° panoramic images for businesses or institutions where a professional solution is needed.

Keywords: 360 imaging, panorama, android, software, hardware.

1. INTRODUCTION

This paper proposes an automated high quality panorama image creating system, composed from multiple images, controllable from any Bluetooth smartphone with Android operating system. The main advantages are:

- After the initial positioning and adjustment of the machine settings, a button is pressed and everything is done automatically, 150 photos being effortlessly made, the speed being approximately one picture at 2-3 seconds (30 pictures per minute, 150 pictures in 5 minutes) at least 10 times faster than manually repositioning the camera. The advantage of short a time span between consecutive frames significantly reduces the possibility of scene changes that may occur during capture of images.
- Control of accurate device rotation and automatic capture minimize the risk of errors, such as missing certain areas in the panorama.

The hardware part of the application was made by using largely recycled components such as stepper motors and toothed wheels from disused printers and other parts that I adapted to my installation.

[1] *PhD., Assistant Prof., Eng., University of Petroşani*
[2] *Ph.D., Eng., Energy Complex Hunedoara*

2. CONCEPT AND IMPLEMENTATION

Panoramic photography is a technique of photography, using specialized equipment or software, that captures images with horizontally elongated fields of view. It is sometimes known as *wide format photography* [2].
Required components for obtaining a stitched panorama (from multiple images):
1. Camera;
2. Tripod, tripod head;
3. Stitching software, available online.

Additional components for automating the process:
- Hardware components:
  - PIC16F88 or PIC16F877 Microcontroller;
  - BTM-222 Bluetooth Module (Class 1) for remote communication;
  - Mitsumi M42SP-7 stepper motor for driving the assembly;
  - CNY-74 – optocoupler for isolation of the camera's tripping circuit from the electrical side of the mounting;
  - ULN2003A Integrated with 7 Darlington gates for step-up motor amplification, each with a capacity of 500mA, for driving the motor.
- Software:
  - Microcontroller program;
  - Android program, for controlling the system.

The camera, that can be triggered electronically, shown in the next part.

In order to trigger the DSLR camera shutter, you need to close two of the camera's circuits, one for auto-focus, the other for exposure. The manual triggers function as a switch that activates each stage. (this was tested o a Nikon camera)

Table 1. ***Trigger the DSLR***

Trigger logic		
Focus	Trigger	Result
0	0	-
0	1	-
1	0	Camera focuses
1	1	Camera shutter is released

The use of an optocoupler, and two gates are needed to perform the focus / trigger operation.

Features of CNY-74
- CNY74-2 includes 2 insulating channels;
- CNY74-4 includes 4 insulating channels;
- DC test voltage of insulation VIO = 2.5 kV;

- Test class 25/100/21 DIN 40 045;
- Low coupling capability of 0.3 pF typical;
- Current Transfer Ratio (CTR) typical 100%;
- Low CTR coefficient;
- Wide range of usable ambient temperature.

The PIC16F877 microcontroller controls tripping and is also used for stepper motor control.

Communication with the Bluetooth module is achieved by linking the RX / TX pins of the microcontroller to the TX / RX pins of the Bluetooth module.

Optionally to reduce the size is enough to use an 18-pin microcontroller like PIC16F88 that has a RS232 hardware port.

The Mitsumi M42SP-7 is a single-pole stepper motor with a common yarn and four windings, which takes 48 steps to complete the rotor's rotation.

Features of the M42SP-7 motor

- Rated voltage - DC 12V;
- Usable voltage - DC 10.8 ~ 13.2V;
- Rated current / phase - 259mA;
- Number of phases - 4;
- DC coil resistance - 50Ω / phase ± 7%;
- Step angle - 7.5˚;
- Driving Method 2-2 (Unipolar);
- Class isolation - Class E;
- Holding torque - 49.0mN · m;
- Pull-out couple - 23.5mN · m / 200pps;
- Pull-in torque - 19.6mN · m / 200pps;
- Frequency max. pulse pulse-out - 600pps;
- Frequency max. pulse pulses – 420pps.

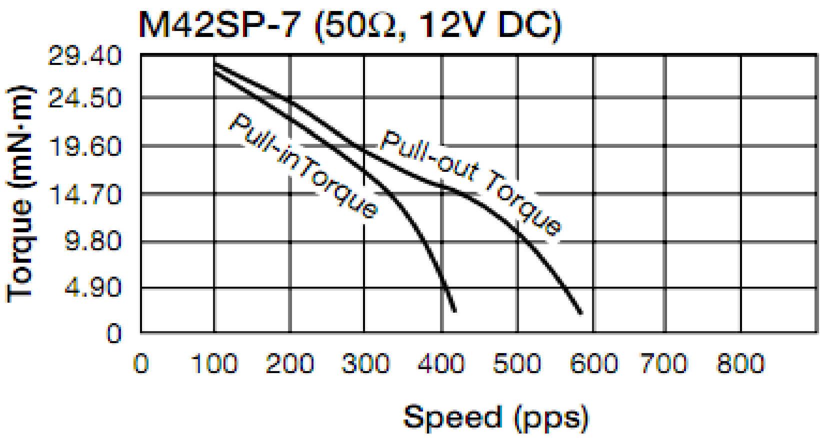

Fig.1. Torque/Speed graph

Between the motor and the microcontroller we used the integrated ULN2003A that has the following features:

- Max. collector-emitter 50 V;
- Input voltage, VI 30 V;
- Collector maximum current 500 mA;
- Output current limitation, IOK 500 mA;
- Emitter-terminal total current -2.5 A.

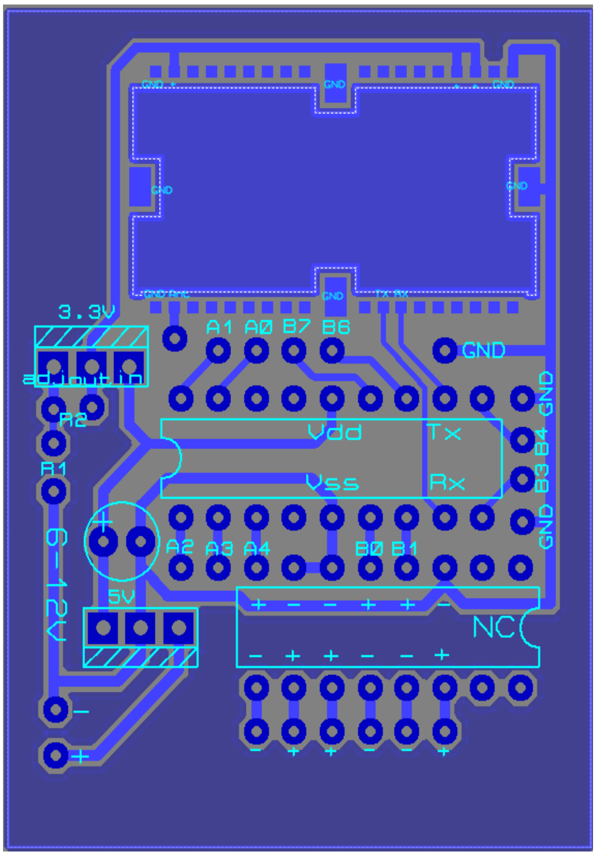

Fig. 2. Complete hardware trace design

A number of four commands were programmed to be transmitted:

• Shutter - with parameters: focus time (0-99 seconds / 10), exposure duration (0-99 seconds), number of exposures (0-999), exposure delay (0-99 seconds);

• Rotation - with parameters: Number of steps (1-9999, one step means 0.2 degrees, one degree = 5 steps, a complete rotation = 1800 steps), delay between steps (0-99 milliseconds), and last but not least (trigonometric and vice versa);

• Auto-panorama - with parameters: total angle (degrees), focal length of the lens (mm), delay time before exposure (0-99 sec / 10) and of course the direction;

• Cancel - at any time if the Cancel button is pressed, the execution of any command is interrupted.

Due to this communication method, once a command is sent, it is executed by the MC even if the wireless connection is interrupted for various reasons.

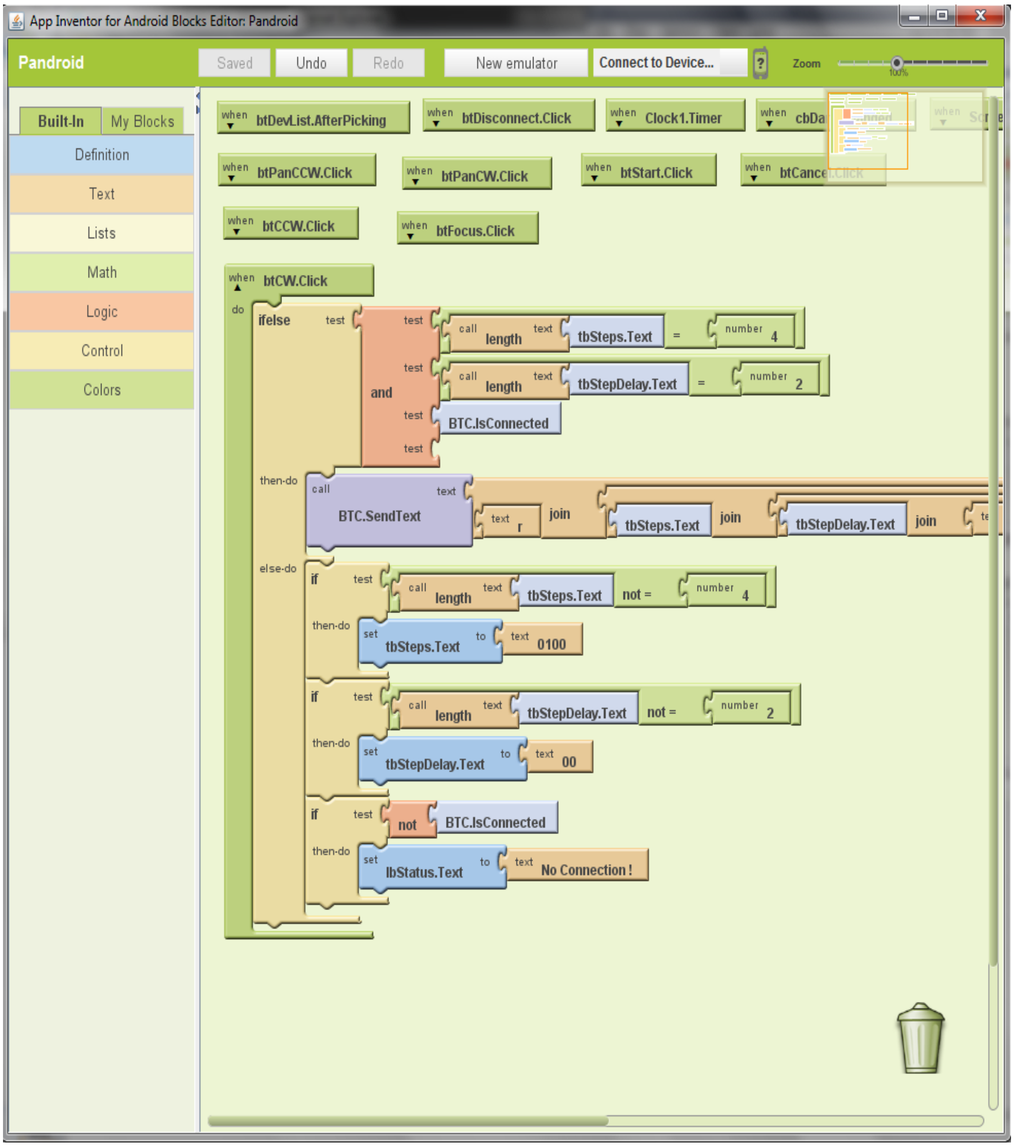

Fig.3. Appinventor complete interface, and click function

Before any transmission can occur between Android Smartphone and microcontroller, the devices must be paired, and a connection must be established. This is the first priority, after powering up the devices.

After that, the controller listens to input from the smartphone, and recognizes the four commands mentioned before. Some of which come with parameters. An example of such a command is given in figure 3.

A good practice is using the microcontrollers interrupts so that receiving commands will work even if the µC is busy carrying out its main task. This is especially important to be able to cancel a running task.

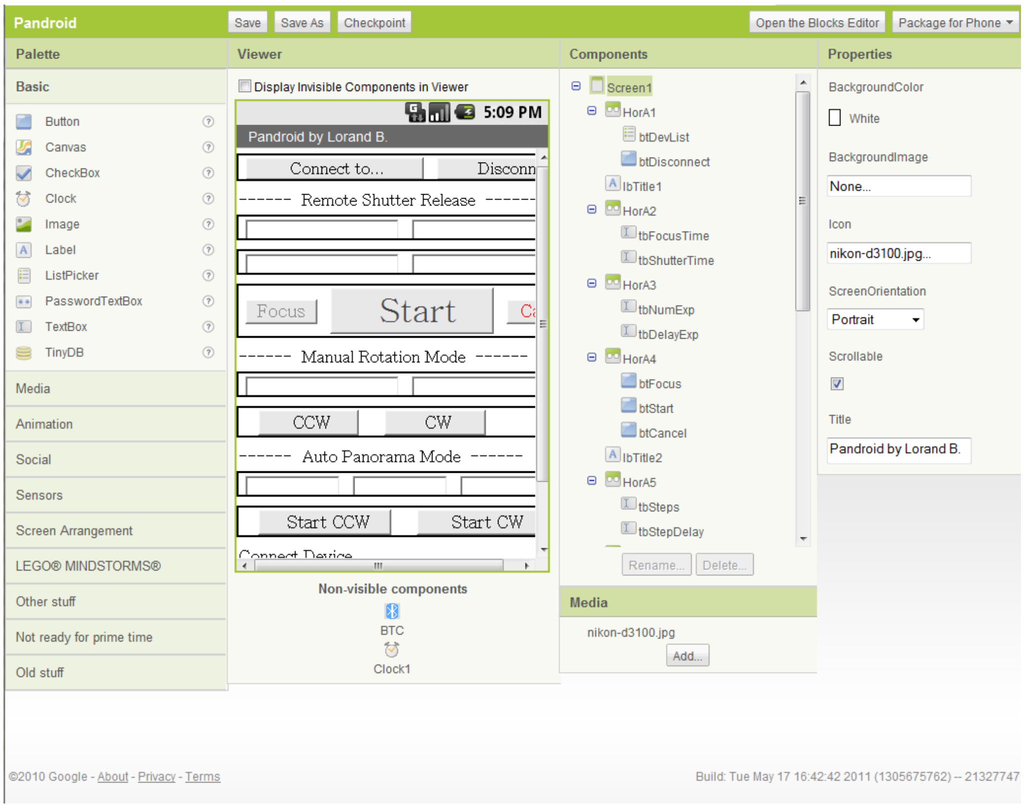

Fig. 2. Designing the interface

```
#int_RDA
void  RDA_isr(void)
{
  ch=getc();
  if (ch=='c')
  {  cancel=1;
     return;
  }
  if (executing==0) switch (ch)
  {
    case 's':{start=1;
          break;}
    case 'm':{startm=1;
          break;}
    case 'a':{starta=1;
          break;}
    default:{data[nrChars]=ch;
          nrChars+=1;
          break;}
  }
```

The above section of code reads and recognizes one of the 4 types of commands. Because it has to run very fast, real-time, as it is attached to an interrupt, the instructions for each command are described in separate functions that are called from within the function handling the interrupt.

The next section is a function to manually position the system. After a parsing sequence, according to the data received, the motor is driven in the direction and to the angle required.

```
void manualMove()       //-------------------
manualMove------------------------
{
  if (nrChars!=7)
  {  data="";
    nrChars=0;
    return; }

  int16 i=0;
  executing=1;

//    Start data parse
  direction=data[0];
  steps=steps+((int16)(data[1]-48))*1000;
  steps=steps+((int16)(data[2]-48))*100;
  steps=steps+(data[3]-48)*10;
  steps=steps+(data[4]-48);
  wait=wait+(data[5]-48)*10;
  wait=wait+(data[6]-48);
//    end of data parse

  nrChars=0;        // resetare nrChars
  data="";          // resetare data

  if (direction=='l')
  {
    for (i=1;i<=steps;++i)
      {
        if (cStep==step4) cStep=step1;
        else cStep=cStep+1;
        output_high(cStep);
        delay_ms(10);
        output_low(cStep);
        if (wait>0) delay_ms(wait);
        if (cancel==1) break;
      }
  }
  if (direction=='r')
  {
    for (i=1;i<=steps;++i)
      {
        if (cStep==step1) cStep=step4;
        else cStep=cStep-1;
        output_high(cStep);
        delay_ms(10);
        output_low(cStep);
        if (wait>0) delay_ms(wait);
        if (cancel==1) break;
      }
  }

  steps=0;
  wait=0;
  startm=0;
  executing=0;
}
}
```

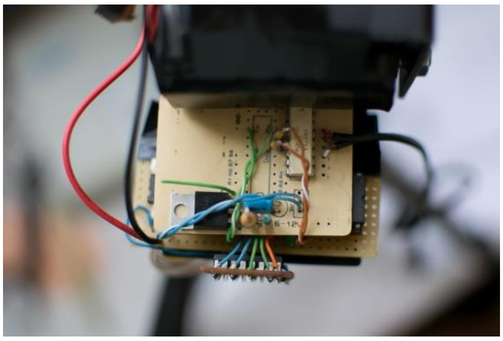

Fig. 5. System close-up, top view

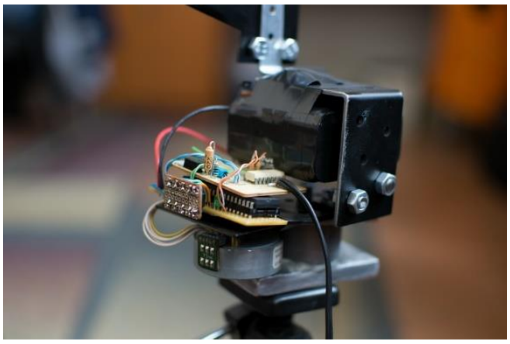

Fig.6. System close-up, side-view

3. CONCLUSIONS

The prototype system lacks a professional mechanical build, but that was not the main purpose, instead we managed to create a communicating system from mostly scrap and recycled material.

Other than that, it's a perfectly usable system, in a real environment as shown with the below results. The programming is the strong point of the system, and required the most effort. The complete program isn't presented in the paper.

To create the final image, from the many images taken with the system, a software is needed for stitching. We chose "Panorama Tools", an open source solution for stitching large panorama images.

The images obtained, if created on a high performance PC, with at least 16 GB of RAM, can be as large as in the scale of GigaPixels.

Fig. 3. Spherical panorama obtained with the system

REFERENCES

[1]. Jones D. W., *Control of Stepping Motors*, 1995 **http://www.yertiz.com/cnc/steppermotor.pdf**

[2]. Kang S. B., Benosman R., *Panoramic vision: sensors, theory, and applications*, Springer, ISBN 978-0-387-95111-9, 2001.

[3]. Pal S., Tripathy N. S., *Remote Position Control System of Stepper Motor Using DTMF Technology*, International Journal of Control and Automation, Vol. 4, No. 2, pp.35-42, June, 2011.

[4]. *** *Documentația tehnică a circuitului integrat ULN2003A*, Texas Instruments, 2016.

Annals of the University of Petrosani, Electrical Engineering, 20 (2018)

SWITCHING ELECTRIC CIRCUITS WITH DC HYBRID BREAKER

TITU NICULESCU[1]

Abstract: The paper presents a method of extinguishing the electric arc that occurs between the contacts of direct current breakers. The method consists of using an LC type extinguishing group to be optimally sized. From this point of view is presented a theoretical approach to the phenomena that occurs immediately after disconnecting the load and the specific diagrams are drawn. Using these, the elements extinguishing group we can choose. At the second part of the paper there is presented an analyses of the circuit switching process by decomposing the process in particular time sequences. For every time interval there was conceived a numerical simulation model in MATLAB-Simulink medium which integrates the characteristic differential equation and plots the capacitor voltage variation diagram and the circuit dumping current diagram.

Keywords: Arc current, DC systems, voltage variation, MATLAB, Simulink.

1. INTRODUCTION

In the DC circuits that contain power breakers, a big problem is the disconnecting the loads, because an electric arc that can destroy its contacts occurs [4], [9]. In these situations we can use an additional circuits that are connected in parallel over the main breaker. These circuits generate a counter current injection which opposes the current breaker and results a current zero through the main breaker and the electric arc will be extinguished [7].

The basic electric circuit for switching DC systems is shown in figure 1:

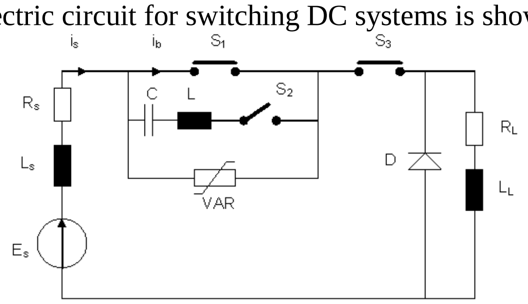

Fig. 1. Electric circuit for switching DC systems

[1] *Ph.D., Associate Prof. Eng., University of Petroşani*

The circuit from Figure 1 contains a DC power E_s which has the intern parameters R_s and L_s, in series with a main breaker S_1. S_3 is an electric separator and at initial moment, a load with R_L and L_L parameters is connected. In parallel with S_1 a switching circuit is connected [2], [8]. This consists in the capacitor C, the inductivity L and the auxiliary switch S_2 (usually is a semiconductor).

For limiting the over voltages, the VAR varistor is applied across the main breaker, and the freewheeling diode D will take the current when its slope is negative[3].

The auxiliary switch S_2 is closed immediately after disconnection to extinguish the arc in the main breaker S_1. Energy stored in the capacitor C, is released and that generates a current that opposes the current through the breaker, resulting a zero current through its contacts. If the arc is not extinguished at the first current zero,the capacitor C and the inductor L form an oscillating circuit which will produce a second current zero. After arc extinguishing, the capacitor C is loaded again from the source E_s and is ready for a new circuit switching.

2. ANALYSIS OF CIRCUIT SWITCHING

We consider the continuous equivalent voltage across of the extinguishing circuit U_{lc}. In this case the equivalent resistance R, the voltage differential equation is given by (1), [5], [6]:

$$LC\frac{d^2u_c(t)}{dt^2}+RC\frac{du_c(t)}{dt}+u_c(t)=U_{1c} \tag{1}$$

where the capacitive current is:

$$i_c(t)=C\frac{du_c(t)}{dt} \tag{2}$$

Equation (1) can be written in the equivalent form:

$$\frac{d^2u_c(t)}{dt^2}=\frac{1}{LC}\left[U_{1c}-u_c(t)-RC\frac{du_c(t)}{dt}\right] \tag{3}$$

Based on equations (2) and (3), the numerical simulation scheme in MATLAB-Simulink medium of arc current through the main breaker S_1 was released (Figure 2):

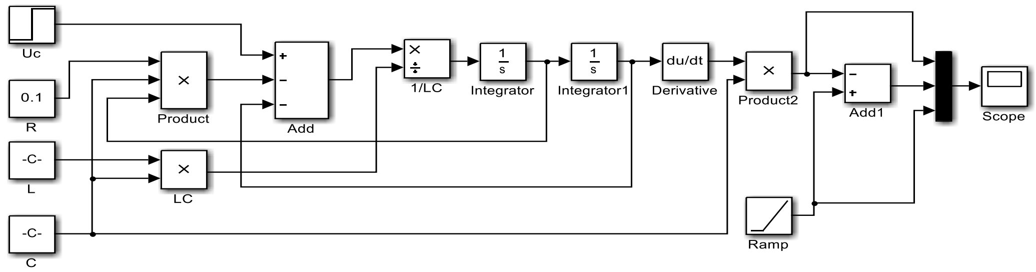

Fig. 2. Simulink model of arc current

The above scheme (Figure 2) generates currents diagram from Figure 3. As is shown in figure 3, the current value i_{t1} is reached at time t_1 (reported at the time of load disconnection). At this moment voltage capacitor C is U_{C1} value. At this time t_1 a counter current injection in opposite to i_s occurs through the main breaker and the breaker current begins to decrease. At time t_2 it becomes zero and the capacitor voltage decreases to U_{C2} value.

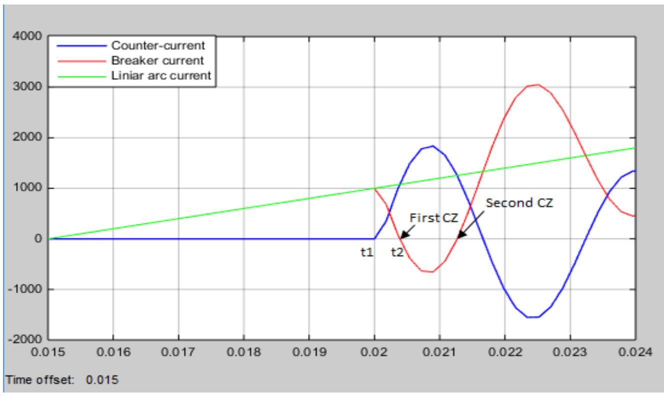

Fig. 3. Currents diagram through the main breaker

Forcing zero current through the main breaker lids to arc extinguishing. The Simulink models presented were made for the following values of electric parameters: U_c=2000[V]; R=0.1Ω; C=500µF; L=500µH.

3. ANALYSES OF SWITCHING PROCESS

For the study of switching process there is used the circuit from figure 4.

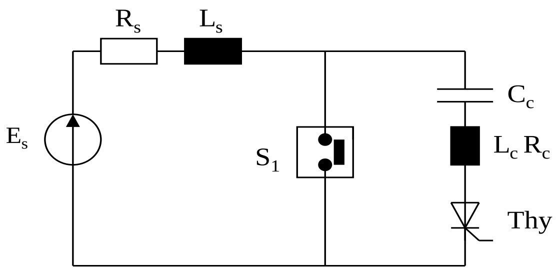

Fig. 4. Switching circuit scheme

The current interrupting process can be split in intervals, where every interval is described by a differential equation. These differential equations can be integrated using the MATLAB-Simulink medium, which allows plotting the variation curves for the current and capacitor voltage [1].

There are considered the following time periods:

- t_1 – time after that S_2 closed and dumping process begins;
- t_2 – time after that occurs the first current zero through the main breaker S_1;
- t_3 – time after that the source current was zero and C capacitor is fully charged at maximum.

3.1. Time interval [0 – t_1]

Throughout this time interval, the E_s source current passes the loop in figure 5 and is described by the differential equation (4):

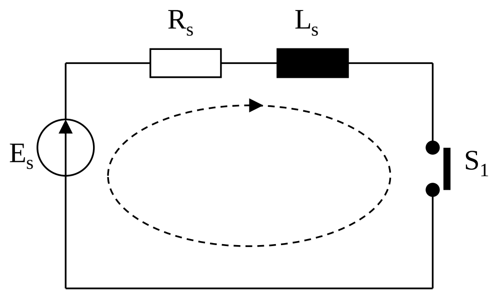

Fig.5. Current flowing for [0-t_1] interval

$$L_s \frac{di_s}{dt} + R_s i_s = E_s \tag{4}$$

If the initial conditions for this interval are took into account, the circuit current expression is:

$$i_s(t) = \frac{E_s}{R_s}(1 - e^{-\frac{t}{T}}) \tag{5}$$

where T = L_s/R_s is circuit time constant.

Its variation is an exponential function.

3.2. Time interval [t_1 – t_2]

At the t_1 moment the oscillation in extinguishing circuit begins, and counter current through the main breaker occurs.

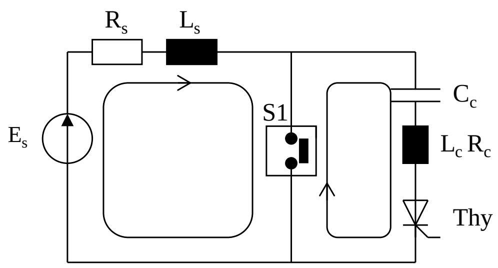

Fig. 6. Current flowing for [t_1-t_2] interval

The capacitor voltage which belongs to the extinguishing circuit is described by the second order differential equation:

$$LC\frac{d^2u_c}{dt^2} + RC\frac{du_c}{dt} + u_c = U_{c1} \tag{6}$$

where U_{c1} is the voltage at which the C_c capacitor is charged at t_1 moment.

Differential equation (6) is integrated using MATLAB-Simulink medium. The numerical simulation scheme which plots the capacitor voltage variation and the current through the extinguishing circuit is presented in figure 7:

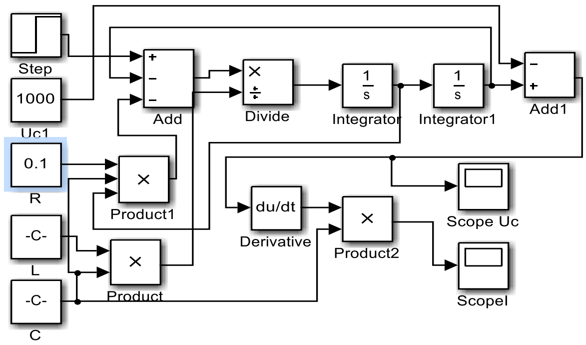

Fig.7. Simulink model for oscillating voltage and capacitor current for [t_1-t_2] interval

This model generates the following diagrams (Figure 8 and Figure 9):

At moment t_2, the current through the main breaker S_1 became zero and the voltage across the capacitor reached U_{c2}.

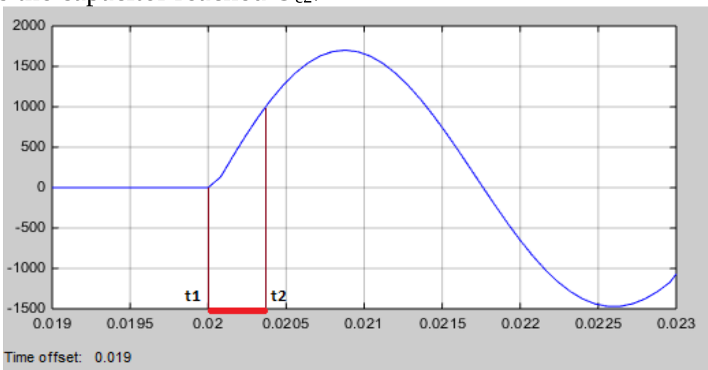

Fig. 8. Current variation in [t_1-t_2] interval

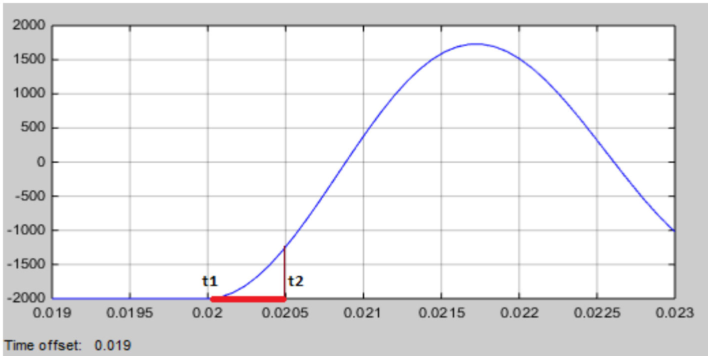

Fig. 9. Capacitor voltage variation in [t_1-t_2] interval

3.3. Time interval [$t_2 - t_3$]

In this interval, source current becomes equal to the capacitor current. The capacitor voltage at the initial moment is $U_{c2,}$ and the current is I_{t2}. After the opening of main breaker, current flowing occurs according to scheme in figure 10:

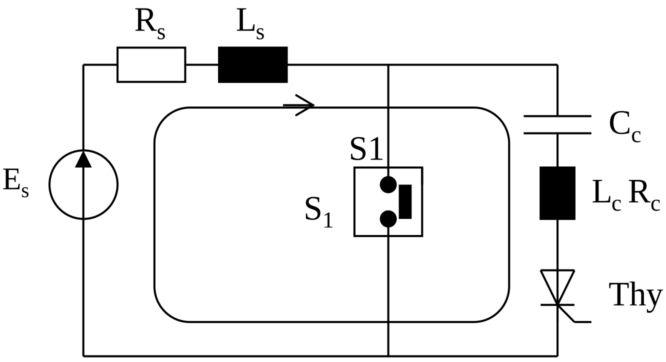

Fig. 10. Current flowing for [t_2-t_3] interval

The capacitor voltage which belongs to the extinguishing circuit, is described by the second order differential equation:

$$C_c(L_s + L_c)\frac{d^2u_c}{dt^2} + C_c(R_s + R_c)\frac{du_c}{dt} + u_c = U_{c2} \tag{7}$$

Differential equation (7) is integrated using MATLAB-Simulink medium. Numerical simulation model which plots the capacitor voltage variation and the current through the extinguishing circuit is presented in figure 11:

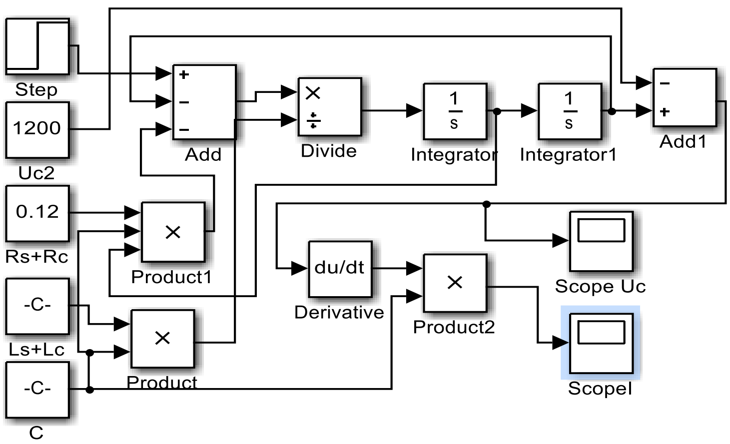

Fig.11. Simulink model for oscillating voltage and current through the capacitor for [t_2-t_3] interval

The Simulink model in Fig.11 generates the following diagrams:

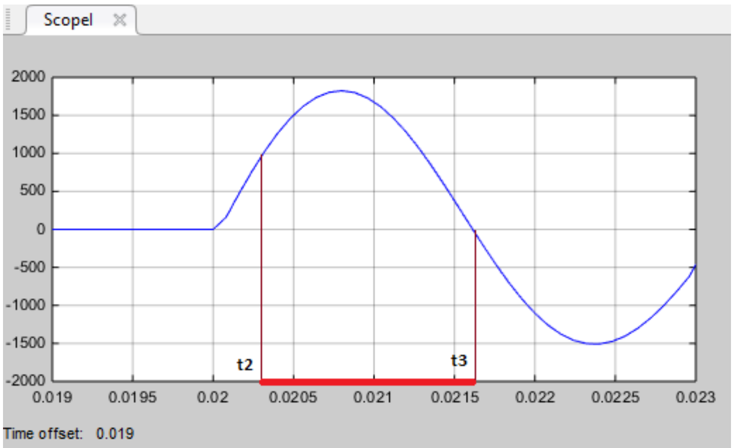

Fig.12. Current variation in [t_2-t_3] interval

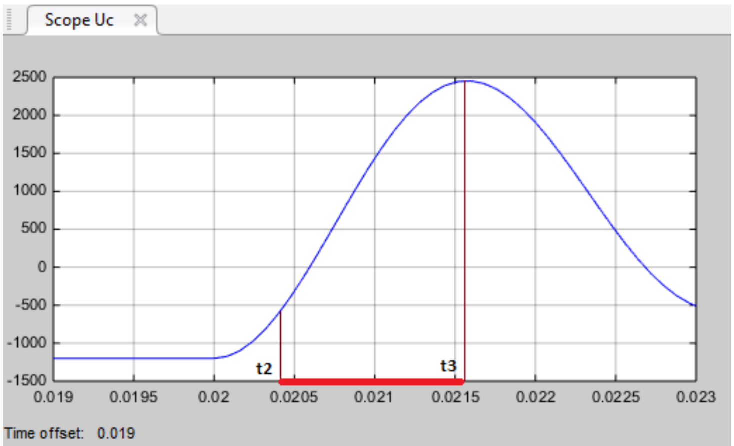

Fig.13. Capacitor voltage variation in [t_2-t_3] interval

At time t_3, the source current will be zero when the capacitor C_c was fully charged, see figure 13.

The Simulink models presented (Figure 7 and Figure 11) were made for the following values of electric parameters: U_c=2000[V]; R=0.1Ω; R_s=0.02 Ω; C=500µF; L=500µH; $L_s \approx 0$.

4. CONCLUSIONS

The auxiliary switch S2 was chosen unidirectional (solid state switch – thyristor) and the counter-current from a resonant LC circuit could provide two current-zeros. For this reason exist two opportunities for circuit interruption.

Another way of interrupting the load current, involves the using of a bidirectional switch (vacuum breaker). In this case, after the source current was commutated, the current oscillation occurs for several time periods according to the circuit damping, until the final capacitor voltage becomes equal with the supply voltage. During oscillation, energy is transferred between source and LC circuit.

Depending on the commutation current value chosen, an appropriate switch might be found from the available power semiconductors. Solid-states switches were commonly vulnerable to increasing slope currents. But the switch had to be able to withstand surge counter-currents when switching on and surge voltages when switching off. The power semiconductors allowed high current to be switched by lowering its frequency. When the frequencies of LC circuit are high, a good method for interrupting the load current, consists of using the vacuum breakers.

REFERENCES

[1]. Ghinea I., Firţeanu V., *MATLAB numerical calculation, graphics,* (in Romanian), Teora Publishing House, Romania, 1994.

[2]. Marcu M., Samoilă L., Popescu F.G., *Power Active Filter Based on Synchronous Reference System Theory,* 1st WSEAS International Conference on Industrial and Manufacturing Technologies (INMAT '13), Vouliagmeni, Athens, Greece, May 14-16, 2013.

[3]. Marcu M.D., Popescu F.G., Niculescu T., Pana L., Handra A.D., *Simulation of power active filter using instantaneous reactive power theory*. Harmonics and Quality of Power (ICHQP), 2014 IEEE 16th International Conference, pp.581 – 585, Bucharest, Romania, 2014.

[4]. Merlin M., Green T., Mitchenson P., Trainer D., Critchley D., Crookes R., *A new hybrid multi level Voltage-Source Converter with DC fault bloking capability*, 9th IET Intenational Conference on AC and DC Power Transmission 2010 ACDC, oct, 2010, pp. 1-5.

[5]. Niculescu T., Niculescu M., *The study of fundamental electrical circuits transitory phenomena using MATLAB software,* Simpozion international multidiscilplinar UNIVERSITARIA SIMPRO 2010, Electrical Engineering and Energetics System Control, Applied Informatics and Computer Engineering, Editura Universitas, octombrie 2010, pp. 31-34.

[6]. Niculescu T., *Technology and Engineering Applications of Simulink, Chapter 2: Study of Inductive-Capacitive Series Circuits Using the Simulink Software Package* ISBN 978-953-51-0635-7, Hard cover, Publisher: InTech, Published: May 23, 2012.

[7]. Niculescu T., Marcu M., Popescu F.G., *Study of switching electric circuits with DC hybrid breaker, one stage,* International Conference on Innovative Research 2016 - ICIR Euroinvent 2016, IOP Conf. Series: Materials Science and Engineering 133, 2016.

[8]. Niculescu T., Popescu F. G., Marcu M., Slusariuc I. R., *Study of Electrical Switching Processes with NI USB Data Acquisition Systems and MATLAB-SIMULINK*, Environment, International Journal of Circuits, Systems and Signal Processing, Vol.12/2018, ISSN: 1998-4464, pp.629-636, 2018.

[9]. Uţu, I., Păsculescu, D., *Power Quality Study in Order to Comply with European Norms*. Publicat in Revista Calitatea, Supplement of “Quality - Access to Success” Journal, Vol.18, S1, January 2017, ISSN 1582-2559, pag. 366-371.

Annals of the University of Petrosani, Electrical Engineering, 20 (2018)

INTELLIGENT SOLUTIONS FOR SUSTAINBILITY OF POWER SYSTEMS

MARIA DANIELA STOCHIȚOIU[1], ALINA DANIELA HANDRA[2]

Abstract: Intelligent solutions provide the necessary features to avoid technical problems in the power systems that increase transmission capacity and system stability very efficiently and they assist in prevention of cascading disturbances. They support the great access of renewable energy resources and reduce the transmission losses by optimization of power flows.

Keywords: sustainable development, flexible systems, power flow.

1. INTRODUCTION

Global demand for renewable energy is pushing renewable energy to the side of fossil fuel energy production. Fossil fuel has limited resources in the world and increasing production has increasing pollution problems. Central power stations are low efficient, high polluting stations which contribute to environmental issues. In order to overcome these problems structural changes are needed in power production to change non-renewable based production to renewable based energy production. Due to public interest, appears a pressure to develop technical solutions to increase amount of renewable energy in power production, and to use opportunities to utilize renewable energy resources and address the technical challenges [1].

Carbon dioxide concentrations are rising mostly because of the fossil fuels that people are burning for energy. Fossil fuels like coal and oil contain carbon that plants pulled out of the atmosphere through photosynthesis over the span of many millions of years; we are returning that carbon to the atmosphere in just a few hundred years.

Small-scale power production is replacing large-scale centralized power production. Intermitted energy as wind power and solar energy are causing negative effects to power quality, voltage, frequency and reliability [5]. An increasing amount of intermittent energy increases problems for the grid.

[1] *PhD., Associate Professor, Eng., University of Petrosani*
[2] *PhD., Trainer, Eng., Soft Skills Training SRL*

2. HVDC AND FACTS CONVERTER TECHNOLOGY

HVDC and FACTS controllers based on line commutated converter technology have a long and successful technology (fig.1). Thyristor was the key components of this converter topology and have reached a high degree of maturity due to their robust technology and their high reliability. HVDC transmission technology offers new dimensions for long distance transmission. In general, for transmission distances above 700km, DC transmission is more economical than AC transmission at least 1GW.

HVDC and FACTS provide the necessary features to avoid technical problems in the power systems that increase transmission capacity and system stability very efficiently and they assist in prevention of cascading disturbances. They support the great access of renewable energy resources and reduce the transmission losses by optimization of power flows.

The power systems work with transmission alternative voltage lines 220kV, 400kV, 750kV and continuous voltage $\pm$ 200kV… $\pm$ 800kV.

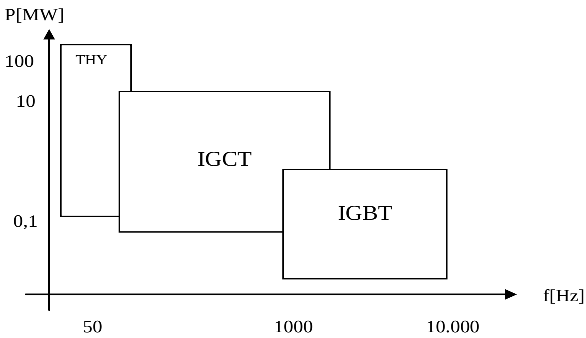

Fig. 1. Evolution of Si power electronics devices

Advances in power electronic technologies together with sophisticated electronic control methods made possible the development of fast static compensators namely Flexible AC Transmission Systems (FACTS). The FACTS technology has become one of the most valuable compensation techniques, because it applies the latest advances in power electronics to achieve additional and more effective control of the parameters of the electrical systems [3]. This represents the most efficient combination of conventional primary equipment, high power semiconductor devices, microelectronics and telecommunications equipment, allowing a most flexible power electric system.

Till today, the thyristor having the highest voltages and currents are used in almost all FACTS technologies and in some HVDC lines having $\pm$ 800kV and power of 8GW. The thyristors are also using in static commutations from LCT (inductance controlled thyristor) and CCT (Capacity switched thyristor) in converters for static VAr compensator.

Especially in applications of wind plants off-shore the devices for HVDC must to have small dimensions so, more devices can be integrated in the same semiconductors structure.

The main definition of FACTS is the A.C. Transmission System which incorporate static commutates based on power electronics which improve the controllability and increase the transmission capacity. Flexible AC Transmission Systems (FACTS) technology helps utilities in reducing transmission congestion and in utilizing more efficiently the existing transmission system without compromising the reliability and security of the system. Their fast response offers high potential for power system stability enhancement apart from steady state flow control [2].

Table 1 ***The semiconductors characteristics for HVDC and FACTS***

Types of semiconductors	Symbol	Characteristics				
		Highest turn-off voltage [kV]	Highest direct current [kA]	The commutation frequency [Hz]	The nominal power	t_{off} [μs]
Thyristor	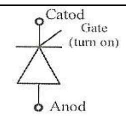	8	5,5	50/60	kW-GW	50
Gate Turn Off Thyristor	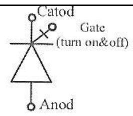	4,5	4	<500	MW	10
Integrated Gate Commutated Thyristor	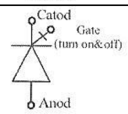	6,5	1,5	<1000	MW	5
Isolated Gate Bipolar Transistor	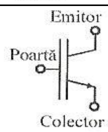	6,5	2,4	<1000	MW	2

The benefits of employing FACTS are many: improvement of the dynamic and transient stability, voltage stability and security improvement, less active and reactive power loss, voltage and power profile improvement, power quality improvement, increasing power flow capability through the transmission line, voltage regulation and efficiency of power system operation improvement, steady state power flow improvement, voltage margin improvement, loss minimization, line capacity and load ability of the system improvement [4]. The abbreviation for used FACTS devices are: TSSC – Thyristor Switched Series Capacitor; SSSC – Static Synchronous Series Compensator; TCVR- Thyristor Controlled Voltage Compensator; CSC – Convertible Static Compensator; SVC – Static VAr Compensator; TCSC – Thyristor Controlled Series Capacitors; STATCOM – Static Synchronous Compensator.

In the last years, some mechanical switchers of parallel capacitors/inductances were being replaced by static switchers with thyristors. The modern devices of serial compensation are TSSC, TCSC and SSSC. The different FACTS devices contain as parallel components as well serial components connected together in the transmission system (as UPFC – Unified Power Flow Controller and IPFC – Interline Power Flow Controller) [4]. These devices can control the important parameters of energy as line voltage, impedance, angle or active power flow and reactive power flow.

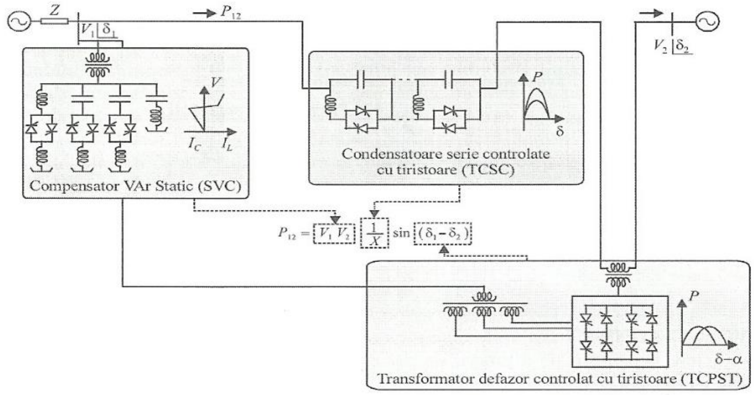

Fig.2. FACTS devices based on the conventional thyristors

3. CONCLUSIONS

Modern power systems are large, interconnected and involves thousands of buses and hundreds of generators. Power system protection devices also form a large part of the system. Environmental as well as economic factors primarily govern the installation of new power system and to transport this power, new transmission line construction are needed to meet the ever increasing load demand.

REFERENCES

[1]. Iakovleva E. V., Momot B. A., *Development of technology for creating intelligent control systems for power plants and propulsion systems for marine robotic systems*, IOP Conf. Ser. Earth Environ. Sci., vol. 87, p. 032010, Oct. 2017.

[2]. Marcu M.D., Niculescu T., Slusariuc R.I., Popescu F.G., *Modeling and simulation of temperature effect in polycrystalline silicon PV cells*, International Conference on Innovative Research 2016 - ICIR Euroinvent 2016, Iasi 2016.

[3]. Marcu M., Niculescu T., Popescu F., Slusariuc R., *Incremental conductance algorithm used in a programmable microcontroller as maximum power point traker*, SGEM 2017 Conference Proceedings, Vol. 17-Energy and Clean Technology, Albena, Bulgaria, pp. 369-376, 29 June-5 July 2017.

[4]. Eremia M., s.a. *Dispozitive FACTS, Concepte si aplicatii in electroenergetica,* Editura Agir, 2017.

[5]. Stochitoiu M.D., Marcu M., Utu I., Niculescu T., Popescu F.G., *Modern concepts and its application for energetically security requirements at different connected sources,* SGEM 2018 Conference Proceedings, Vol. 18- Informatics, Geoinformatics and Remote sensing, Albena, Bulgaria, 29 June-5 July 2018, pp. 591-596.

Annals of the University of Petrosani, Electrical Engineering, 20 (2018)

ASYNCHRONOUS MOTOR PROTECTIVE RELAY WHEN ONE OF THE ROTOR PHASES GETS INTERRUPTED

LILIANA SAMOILĂ[1], SUSANA ARAD[2], DUMITRU SFARLOAGA[3]

Abstract: The electronic relay for protecting the asynchronous motor rotor against remaining in two phases can be used in electrical driving with slip-ring asynchronous motors. It is meant to control and turn off the supply network when one of the phases is missing in the rotor circuit, respectively in the case of an unbalanced three-phase system.

Key words: asynchronous, motor, protection.

1. INTRODUCTION

The problem of diagnosis is indeed related to that of the maintenance, utilizing economic factors that are difficult to evaluate [4]. The issues of preventive and condition-based maintenance, online monitoring, system fault detection, diagnosis, and prognosis are of increasing importance [2], [3].

The key issues for a successful motor operation are a quality motor, understanding its application, choice of the proper one for the application, and its proper maintenance. The use of induction motors in today's industry is extensive and they can be exposed to different hostile environments, manufacturing defects, etc. [5]

These types of faults usually refer to the gradual deterioration of the motor that can lead to motor failure if undetected [5].

Monitoring of the current per phase can provide indications on the motors state. This is preferable, compared to other methods since it is easy for physical measurement. The fault affects the spectrum current signal while the induction machine is sufficiently loaded and generally, we can extract from that the number of the broken bars. The motor current based fault detection relies on interpretation of the frequency components in the current spectrum that are related to rotor asymmetries.

[1] *PhD, Associate Professor, Eng., University of Petrosani, branaliliana@gmail.com*
[2] *PhD, Professor, Eng., University of Petrosani, susanaarad@yahoo.com*
[3] *PhD, Student, University of Petrosani*

2. ASYNCHRONOUS MOTOR ABNORMAL WORKING REGIMES

The overload and short-circuit currents produce the winding temperature increment above the maximum admissible value that leads to the motor break down [1]. It is necessary to take certain measures in order to avoid such situations.

An overload current may appear when [5]:

- the driven mechanism is over loaded, that is the load torque overpasses the maximum motor torque for a long time; in this case, the motor stalls and the current reach the starting current value;
- the supply voltage lowers, which determines the rotor, respectively stator current diminution; the speed goes down up to the motor stop; when the supply is reestablished, if the motor hasn't been disconnected, the current is high (starting current).
- one of the stator or rotor phase is interrupted, which determines 1.7 – 1.8 times increment of the other two currents.

The interruption of one of the rotor phases causes the following effects:

- the motor speed goes downward;
- some strange specific noise appears;
- the zero voltage in the rotor star connection shifts and a shift voltage appears;
- the rotor voltage frequency modifies;
- the currents in the other two phases grow by $\sqrt{3}$;
- the motor slip changes.

3. ELECTRONIC RELAY FOR PROTECTING THE SLIP-RING ASYNCHRONOUS MOTORS WHEN ONE OF THE ROTOR CIRCUIT PHASES IS INTERRUPTED

The belt conveyors in the lignite quarries are driven with 1 – 5 slip rings asynchronous motors.

The motors connection to the 6 kV network is made using an interrupter CA – 100 A, for one motor, or CA – 200 A for two simultaneously connected motors.

Measurements made in the lignite mining area of Oltenia showed that, when driving a belt conveyor with several motors, the motor power is over dimensioned, considering the heavy working regimes [2].

Practice highlighted that the asynchronous motors rotor circuit frequently remains in two phases due to the imperfect contact between the brush and the collecting rings or between the mobile electrodes and the stationary ones at the starting rheostat.

If the trouble appears during the motor running, the overload in the motor stator isn't sensed immediately by the existing protection because of the derivation connection of the two motors. When the conveyor restarts and one of the motors has the rotor circuit in two phases, the staring time being usually long and the torque and the starting current having high values, the collecting rings or the windings are destroyed.

To eliminate these defects and to reduce the electric energy consumption, we designed and achieved an electronic protection relay Re (figure 1).

In short, a protection relay is a device that receives inputs, compares them to set points, and provides outputs which prevent the system from breaking.

In our case, this relay senses the rotor circuit remaining in two phases during operation and does not allow restarting while the trouble is not solved.

The motors start is accomplished using a liquid rheostat, in star connection, whose neutral point has a null potential when the motor works normally.

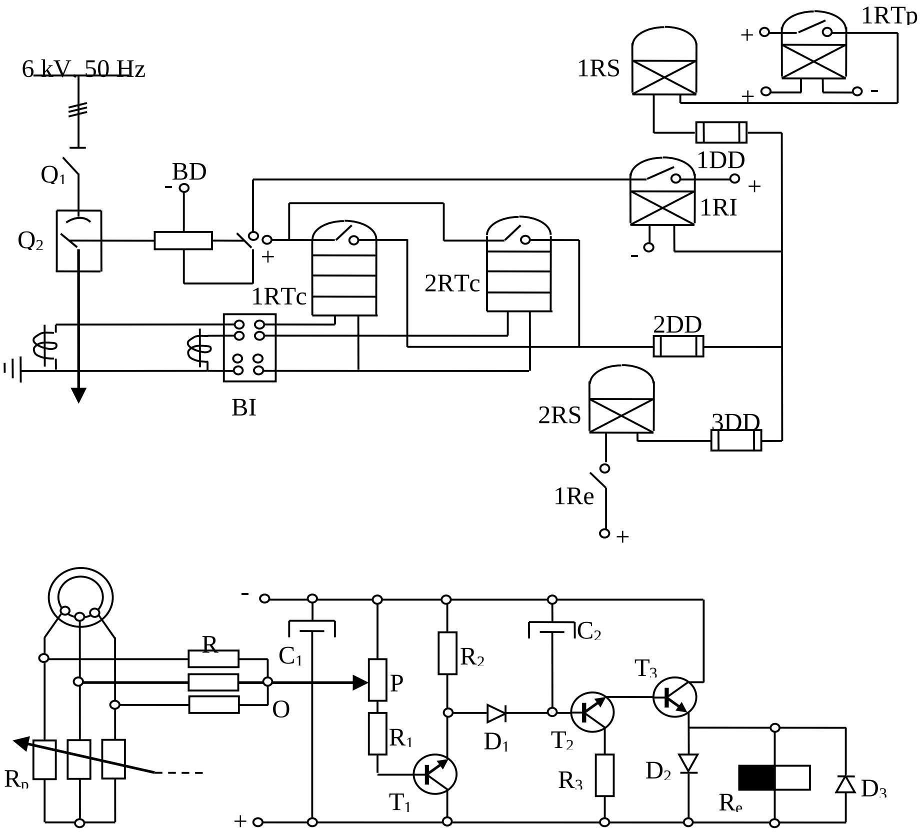

Fig. 1 Operating principle of the protection relay

When the rotor circuit remains in two phases, the null shifts and the protection relay is supplied. The use of the 2RS relay gives the warning “rotor in two phases” and, through the time relay 1RTp, it transmits the trip signal through the tripping coil BD to the interrupter Q2.

The potentiometer P resistance is modified depending on the zero-shifting voltage.

4. CONCLUSIONS

The asymmetrical working regime of the asynchronous motor raises important problems related to the operation and the integrity of the motors.

The protection against one of the supply phase interruption is solved in several options.

The interruption of a rotor phase isn't sensed by any of these solutions. So, it was necessary to design an adequate specific protection, which we managed.

Using the protective device that we made, important economic effects were obtained, related to avoiding the motors braking down.

The relay was achieved end experimented in our laboratory and some of the motors at the Rovinari opencast mining company.

REFERENCES

[1]. Arad S., Pana L., Popescu F., *Improving the energetic efficiency at electric drives compressors of EM Lonea*, International Multidisciplinary Scientific GeoConference: SGEM: Surveying Geology & mining Ecology Management, 2013, pp. 153-160.

[2]. Marcu M., Utu I., Pana L., Orban M., *Computer Simulation of Real Time Identification for Induction Motor Drives*. Proceedings of the International Conference on Theory and Applications of Mathematics and Informatics - ICTAMI 2004, Thessaloniki, Greece, pp. 295-305.

[3]. Popescu F.G., Slusariuc I.R., Uțu I., *Mașini și acționări electrice - lucrări de laborator (Electric machines and drives - laboratory work),* Universitas Publishing House, 2017.

[4]. Stochitoiu M.D., Marcu M., Utu I., Niculescu T., Popescu F.G., *Modern concepts and its application for energetically security requirement at different connected sources*, 18th International Multidisciplinary Scientific Geoconference, SGEM 2018; Volume 18, Issue 2.1, 2018, pp. 591-596.

[5]. Tabacaru T., Utu I., *Masini electrice si actionari (Electric machines and drives),* Universitas Publishing House, 2012.

INDEX OF AUTHORS

REVIEWERS:

Susana Arad PhD.,
Marius Marcu PhD.,
Nicolae Pătrășcoiu PhD.,
Dragoş Păsculescu PhD.,
Florin Gabriel Popescu Ph.D.,
Liliana Samoila PhD.,
Răzvan Slusariuc PhD.,
Olimpiu Stoicuta PhD.,
Ilie Uţu PhD.